Possible unexpected peaks from oil drop size measurements in milk

Rodrigo Olmedo Sotomayor
Laura Schalkwijk

Supervisor: Andreas Håkansson
Assistant supervisor: Fredrik Innings

KLTM01 - Degree Project in Food Engineering
Master of Food Technology and Nutrition

June 2020

Department of Food Technology and Nutrition
Lund University

Preface

This report is a thesis of the master's degree of Food Technology and Nutrition at Lund University in Lund. The assignment is completed by Rodrigo Sotomayor Olmedo and Laura Schalkwijk in collaboration with Tetra Pak and CR Competence in Lund from the end of January until the beginning of June 2020.

We would like to thank our mentors from Tetra Pak and CR Competence, Eva Ransmark, Gunnhildur Gudmundsdottir, Pavlos Kouroutsidis, Anna Stenstam, Marta Gubitosi and Dan Lundberg for their expert advice, assistance during experiments and valuable input during our meetings throughout the course of the assignment. Additionally, we would like to thank Tetra Pak and CR Competence for the possibility to perform part of our experiments there and using their equipment. We would also like to thank our second supervisor at Tetra Pak, Fredrik Innings, for his guidance during the assignment. Furthermore, we would like to thank our classmates for creating an enjoyable working environment, wonderful fika's and a pleasant time at the university.

Lastly, we would like to thank Andreas Håkansson, our main supervisor from Lund University, for his guidance, commitment and advice. We really appreciate all the help and support you have given us during the last twenty weeks.

Rodrigo Olmedo Sotomayor

Laura Schalkwijk

Lund, Sweden, June 2020

Abstract

The shelf life of milk is amongst others dependent on the size of the oil droplets. These droplets can be measured using the laser diffraction (LD) technique. LD is a popular technique to measure particle size distributions (PSD) that has an outstanding broad measuring range capability, is easy-to-use and has a high reproducibility. While this technique is extremely popular, there are some conditions under which LD shows unexpected results in the form of unexpected peaks. The purpose of the current study was to determine under which conditions unexpected peaks appear or do not appear while measuring the PSD of oil droplets on LD equipment. Samples of pasteurized milk were measured on two versions of LD equipment to investigate and identify the conditions under which the LD gives these unexpected peaks, including the variables: pretreatment, sample concentration (i.e. obscuration rate) and dispersing unit stirring speed. A more simplified system (i.e. model emulsion) and a complementary technique (dynamic light scattering) were used to further investigate the unexpected peaks. Results showed that the right sided unexpected peaks are believed to be caused by the incorporation of air. Right sided unexpected peaks can also be caused by dirt in the equipment and a too low sample concentration (i.e. obscuration rate). The second finding of this study is focused on left sided unexpected peaks. These peaks are believed to be caused by a too high sample concentration, which results in the effect of multiple scattering. Another type of left sided unexpected peaks is an increased standard deviation caused by using unoptimized variables of the LD equipment (e.g. too high stirring speed or too low sample concentration). As a result of the increased sensitivity in one of the models of the LD equipment, it was found that it is even more crucial to introduce the adequate optical parameters values (e.g. absorption index). When increasing the absorption index blue light, the discrepancies between different models can be reduced. However, more research needs to be done to confirm this theory. All in all, unexpected peaks can be caused by air, sample concentration, dirt and differences between LD equipment.

Popular Science Summary

Chasing unexpected results in the particle size analysis of oil droplets.

Imagine that 90% of the results given by the most popular particle size distribution determination technique are unreliable and a large scientific community have been using these results over the past years without critically thinking about them.

In the engineering world, accuracy and precision are two concepts that are extremely important to consider when measuring the efficiency of any process. In the food industry as well as in many applications, the need to measure small particles has led to different technologies. Some of them used in a major extent compared with others. Together with advances in laser and light technology, especially after the increasing interest of nanoparticles by the pharmaceutical industry, several techniques have been developed in order to improve the accuracy and reliability of the small particle measuring techniques.

Automatized laser diffraction (LD) techniques are the most used and popular instrument to measure particle size distributions. Its high popularity is due to its outstanding broad measuring range capability and its easy-to-use and high reproducibility. These instruments utilize the principle of laser technology. Together with a complex mathematical algorithm the technology interprets the signal and in an indirect way measure macroparticles, microparticles, nanoparticles and mixtures of those. This makes it an all-purpose technique. However, this technique has its problems and limitations, which are not easy to overcome. These are quite often overseen, underestimated or simply unknown to the user.

Having a deeper understanding under which conditions the instrument can give precise, accurate and reliable results will be highly beneficial for most of the scientific community interested in micron and submicron particle populations. For example, product developers, process engineers, food scientists, just to mention some. However, there are some conditions under which the LD technique shows unexpected results in the form of unexpected peaks. To tackle this problem, this study was started.

In this master thesis, conditions are studied under which unexpected peaks appear or do not appear while measuring oil droplets on commonly used LD equipment. A comparison between two commonly used LD models is presented in order to highlight significant differences in volume PSD and the occurrence of unexpected peaks.

Experiments were preformed using primarily pasteurized milk. However, since milk is such a complex system a model emulsion was studied, which is a more basic system to analyze. This also provided insights to discard some of the hypotheses that might cause the appearance of the unexpected peaks. In order to evaluate the accuracy and detection capability of LD equipment, a technique using dynamic light scattering was used as a complementary technique.

Furthermore, this thesis describes usage recommendations and best practices in detail. This can provide insights in how such equipment should be operated to limit the incidence of unexpected peaks and how to interpret the unexpected peaks when they do occur.

Table of Contents

1. Introduction

Milk is a complex emulsion system that is constantly studied by the food industry, including food manufacturers and packaging material companies. The companies invest many resources in trying to obtain a deeper understanding of the science behind the milk. One of their interests is to try to prolong the shelf life of the milk, which is amongst others dependent on the cream layer of the milk. As the process of creaming can be delayed when the fat droplets in the milk have a smaller particle size, it is crucial to measure the particle size to predict the shelf life.

A widely used particle sizing technique is laser diffraction (LD), which can be used for material ranging from hundreds of nanometers up to several millimeters in size. The main reasons for its success are its wide dynamic range, rapidity during measurements, easy use and repeatability. The biggest advantage of this instrument is its broad measuring range, that can be applied for microparticles, macroparticles, nanoparticles and mixtures of those, making this technique an all-purpose technique and becoming the standard particle sizing technique across many industry sectors (Malvern, 2019). However, this technology has limitations and problems, which are not easily overcome, as they are often overseen, underestimate or unknown to the user of the LD instrument (Keck & Müller, 2008).

In addition, laser diffractometry is also in focus of criticism, because the comparability of results between different laboratories or even between different experiments often fails due to unknown reasons (Keck & Müller, 2008). There is at least one publication which reports the ineffectiveness of the equipment when measuring multimodal samples (Driscoll et al., 2001). The authors state, that the reliability of the method is not appropriate for analyzing multimodal samples (i.e. multiple populations, such as large particles besides a small sized main population) and therefore suggest using different methods rather than laser diffractometry. Nevertheless, laser diffractometry is a frequently applied technique for the size characterization of submicron particles. Even though it is mostly used for a simple particle size characterization; its purpose should be to investigate multimodal samples. This is because there are other more suitable methods to characterize just small particles in the submicron range (e.g. dynamic light scattering technologies (Müller & Schumann, 1996)). However, on the other hand, there are not many methods for the detection of larger particles besides a small sized main population, because the upper detection limit for most of the methods is only a few micrometer (Müller & Schumann, 1996). Hence LD is the method of choice for the detection of larger particles within a submicron system, which can occur due to stability problems (e.g. agglomeration of particles or coalescence in emulsions).

When measuring pasteurized milk using the LD technique, a typical particle size distribution (PSD) shows a main distribution at approximately 0.6 µm, smallest particles at ~0.1 µm and largest particles at ~2 µm (Figure 1).

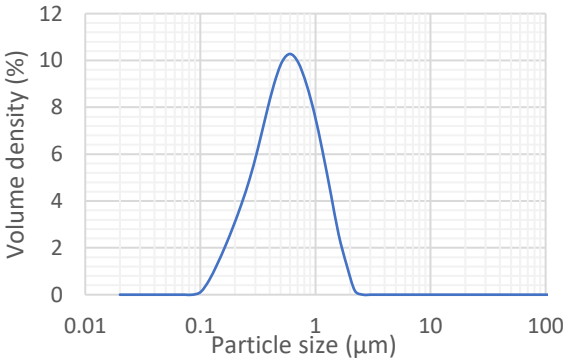

Figure 1: Characteristic PSD of pasteurized milk measured on the Mastersizer 2000.

The LD technique sometimes shows unexpected peaks in the PSD, as found by companies such as Tetra Pak and CR Competence (Obiols-Rabasa, Grusch, Persson & Lundberg, 2019). This creates uncertainty in the reliability and performance of the LD equipment, which is used to determine the efficiency of the homogenization processing of milk. These peaks can be split into two categories: the right and left sided unexpected peak. The right sided unexpected peak (Figure 2.A) can be defined as a free-standing bimodal distribution, as it shows a peak on the right side of the main distribution that is not connected to the main distribution. The unexpected peak appears at particle sizes higher than 3 µm when measuring homogenized milk and likewise products. It shows either a small distribution of approximately 3-6 µm (Figure 2.A, continuous line) or a larger distribution at a particle size of approximately 50-100 µm (Figure 2.A, dash line). The left sided unexpected peak (Figure 2.B) can be defined as deviations from monomodality, as this peak shows a tail or shoulder on the left side of the main peak which is always connected to the main distribution. A tail can be described as a gradual increment within the monomodal distribution (Figure 2.B, continuous line). A shoulder can be described as a more abrupt increment within the monomodal distribution (Figure 2.B, dash line).

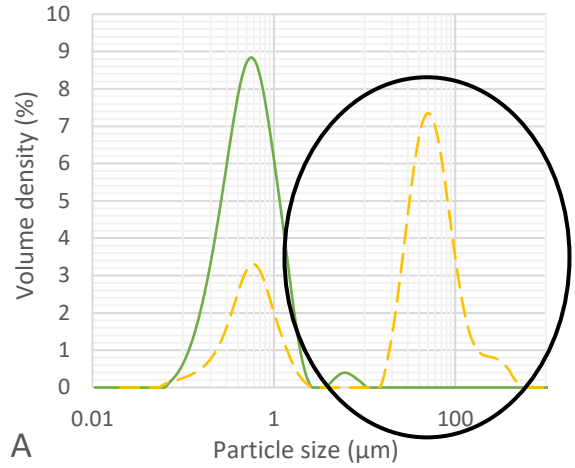

Figure 2.A: PSDs of two examples of variations of the right sided unexpected peak, showing a free-standing bimodal distribution with the expected main distribution on the left side of the distribution at a particle size below 2 µm.

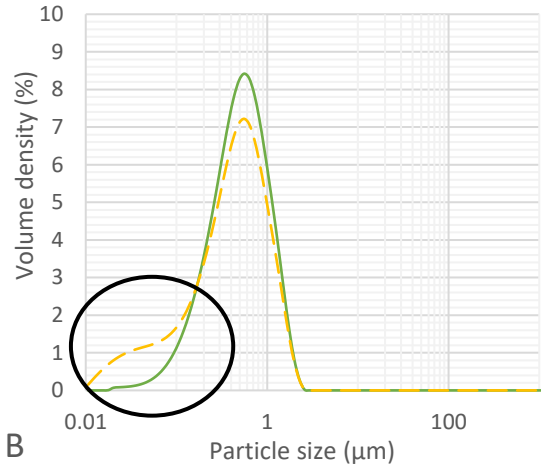

Figure 2.B: PSDs of two examples of variations of the left sided unexpected peak, showing deviations from monomodality as a tail or shoulder can be seen on the left side of the main distribution.

The study started by investigating and identifying the conditions under which the laser diffraction technique gives these unexpected peaks when measuring milk, including the variables: pretreatment (addition of a surfactant, solution A), sample concentration and dispersing unit speed. First experiments were performed on pasteurized milk, repeating some of the experiments for Extended Shelf Life (ESL) milk and non-homogenized milk. A model emulsion was used to evaluate these unexpected peaks in a more simplified system. A complementary technique, Dynamic Light Scattering (DLS), was used to investigate the results obtained from the LD equipment in more detail.

The objective of this master thesis is 'to identify the conditions under which the light scattering technique gives unexpected peaks when measuring different types of milk including the parameters pre-treatment, sample concentration and dispersing unit speed within 20 weeks'. To achieve this objective, the following hypothesis were formulated:

- If the concentration of solution A is reduced, then it will affect the PSD by showing an increased number of small particles (i.e. casein micelles).
- If the stirring rate is increased, then it will affect the PSD by inducing coalescence or incorporating air.
- If the sample concentration is too low, then it will affect the PSD by creating interference between the sample and the background signal.

- If the background shows disturbances, then it will affect the PSD by showing an unexpected peak.
- If the sample concentration is too high, then it will affect the PSD by showing multi scattering.
  To answer this the following sub hypothesis are formulated:
  - If the sample concentration is too high, then aggregation of fat droplets will occur.
  - If the sample concentration is too high, then it will affect the PSD by showing an unexpected peak created by casein micelles
  - If the sample concentration is too high, then it will affect the PSD by showing an unexpected peak created by an artifact.
  - If the sample concentration is too high, then it will affect the PSD by showing an unexpected peak created by small oil droplets.
- If the variables of the LD equipment are not optimized, then it will increase the standard deviation of the PSD.
- If the sensitivity of the LD equipment is increased, then it will affect the PSD.

The intention of this thesis is to raise awareness of the different variables that will cause the creation of an unexpected peak and have an impact in the PSD. The study has been organized in the following way. First, the background will be given in chapter two, which discusses the model emulsion, several techniques used, particle size distribution and a comparison of different versions of the LD equipment. After that, chapter three lays out the theoretical dimensions of the research and looks at LD and milk in detail. Chapter four is concerned with the equipment and methodology used for this study. The fifth chapter presents the findings of the research, focusing on the right and left sided unexpected peak and variations that may cause these peaks to appear. Chapter six contains the conclusions of this study. Chapter seven provides insights in how to use the equipment to obtain more reliable and accurate results, named ‘Best practices’. Lastly, chapter eight presents the suggestions for further research.

2. Background

In this section, model emulsion and techniques such as DLS homogenization are discussed, as well as concepts of PSD and a comparison of LD equipment used for this thesis are explained. Milk and LD will be further discussed in section 3 'Theory'.

2.1 Model emulsion

To mimic the particle size of oil droplets in milk as much as possible, a model emulsion is used. The model emulsion consists of water, sunflower oil and Tween 80, no proteins are included, since they are usually dissociated in the milk samples analyzed due to the addition of Solution A (a mix containing a surfactant). Tween 80 has a similar role as EDTA and Tween 20 used in Solution A, as it also prevents the fat droplets from aggregating and stabilizes the emulsion (Nielsen, Kjems, Mygind, Snabe & Meyer, 2016).

The amount of emulsifier that needs to be used depends both on the fraction of oil in the solution and the size of the droplets suspended in it. The lowest concentration of emulsifier used in a sample must be enough in order to cover the surfaces of all oil droplets (see equation 1). A critical micelle concentration, $CMC_{emulsifier}$, is the lowest amount of emulsifier required to start micelle formation, which is a necessary occurrence before the emulsifier can start to cover the oil droplets. See the derivation in Appendix A.

$$V_{emulsifier} = \frac{M_{emulsifier} \cdot CMC_{emulsifier} \cdot V_{emulsion} + n \cdot \Gamma \cdot A_{oil\ droplet}}{\rho_{emulsion}} \quad (1)$$

In the equation $M_{emulsifier}$ is the molar mass of the Tween 80 (g/mmol), $CMC_{emulsifier}$ is the critical micelle concentration (mmol/l), $V_{emulsion}$ is the total volume of the emulsion (l), *n* is the number of droplets in the emulsion, Γ is the amount of emulsifier required to cover the oil drops (g/m^2), $A_{oil\ droplet}$ is the surface area of one oil droplet (m^2) and $\rho_{emulsion}$ is the density of the emulsion (g/l).

To get a similar particle size to milk, which is a commercial sample and thus already homogenized, the model emulsion is also homogenized. Homogenization will be further described in '2.2.2 Homogenization'. When homogenizing this model emulsion, the particle size can be reduced depending on the pressure and the number of homogenization cycles. By choosing a pressure and number of cycles with a particle size similar to milk, the two can be compared. This can provide valuable information when analyzing particle size measurements using LD, since the particle size of the model emulsion cannot be influenced by protein and is dominated by the fat droplets while milk still contains protein. Therefore, the model emulsion can be seen as a less complex system and is used to verify measurements done using LD.

2.2 Techniques used

2.2.1 Dynamic Light Scattering

DLS is based on similar techniques as LD, as they are both based on the scattering of light. The main difference between the two techniques is that LD focusses on particles between 0.1 – 3500 µm by using the scattering angle and intensity of the scattered light. While the DLS technique can measure in the range of 10 nanometers to tens of micrometers by illuminating a sample with a laser beam and measuring the fluctuations of the scattered light (Malvern Instruments, 2020). In DLS, a laser is used to illuminate the particles in a sample and the intensity over time is measured. As the intensity fluctuates, this fluctuation is a measure of the intensity of scattered light over time. The intensity of a small particles will fluctuate rapidly, meaning that the intensity will lose correlation fast. On the other hand, for large particles, the intensity will fluctuate slowly, and the correlation will remain for a long time. The difference fluctuations of the intensity and correlation for small and large particles can be seen in Figure

3. These fluctuations are associated with the Brownian motion of dispersed particles, which can be described as the random movement of particles as they collide with other molecules (Malvern Instruments, 2020). Algorithms are then used to extract information of the time it takes for the scattered intensity to lose its correlation (i.e. decay time). Since small particles show rapid fluctuation in intensity of scattered light, this results in a faster decay time of the correlation function compared to larger particles (Figure 3). The decay times can be interpreted as a PSD based on intensity. The data can also be converted to a particle size using volume distribution. They are valid under the assumption of spherical non-interacting particles present in the system. (Malvern Panalytical, 2020)

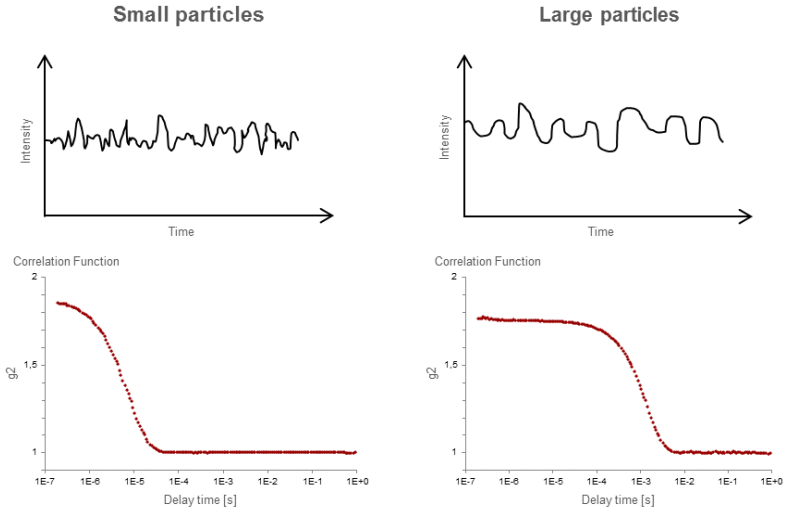

Figure 3: Differences in the intensity (top) and correlation function (bottom) of small and large particles (Anton Paar, n.d.).

Another factor that affects DLS measurements is the temperature, as this could influence the viscosity and microscopically the Brownian motion (Malvern Panalytical, 2020). Therefore, this is also monitored and controlled by the DLS equipment (Malvern Instruments, 2020). While results between LD and DLS should be similar, manufacturer Horiba has stated that results between the two techniques are likely to differ 10-20 % (Horiba, n.d.).

2.2.2 Homogenization

The objective of homogenization process in milk is to reduce the size of the fat globules in the milk, in order to reduce or prevent creaming. It also prevents globules to aggregate or coalesce. During homogenization, a liquid is forced through a small passage at high velocity. Phenomena such as turbulence and cavitation are responsible for the disintegration of the original fat droplet. The fat globule size of pasteurized milk is reduced from an average of 3.5 µm to below 1 µm in diameter (Bylund, 2015). There is an increase in the fat/plasma interfacial surface are by a four- to six-fold. The newly created fat globules are surfaced with a mixture of proteins adsorbed from the plasma phase.

The physical state and concentration of the fat phase during homogenization is highly relevant since it contributes to the size and dispersion of the resulting new fat globules. Homogenization pressure is usually applied between 10 and 25 MPa (100-250 bar), depending on the product (Bylund, 2015).

Single-stage and two-stage homogenizer

A homogenizer is a pump with a homogenization device. The product enters the pump block and is pressurized by the piston pump. The back-pressure determines the pressure that is achieved, it is given by the distance between the forcer and seat in the homogenization device. This pressure (P_1) is designated as the homogenization pressure. P_2 is the back-pressure to

the first stage (Bylund, 2015). A homogenizer can be equipped with single-stage homogenization or two-stage homogenization connected in series (Figure 4). In the case of the two-stage homogenization, the back pressure (P_2) is created by the second stage and can be chosen to achieve optimal homogenization efficiency, when the relation P_2/P_1 is about 0.2, the best results are obtained. In addition to this, the second stage reduces noise and vibrations in the outlet pipe. Optimal homogenization results are achieved by using two-stage homogenization since it breaks up fat clusters in products with high fat content (Bylund, 2015).

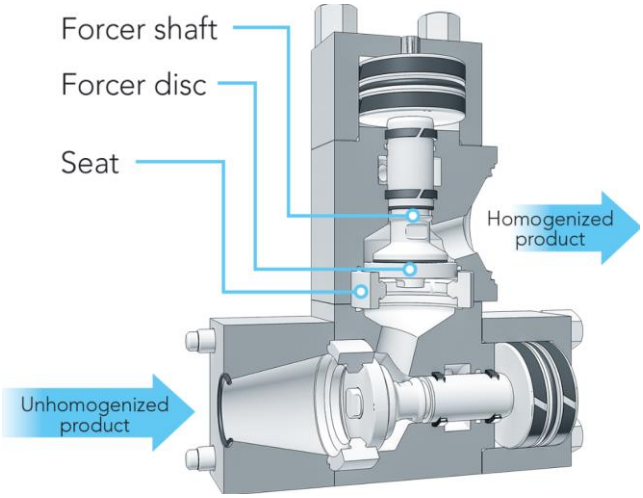

Figure 4: The components of a two-stage homogenization device (Bylund, 2015).

Effect of Homogenization

The homogenization effect in physical structure of milk has several benefits:

- Smaller fat globules leading to less cream-line formation, which is critical for shelf life determination.
- Whiter and more appealing color.
- Lowered sensitivity to fat oxidation.
- More full-bodied flavor, and better mouthfeel experience by the consumer.
- Improved stability of cultured milk products.

However, homogenization also has certain disadvantages:

- Somewhat sensitivity to light is increased, giving a “sunlight flavor”
- The milk might be less suitable for production of semi-hard or hard cheeses since the coagulum will be too soft and difficult to dewater.

Homogenization efficiency

According to Stokes´s Law (equation 2), it can be observed that decreasing the particle size is an effective way of decreasing the rising velocity. Therefore, reducing the size of fat droplets in milk reduces the creaming rate. (Bylund, 2015)

$$v = \frac{2}{9}\frac{(\rho_p - \rho_f)}{\mu} g\, R^2 \qquad (2)$$

In the equation v is velocity (m/s), ρ_p is the mass density of the particles (kg/m^3), ρ_f is the mass density of the fluid (kg/m^3), μ is the dynamic viscosity (kg/(m·s)), g is the gravitational field strength (m/s^2) and R is the radius of the spherical particle (m).

The efficiency of the homogenization process can be measured by using the LD technique, which results in size distribution curves. The percentage of volume (fat) is given as a function of the particle size (fat globule size). As a common rule the curve shifts to the lower size class as a higher homogenization pressure is used (Bylund, 2015).

2.3 Particle size distribution

Several properties of dispersions, especially physical stability, can depend on the size of the particles. As the particles within a dispersion generally vary considerably in size, the size distribution must also be considered. Therefore, in this section some basic aspects of these distributions are briefly discussed for spherical particles.

Distribution Statistics

In order to simplify the interpretation of PSD data, several values can be calculated and extracted. In the industry there is no standard set of what to use, but values of D [4,3] (volume moment mean), D [3,2] (surface area moment mean), Dv10, Dv50 and Dv90 (volume percentiles whereof 10, 50 and 90% of the volume is smaller than) are frequently reported (Ransmark et al., 2019).

Surface area moment mean D [3,2] or Xsv

The surface area mean (Sauter Mean Diameter) is most relevant when specific surface area is important. It is most sensitive to the presence of fine particles in the size distribution (Malvern Instruments, 2015).

Volume moment mean D [4,3] or Xvm

The volume area mean (De Brouckere Mean Diameter) is relevant for many samples as it reflects the size of those particles which constitute the bulk of the sample volume. It is most sensitive to the presence of large particulates in the size distribution (Malvern Instruments, 2015).

Percentiles

For volume weighted PSDs, such as those measured by LD, it is often convenient to report parameters based upon the maximum particle size for a given percentage volume of the sample.

Percentiles are defined as XaB where:

X = parameter, usually D for diameter
a = distribution weighting, e.g. v for volume
B = percentage of sample below this particle size e.g. 50%.

The Dv50 would be the maximum particle diameter below which 50% of the sample volume exists, also known as the median particle size by volume. The most common percentiles reported are the Dv10, Dv50 and Dv90, as can be shown in the Figure 5 (Malvern Instruments, 2015). By checking these parameters, it is possible to see if there are significant changes in the main particle size, as well as changes at the extremes of the distribution, which could be due to the presence of fines, or oversized particles/agglomerates.

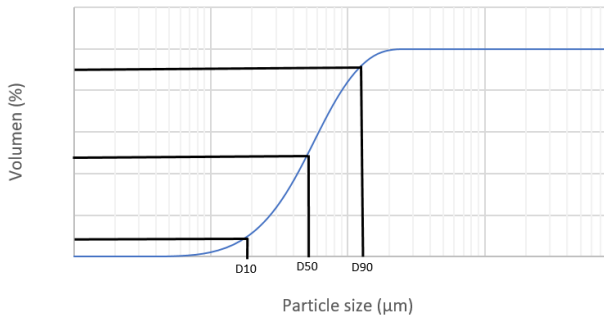

Figure 5.A: Cumulative plot of the most common percentiles (reproduced from Malvern Instruments with permission from the publisher).

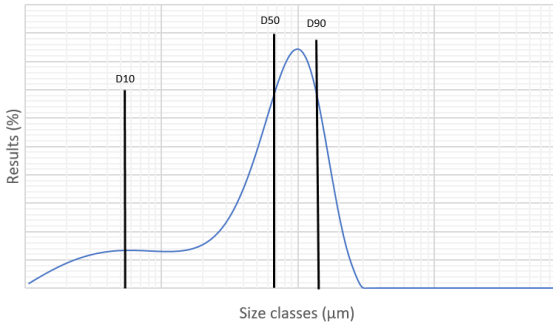

Figure 5.B: Illustration of the Dv10, Dv50 and Dv90 on a typical PSD where a significant proportion of fines are present.

2.4 Comparing Mastersizer 2000 and 3000

While the Mastersizer 2000 and 3000 are both based on LD as their main technique, there are some differences which may cause a difference in PSD. One of the differences between the Mastersizer 2000 and 3000 is the laser path alignment of the lasers. The Mastersizer 2000 has a different path for the red and blue lasers which requires a different setup for the detectors (Figure 6). However, the Mastersizer 3000 has the same path for both the blue and red laser, meaning they can utilize the same detectors.

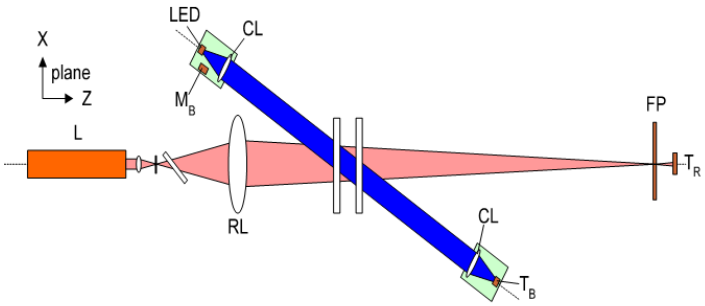

Figure 6: View of blue and red laser orientation in Mastersizer 2000 (Malvern Instruments, 2015).

Other differences between the equipment is that the Mastersizer 3000 has a stronger laser for blue light, as the power of the blue light laser was increased to 10 milliwatt instead of 0.3 milliwatt on the Mastersizer 2000 (Table 1). Furthermore, the Mastersizer 3000 has an increased number of detector channels, backscatter detectors, large angle detectors and measuring angle. Due to the increased measuring angle, there is an increased number of large angle detectors and detector channels. The backscatter detectors collect some of the light scattering information from the sample. The increased number of detector channels on the Mastersizer 3000 causes an increase in the measurable range of small particle size. This increases the detection limit for blue light to 0.01 µm on the Mastersizer 3000. While the detection limit for blue light on the Mastersizer 2000 is 0.02 µm. The detection limit for red light is 0.1 µm for both equipment. Even though the red laser is unchanged, the new laser path alignment for the blue light, stronger blue light laser and increased number of detectors make the Mastersizer 3000 more sensitive to smaller particles. This increase in sensitivity leads to the need of a different algorithm in order to convert the diffraction pattern into a PSD. However, since the Mastersizer 3000 is more sensitive to smaller particles, the equipment is more sensitive to equipment and material parameters deviations as well. (Malvern Instruments, 2015; Malvern Panalytical, 2017; M. Larsson, personal communication, April 8 and May 18, 2020)

Table 1: Some of the differences in the specifications of the Mastersizer 2000 and 3000

	Mastersizer 2000	**Mastersizer 3000**
Laser path alignment	Different pathway for red and blue laser	Same pathway for red and blue laser
Detection limit blue light laser	0.02 µm	0.01 µm
Number of detector channels	52	63
Laser power blue light	0.3 milliwatt	10 milliwatt

3. Theory

In this section the theoretical background of milk and laser diffractometry will be described in detail.

3.1 Milk

Milk is a very complex product. The main components of milk are water (87.5%), fat (3.9%), proteins (3.4%), lactose (4.8%) and minerals (0.8%), meaning about 87% water and 13% dry substance. Dry matter is either suspended or dissolved in the water depending on the type of matter and size of particle. Fat globules are present in an oil/water type emulsion, usually in the size range between 1-10µm (Bylund, 2015). The emulsion is stabilized by a very thin membrane of only 10-20nm thick (1 nm = 10^{-9} m) which surrounds the globules and has a complicated composition, mainly consisting of phospholipids, lipoproteins, cerebrosides, proteins and other components. Fat globules are not only the largest particles in the milk but also the lightest (density at 15.5 °C = 0.93 g/cm^3), fat globules tend to rise to the surface when milk is left to stand for a while. The rate of rise follows Stokes´s Law (equation 2), but the small size of fat globules makes creaming a slow process. (Bylund, 2015).

Proteins in milk can vary in many different types, most of them in very small amounts, they can be grouped in into casein, albumin and globulin, they vary widely in terms of behavior and form of existence. Caseins are easily precipitated from milk in a variety of ways, while the serum proteins usually remain in solution. Casein is the dominant class of proteins in milk, constituting about four-fifths of the milk proteins, the casein self-associate and form large clusters called micelles. The micelles are built up of hundreds and thousands of individual casein protein molecules and vary in size from 50 to 500nm. Since the micelles are of colloidal dimensions, they are capable of scattering light. The casein micelles scatter light which appears as a white color, which explains the fact that also skim milk has a slight white appearance, in absence of fat globules (Bylund, 2015).

Milk as a colloidal system

Figure 7 shows the main structural elements of milk schematically. The figure shows that aspects of colloid chemistry are essential for understanding the properties of milk and the many changes that can occur in it. All particles exhibit Brownian motion; they have an electrostatic charge, which is negative at the pH of milk (pH at 25 °C = 6.7) (Bylund, 2015). Their total surface area is large.

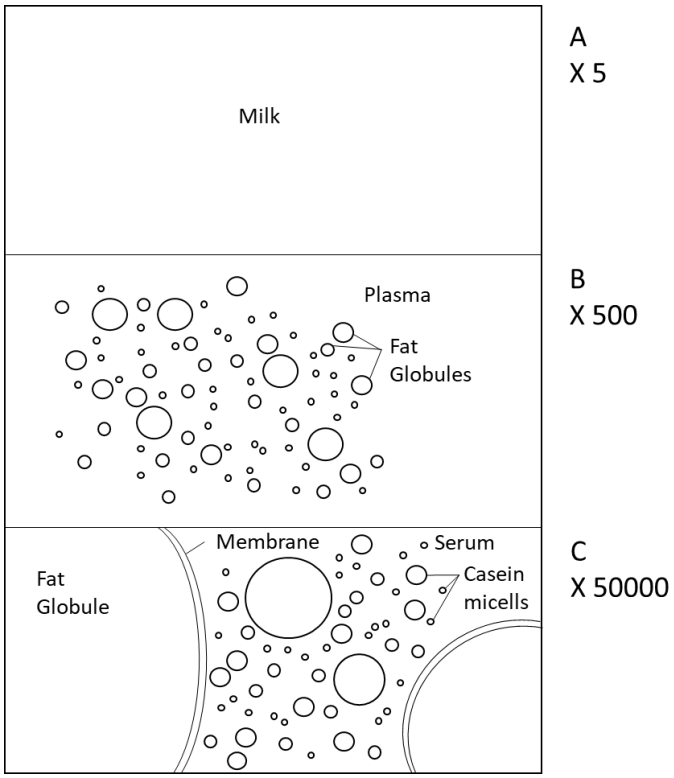

Figure 7: Milk viewed at different magnifications, showing the relative size of structural elements (A) Uniform Liquid. However, the liquid is turbid and thus cannot be homogeneous. (B) Spherical droplets, consisting of fat. These globules float in a liquid (plasma), which is still turbid. (C) The plasma contains proteinaceous particles, which are casein micelles. The remaining liquid (serum) is still opalescent, so it must contain other particles. The fat globules have a thin outer layer (membrane) of different constitution (reproduced from H. Mulder and P. Walstra, *The Milk Fat Globule,* Pudoc, Wageningen, 1974 with permission from the publisher).

Milk is a dispersion and contains many particles of colloidal dimensions (~10 nm and 100 µm in diameter), especially fat globules and casein micelles; together they make up 12 to 15% of the milk by volume (Walstra et al., 2005).

The presence of these particles has several consequences:

- Some substances (fat globules) are present in separate particles. This means that interactions with compound in the serum must occur via the surface of the particles, which may act as a barrier.
- The particles can be subject to various instabilities such as creaming, aggregation, coalescence, partial coalescence and/or Ostwald ripening.

Basic colloid and surface science in milk

In this section some fundamentals of colloid and surface science will be discussed briefly for the benefit of readers.

Two kinds of colloids can be distinguished:

- Lyophobic colloids. They are, in principle unstable and all the physical instabilities such as creaming, aggregation, coalescence and so on will take place. Although the rate of change may be extremely small in some conditions. Lyophobic particles constitute a true phase. They have a phase surface onto which such substances can adsorb. In milk, the fat globules and any gas bubbles present are of the lyophobic type.
- Lyophilic colloids. There are, in principle stable and can form spontaneously. They have no phase surface and can only undergo physical changes if conditions change, e.g., pH in milk, the term refers to the casein micelles.

The terms lyophobic and lyophilic imply “solvent-hating” and “solvent-loving” respectively. Milk serum has a continuous aqueous phase. Thus, in this system lyophobic and lyophilic imply

that the colloidal particles are hydrophobic and hydrophilic, respectively. It is important to mention that creaming, or more generally sedimentation, is not due to colloidal interaction but due an external force caused by gravity or centrifugation (Walstra et al., 2005).

Various types of interfaces can exist between two phases, this study focuses in liquid-liquid, which possess a fluid interface that can be deformed.

Surface Tension

An interface between two phases contains an excess of free energy which is proportional to the interfacial area. Consequently, the interface will try to become as small as possible, minimize the interfacial free energy. This then means that one has to apply an external force to enlarge the interfacial area. The reaction force in the interface is attractive and acts in the direction of the interface. If the interface is fluid, the force can be measured, and the force per unit length is called the surface or interfacial tension (γ) units $N \cdot m^{-1}$. The magnitude of γ mainly depends on the composition of the two phases but also on temperature, nearly always decreases with increasing temperature (Walstra et al., 2005).

Adsorption

Some molecules in a solution that is in contact with a phase surface can accumulate at this surface, forming a monolayer. This is called adsorption. Molecules that have the capability to absorb are called surfactants. They adsorb in such a conformation that provides a lower surface free energy – hence, a lower surface tension. It is known that the surface tension decreases depending on the surfactant concentration left in solution after equilibrium has been reached. (Walstra et al., 2005)

Surfactants

Surfactants come in two main types, small-molecule amphiphilic compounds and polymers, especially proteins.

1. Amphiphiles. These substances are surface active because they are amphiphilic. The molecules have a hydrophobic tail, generally of a fatty acid, and a hydrophilic head group. Most amphiphiles in the presence of water tend to form micelles above a certain concentration, the critical micellization concentration (CMC).
   Some important amphiphiles are monoglycerides and Spans (i.e., fatty acid sorbitan esters), which have low to medium HLB-values. The later variable is the hydrophile-lipophile balance of the molecules. Tweens are derived from Spans by attaching a few polyoxyethylene chains to the sorbitan moiety, they have higher HLB numbers (Walstra et al., 2005).

2. Proteins. These are also amphiphilic molecules, but the main cause for their high surface-active activity is the large size. They tend to change conformation upon adsorption. Globular proteins often become irreversibly inactivated after adsorption, and often become denatured to some extent. Micellar casein and serum proteins are adsorbed onto fat globules during homogenization (Walstra et al., 2005).

Functions of Surfactants

The presence of surfactants in a system can have several different effects. Hence, surfactants are applied to fulfil several functions. Some changes leading to important effect in milk are (Walstra et al., 2005):

1. Laplace pressure. Addition of a surfactant generally lowers surface tension, hence the Laplace pressure. This facilitates the deformation of fluid particles and thereby the formation of small particles during emulsion and foam formation.
2. Surface tension gradients. Variations in the tension gradients makes the formation of foams and emulsions possible. Without surfactant, a liquid will flow very rapidly away from the gap between two bubbles (or two drops), this will generally cause immediate

coalescence of the bubbles. If a surfactant is present, the drainage will be significantly slowed down.

3. Colloidal interaction. The adsorption of a surfactant onto particles can greatly affect (in most cases increase) the repulsive colloidal interaction forces between these particles, and thereby determine if they will aggregate or not. A main function of surfactants is to prevent particle aggregation.
4. Coalescence. Another main function of surfactants is to prevent coalescence of emulsion droplets and foam bubbles. In most situations, this function depends for a considerable part, though not exclusively, on the colloidal repulsion provided. Surfactants greatly vary in their effectivity to prevent coalescence.
5. Micellization. As mentioned, many small-molecule surfactants form micelles in water above the CMC.

Aggregation

Aggregation occurs if particles being close together remain in that state for a much longer time that they would do in the absence of attractive forces between them. The terms flocculation and coagulation are also used, in which the former especially refers to weak, i.e., reversible, aggregation and the latter to irreversible aggregation.

Aggregation is of importance because the aggregates have properties that differ from those of the individual particles, such as faster sedimentation or causing an increase in viscosity. Aggregation is often needed for drops to coalesce, as drops generally must stay close together for a rather long time for coalescence to occur, this is an important phenomena to consider since it might lead to creaming in milk, which is a critical parameter for food producers since creaming is crucial when determining milks shelf life.

Fat Globules

Size Distribution

The milk fat globules vary in diameter from about 0.1 to 15 µm. Globules smaller than 1 µm make up about 75% of the number of globules, about 2% of the globular fat, and about 7% of the fat globule surface area (Walstra et al., 2005).

An emulsion is characterized by its droplet size distribution and the volume fraction of droplets. Volume- surface average diameter is on average about 3.4 µm for milk of several breeds of cows. Of course, the size distribution can be altered by treatment, especially by homogenization (Walstra et al., 2005).

Each fat globule of milk is surrounded by a surface layer or membrane. The layer functions to prevent the fat globules from coalescence. Its composition is completely different from either milk fat or milk plasma and is like that of a cell membrane, from which the fat globule membrane largely derives.

Releasing part of the membrane from the surface of a fat globule causes surface-active substances (mainly protein) to adsorb from the plasma onto the denuded fat-water interface. Increasing the fat surface area by reducing average globule size creates an uncovered interface, which subsequently acquires a coat of plasma proteins. This specially happens during homogenization (Walstra et al., 2005).

Types of instability

Various kinds of instability can be distinguished. These instabilities can to some extent occur simultaneously. Moreover, the changes can influence each other. All changes that cause an increasing particle size promote creaming, and thereby demixing. Aggregation thus enhances creaming, but the creaming also enhances aggregation. (Walstra et al., 2005).

Walstra et al. (2005), define three types of ways in which fat globules can *aggregate*, as illustrated in Figure 8:

1. In *floccules*, attractive forces between globules are week, and stirring disrupts the flocculates. Flocculation does not happen normally with milk fat globules because electrostatic and steric repulsion prevents it.
2. In *clusters*, two globules share part of the membrane material, generally micellar casein. Examples are so-called homogenization clusters and heat-coagulated fat globules. Clusters usually cannot be disrupted by stirring.
3. In *granules,* fat touches fat. Aggregation to granules can only occur if the fat globules contain a network of fat crystals, giving the globules a certain rigidity. Granules usually cannot be disrupted.

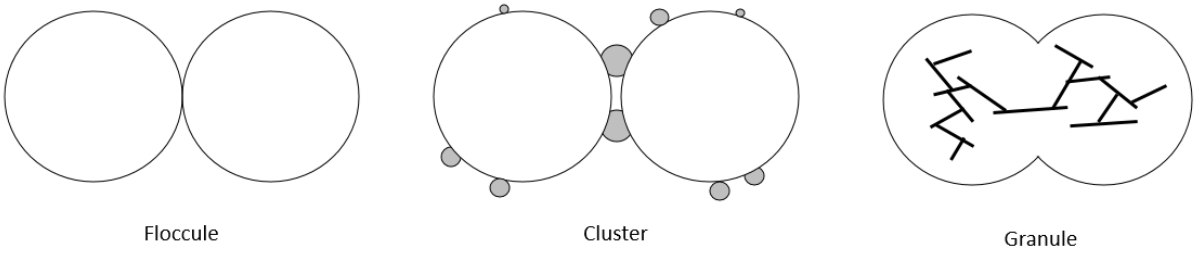

Figure 8: Different types of aggregates of fat globules. Gray dots denote (parts of) casein micelles; heavy lines denote fat crystals. Highly schematic, not to scale (reproduced from Walstra et al, 2005 with permission from the publisher).

Creaming

Because of the difference in density between milk plasma and fat globules, the globules tend to rise. This property is of great importance because it causes (undesirable) creaming during storage, and it enables milk to be separated into cream and skim milk. Creaming is much enhanced if the fat globules have been aggregated into floccules or clusters.

Regarding pasteurized milk, creaming of single fat globules may occur. This can be predicted using Stoke's Law (equation 2), since the velocity of a rising globule can be obtained from this equation.

Casein Micelles

The fact that casein in milk is not present in solution but in micelles has important consequences for the properties of milk. To a large extent the casein micelles determine the physical stability of milk products during heat treatment, concentrating, storage and have a fundamental role in the rheology of fermented and concentrated dairy products (Bylund, 2015). Almost all casein in fresh uncooled milk is present in roughly spherical particles, mostly 40 to 300 nm in diameter. On average, the particles comprise approximately 10^4 casein molecules. There is still disagreement among the molecular research community on the supramolecular structure of casein micelles, although several aspects of it are common ground. An important element is that the micelles is built of mixed-composition submicelles, each 12 to 12 nm in size, and containing some 20 to 25 casein molecules. Some of these submicelles would contain one or two polymers of κ-casein and are at the outside of the micelles. The other micelles would contain no or very little κ-casein (Walstra et al., 2005).

The micelles show a distinct size distribution, a typical example being given in Figure 9. Note the great number of very small particles. These appear to be loose submicelles, which make up only a small part of the total casein (often called "soluble casein"). Walstra et al. (2005), estimate the volume-surface average diameter (d_{vs}), excluding the loose submicelles, to be 120 nm.

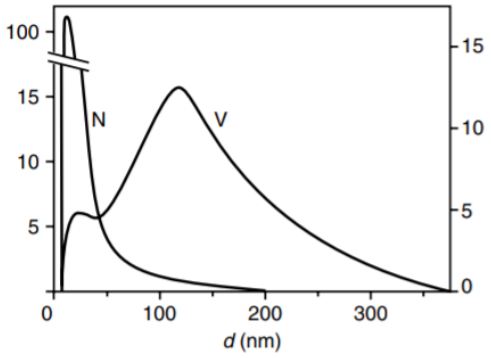

Figure 9: Estimate of the average size frequency distribution of casein micelles. Number (N, left-hand ordinate) and volume frequency (V, right- hand ordinate), both in percentage of the total per 20-nm clase width, against micelle diameter (d) (reproduced from Walstra et al, 2005 with permission from the publisher).

Solution A

Casein micelles, fat globules and fat/protein aggregates are milk components that will scatter light. The most relevant variable to evaluate when measuring homogenization efficiency, is the size of single fat globules. As the droplet size of fat globules determines the creaming rate, this is of importance when estimating the shelf life. Casein micelles are attached together by small regions of calcium phosphate (CCP – colloidal calcium phosphate), which can be removed by acidification or addition of EDTA or citrates, leading to disintegration of the micelles (Bylund, 2015). In this research, in order to dissociate casein micelles and potential fat globule aggregates a reactant solution should be mixed with the milk sample (Ransmark et al., 2019). It is important that reactant solution contains substances not only to dissociate casein micelles but also an emulsifier that prevents fat droplets from aggregating. EDTA can be used as a casein dissociating substance and SDS or Tween have been reported as emulsifiers to prevent fat droplets from aggregating (Qi, 2007; Haugaard & Pettinati, 1959; Michalski et al., 2001). When using LD technique, knowledge of refractive index and absorption coefficient of milk fat is highly relevant since Mie Theory uses them to calculate the PSD, assuming a volume equivalent sphere model, this is well described by Michalski et al. (2001), who found that the refractive index did not change during homogenization process of the milk or by washing the fat globules to remove attached casein micelles.

3.2 Laser Diffractometry

The LD technique can be used for the determination of PSDs. The technique is based upon the phenomenon that the angular distribution of the intensity of scattered light by a particle (scattering pattern) is dependent on the particle size. When the scattering is from a cloud or ensemble of particles, the intensity of scattering for any given class is related to the number of particles and their optical properties present in that size (Hulst, 1981).

A test sample, dispersed at an adequate concentration in a suitable liquid or gas, is passed through the beam of a monochromatic light source, usually a laser. The light scattered by the particles at various angles is measured by an array of photo detectors. The numerical values form each detector are recorded for subsequent analysis. Within certain limits, such as of particle concentration in measuring zone, the scattering pattern of an ensemble of particles is identical to the sum of the individual scattering pattern of all particles. The theoretical scattering patterns of unit volume of particles in selected size classes are used to build a matrix. Together with a mathematical procedure these are used to solve the inverse problem, providing a volumetric PSD, iterated to provide a best fit to the measure scattering pattern (Heuer & Leschonski, 1985).

Four types of interaction between the incident light and the particle influence LD measurement (Born & Wolf, 1999):

- diffraction at the contour of the particle;
- reflection at the boundary of the particle, both outside and inside the particle;
- refraction at the boundary of a particle coming from medium to particle and vice versa;
- absorption within the particle.

These interactions lead to interference phenomena, which cause a characteristic pattern of scattered light. Both scattering pattern and extinction are dependent on the size, shape and optical properties (refractive index) of the particle. Thus, they form the basis for particle size analysis by lases diffraction.

The characteristic scattering patterns form the basis for application of the LD technique for measurement of particle size. In LD, a PSD is formed for an ensemble of particles passing through a measurement zone. Thus, the light scattered by a single spherical particle shall be extended to an ensemble of particles. This is possible provided that (ISO, 2020):

- each particle scatters as an independent entity, i.e. there is no significant multi scattering, which means that particle concentration should be low;
- there is no optical interference between the scattered radiations from different particles, this is satisfied if all particles move randomly with respect to each other and if the overall scattering pattern is sampled many times.

Optical Parameters

When using Mie formula, which will be further explained below, the optical properties of the dispersant are usually relatively easy to find from published data, and many modern instruments will have integrated databases that include common dispersant. Mie theory to explains that for a correct analysis result, the use of optical parameters is necessary if the particle size is smaller than six times the wavelength applied for analysis (Keck & Müller, 2008). The FDS stablished ISO guidelines in 1999, which suggest that optical parameters should be applied in order to obtain a correct analysis of submicron particles. Römpp and Rawle found in their studies that optical parameter are compound specific and they are not known for most of the solid pharmaceutical compounds and/or hard to access. (Römpp, 1995; Rawle, 2006).

The optical parameters are expressed in two terms – the real refractive index $\underline{n}_p$, which is mostly referred to as the refractive index (RI) and the imaginary refractive index ik_p (IRI), this index can be referred to as well as absorption index. The absorption can be described by how much laser light is absorbed by the sample during an experiment. A higher absorption index indicates less light passing through the sample, resulting in less light being diffracted. While a lower absorption index means more light passing through the sample and being diffracted. In general, absorption index is often established empirically or by experience and has typical values between 0.001 to 0.1 (ISO, 2020). Both indices are compound specific and change with changes in temperature and wavelength. The RI symbolizes the ratio of the light velocity v in the medium itself (i.e. in the particle) (Keck & Müller, 2008).

The RI gives information, where the light intensity which did not arrive due to diffraction but from refraction can be expected on the ring detector of the instrument. The same applies for the IRI, depending on the value that is introduced by the user, the software calculates how much light was absorbed by the particles of the sample. Therefore, using Mie theory for LD analysis requires the input of both the real refractive index and the imaginary index (Keck & Müller, 2008).

Milk fat has been thoroughly studied as well as its refractive index and absorption coefficient and the use in PSD measurements is well described by Michalski et al. (2001), who found that neither homogenization of the milk or by washing the fat globules to remove attached casein micelles have any impact in the refractive index of milk fat (Ransmark et al., 2019).

Extinction

For particles that are very large compared with the illuminating wavelength, the quantity of light extinguished from the incident beam is equal to twice the quantity of light that is incident on the geometrical cross-section of the particle. This is the case when the extinction is measured at a significant distance from the particle, in the so-called “far field” (ISO, 2020).

In general, the quantity of light extinguished by a particle in a beam of light depends upon:

- particle size and shape (scattering cross-section);
- refractive index relative to the medium in which the particle is embedded;
- wavelength of the illuminating source.

The refractive index value of particles ($\underline{n_p}$) is a complex number calculated by $\underline{n_p} = n_p - ik_p$ with a real term n_p, and an imaginary term, ik_p. The real part can be established by direct measurement using one of several techniques. The determination of the imaginary part is more often empirically arrived at. The absorption index, k_p, can be defined as a reduction of intensity of a light beam not due to scattering.

Scattering

The quantity of scattered light emanates at refractive index boundaries or gradients. Therefore, the relative refractive index, m_{rel}, of particle and dispersion medium is decisive in determining the quantity of light scattering that occurs.

In LD, the understanding of how light is scattered by particles is decisive for the determination of particle size and quantity. There are several factors that influence how the light is scattered by the particles:

- angular dependence;
- amplitude dependence;
- wavelength dependence;
- polarization influence.

The property of the sphere is utilized as being a shape that can be fully characterized by a single value, namely its diameter. Present LD instruments report their size distributions based upon scattering patterns deduced for spheres.

The principle of LD is the detection of the created diffraction pattern derived from an illuminated particle (Horiba-Instruments, 2004). LD measures the intensities and the distance of the rings in the diffraction pattern, which are created upon illumination of a particle, large particles scatter light at small angles relative to the laser beam and small particles scatter light at large angles, as illustrated below. A basic set-up of laser diffractometer consists of a light source (laser) to illuminate the particles, an optical system to widen the light beam, the sample cell, a Fourier lens to collect the diffracted light and a ring detector system to detect the created pattern. Finally, the angular scattering intensity data is then analyzed to calculate the size of the particles responsible for creating the scattering pattern, using the Mie theory of light scattering. This information is used to calculate the particle size via the software and the particle size is reported as a volume equivalent sphere diameter (Figure 10) (Müller & Schumann, 1996). For analysis, the particles need to be dispersed as a dispersion medium can be either a transparent liquid (e.g. water, alcohol, etc.) or a gas medium (e.g. air).

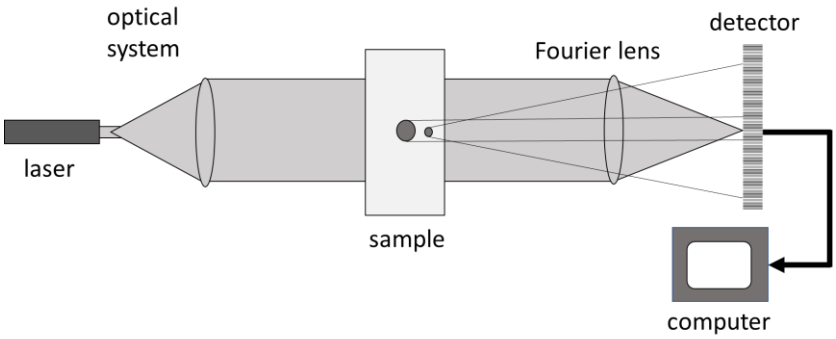

Figure 10: Basis setup of a laser diffractometer (reproduced from Müller & Schumann with permission from the publisher).

In the case that light strikes a particle, it is not only a diffraction pattern, which is created, but a more complex patter which spreads light in every direction (Stratton, 1941). All phenomena together are named scattering. The shape of a scattering pattern depends on the size of the particle. The shape of the scattering will not only change due to a change in the particle size with a constant wavelength, but it will also change if the particle size remains constant and the wavelength of the incident beams is changed. There are three major shapes of scattering patters depending on the radio of particle size to wavelength, these are (Keck & Müller, 2008):

1. Fraunhofer scattering
2. Mie scattering and
3. Rayleigh scattering

Fraunhofer scattering pattern occurs when a particle is much larger than the incident wavelength and Rayleigh scattering occurs with particles sized much smaller (i.e. 10x) that the incident wavelength. All particles in the intermediate region show Mie scattering (Stratton, 1941). In Figure 11 the shape of the three different scattering shapes explained above are shown.

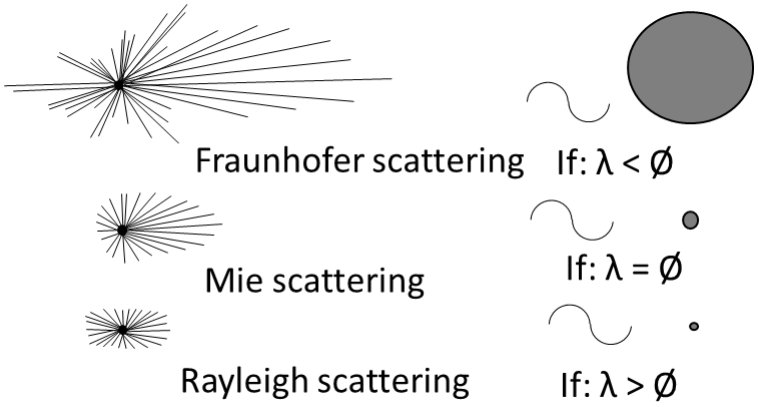

Figure 11: Envelops of scattering as function of ratio particle size to wavelength, where λ = wavelength, (reproduced from Keck & Müller with permission from the publisher).

Fraunhofer scattering is characterized by a strong forward scattering and a relatively weak backward scattering. With Mie scattering the ratio of forward scattered light to backward scattered light is much smaller, when compared to Fraunhofer. With Rayleigh scattering the intensity of forward scattered light is about the same as the backward scattered light intensity (Keck & Müller, 2008). All these phenomena need to be considered for a correct LD analysis result.

The interpretation of LD “spectra” to PSDs depends on two major operations. The first requires that mathematical models be created on how homogeneous particles scatter light. The second involves the de-convolution of the measured scattering pattern into a PSD (ISO, 2020).

Light is an electromagnetic wave with the electric and magnetic vectors at 90 degrees to each other. The influence of these two vectors are expressed in the terms $S_1(\theta)$ *and* $S_2(\theta)$.

The angular intensity distribution of polarized light scattered by a single, optically homogeneous spherical particle, *I(w)* can be written as

$$I(\theta) = \frac{I_0}{2k^2 l_a^2}\{[S_1(\theta)]^2 + [S_2(\theta)]^2\} \quad (3)$$

Where *k* is the wave number in the medium, l_a is the distance from scattering object to detector, I_0 is the intensity of the incident polarized light, $S_1(\theta)$ and $S_2(\theta)$ are dimensionless, complex functions defined in general scattering theory, describing the change of amplitude in the perpendicular and the parallel to the scattering plane respectively, as a function of angle θ with respect to the forward direction.

Mie theory

In 1908, Gustav Mie described the light-scattering properties of homogeneous spheres of know optical properties, when illuminated by an infinite plane wave of known wavelength, by solving Maxwell´s equations for defined boundary conditions. In this way, he solved the complex functions $S_1(\theta)$ *and* $S_2(\theta)$ (ISO, 2020).

Mie theory provides a rigorous solution that is valid for all sizes of spheres (Hulst, 1981). When using this theory, it is assumed that:

- all particles are optically homogeneous and spherical (although some special or regular shapes can be considered as well, i.e. coated spheres);
- the particle is illuminated by a plane wave of know wavelength;
- the refractive index of the particle, both real and imaginary, and that of the medium it is dispersed in are known;
- the particles have no surface charges and no surface currents.

Mie formula describes all phenomena, which occur if light hits a spherical particle (Mie, 1908). A simplified version of the Mie formula is shown in Equation (3).

$$I(w) = E\{k^2 A^4 [J1]^2 W^{-1} + [K_1 W]^1 + [K_2 W]^3 + [K_3 W]^5 + k^4 A^6 (m-1)^2 W^6 / 8\pi^2\} \quad (4)$$

Fraunhofer Term — RayleighTerm

In the equation I is the intensity of scattered light, E is the flux per unit area of incident light, k, K are constants, A is the particle radius, J1 is the first order Besser function of first kind, W is the angle of scatter and m is the complex refractive index. From this formula three influencing parameters remain. They are the:

1. Particle radius (A), which is the parameter of interest and to be measured.
2. Angle of scatter (W) which is measured on the detector and the
3. Optical parameters (m) = imaginary and real refractive index (expressed as complex refractive index).

In summary by using the Mie formula, the particle radius can be determined if the angle of scatter and the optical parameters are known. From this it is important to consider that if the optical parameters are not known, not correct results can be expected from theory (Keck & Müller, 2008). It should be noted that this knowledge may not be readily available: especially

the imaginary (absorptive) part. This part is often strongly dependent on the wavelength of the light and is often given a finite value in order to account for specific surface structure of the particles.

$S_1(\theta)$ and $S_2(\theta)$ are given as (equation 5 and 6),

$$S_1(\theta) = \sum_{n=1}^{\infty} \frac{2n+1}{n(n+1)} [a_n \pi_n(cos\ \theta) + b_n \tau_n(cos\ \theta)] \qquad (5)$$

$$S_2(\theta) = \sum_{n=1}^{\infty} \frac{2n+1}{n(n+1)} [a_n \tau_n(cos\ \theta) + b_n \pi_n(cos\ \theta)] \qquad (6)$$

The complex formulae (3) and (4) have been encoded into open source software available by a search of the “World Wide Web” and yields Mie calculation facilities (ISO, 2020).

Laser diffraction particle sizing problem is to measure the composite forward angular scattering distribution from a particle field and perform a mathematical inversion to obtain an estimate of the size distribution. (Hirleman, 1988).

Sample concentration

The scattered light intensity from many particles rises in proportion with the number of particles that have that size. In the low concentration region this process is linear. However, at some point the concentration is such that a significant amount of the light scattered by individual particles is further scattered by neighboring particles. The point at which this multi scattering changes the size distribution in a significant way mark the maximum allowable particulate concentration for accurate size distribution determination (Hulst, 1981).

Hulst (1981) also proposes that the onset of multiple scattering commences if particles are regularly respirated from their neighbors by 3 times their diameter. As the number of particles increases proportional to D^{-3} for the same volume concentration the smallest particles have the highest number per unit volume. It therefore follows that the smallest sizes in any distribution determine the onset of multiple scattering due to their possible proximity.

LD instruments are often provided with a measure of the attenuation of the incident laser beam due to the presence of particles within the measurement zone. This is referred to as either an obscuration or a transmission detector. Such detectors almost subtend 0° of scattering and, thus, may be regarded as a measured value of extinction.

The effect of multiple scattering is generally to increase the angle of scattering and, thus, to shift the size distribution results to lower sizes (ISO, 2020).

4. Materials and Method

4.1 Materials

Two different techniques were used to measure the particle size of the samples, LD and DLS. An older and newer version of the LD technique were used, the Mastersizer 2000 and Mastersizer 3000, both Malvern Instruments equipment. The setup of the Mastersizer 2000 can be seen in Figure 12. As can be seen, a small volume (SV) dispersing unit is used. Stirring speed is adjusted manually. A significant difference between the Mastersizer 2000 and 3000 is the dispersing unit, as the Mastersizer 3000 uses a large volume (LV) dispersing unit while the Mastersizer 2000 uses a small unit, shown in Figure 13. The speed of the dispersing unit of the Mastersizer 3000 is adjusted within the software. As for the DLS, a Malvern Zetasizer Nano ZS instrument was used (Figure 14).

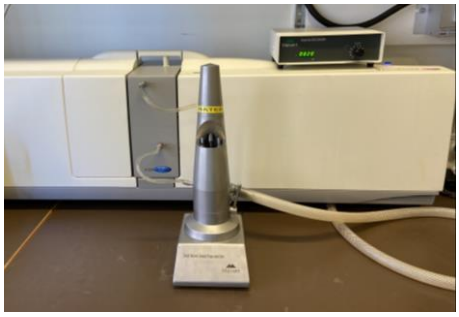

Figure 12: Set up of the Mastersizer 2000.

Figure 13: Set up of the Mastersizer 3000.

Figure 14: Malvern Zetasizer Nano ZS.

The model emulsion was made by pre-emulsifying the emulsion using an Ultra Turrax (Figure 15), followed by homogenization using Panda Plus GEA Niro Soavi equipment (Figure 16), the oil droplet size was aimed to be as closest as possible to pasteurized milk (~1 µm), the PSD was decreased by fractionation using centrifuging. This was done by using the Allegra X-15R (Figure 17).

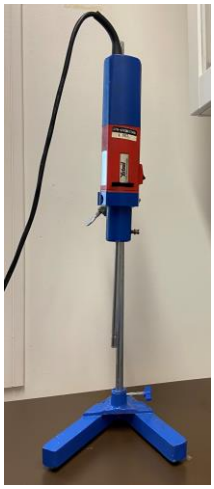

Figure 15: Ultra Turrax.

Figure 16: Set up of the Homogenizer.

Figure 17: Allegra X-15R centrifuge.

4.2 Methods

4.2.1 Sample preparation

4.2.1.1 Preparation of milk samples

At the start of the study, commercial samples of pasteurized milk were analyzed. Three variables were tested on the Mastersizer 2000. These variables were the sample concentration (i.e. obscuration rate), pre-treatment and stirring speed. Each of these variables were tested at different settings. Obscuration rate was tested at 0.5, 2, 5, 10 and 20%. Pre-treatment is tested at 0, 20, 33 and 50% v/v solution A of the total volume, this corresponds to the addition of 0, 1, 2 and 4 mL respectively. Stirring speed was varied at 380, 800, 1800 and 2500 rpm. This can be seen schematically in Table 2.

Table 2: Settings used to measure samples

Variable	Setting
Obscuration rate (sample concentration)	0.5%
	2%
	5%
	10%
	20%
Pre-treatment (solution A)	0%
	20%
	33%
	50%
Stirring speed	380 rpm
	800 rpm
	1800 rpm
	2500 rpm

These variables were tested using the Tetra Pak method as a standard and reference. The Tetra Pak method uses an obscuration rate of 2%, 2 mL of solution A (33% v/v) and a stirring speed of 800 rpm (Tetra Pak, 2019). As an example, when stirring speed was tested at 2500 rpm, obscuration rate was kept at 2% and solution A at 2 ml, following the Tetra Pak procedure.

The main focus of the experiments was on pasteurized milk, but some experiments were repeated for Extended Shelf Life (ESL) milk and non-homogenized milk as well. Where ESL milk was commercially bought and non-homogenized milk was made by combining skim milk (0.2% fat) with non-homogenized cream (40% fat) to a final fat content of 3%, stirring with a spoon.

Preparation of solution A

As described above, solution A is added in order to disintegrate the micelles and avoid aggregate of fat droplets. Solution A consists of EDTA, which can be used as a casein dissociating substance and Tween, which prevents the fat droplets from aggregating. Solution A is made by adding 400 mL of deionized water into a Duran bottle and weighing 6.25g of Tween 20 and 18.75g EDTA into the bottle. This is heated while stirring to 40 °C. After this, a 0.1 M NaOH ampoule is emptied into a beaker and added to the mixture while stirring with the magnetic stirrer, measuring the pH continuously until the pH is 10.

4.2.1.2 Preparation for model emulsion

The model emulsion was made by adding 3 wt% sunflower oil, 0.018 wt% Tween 80 and 96.98 wt% water in a beaker, then the blend is mixed by using an Ultra Turrax at 2500 rpm. A 1.2% stock solution of Tween 80 was prepared beforehand by adding 12 g of Tween 80 to a 1 L volumetric flask, which was let stand overnight to ensure the dissolution of Tween and avoid extra foaming. The amount of emulsifier that is needed to be used depends both on the fraction of oil in the solution (3 wt%) and the size of the droplets suspended in it (1 µm). A critical micelle concentration, C_{CMC}, was defined to 14.73 g/m^3. The lowest emulsifier concentration required was then calculated, $V_{emulsifier}$ = 0.008 L, see the derivation in Appendix A. Once the blend is premixed, the blend is homogenized twice in a Panda Plus GEA Niro Soavi equipment using a homogenization pressure of 750 bar. Lower pressures were tested (250, 350 and 400 bar), but a pressure of 750 bar resulted in a narrow PSD with a large population of particles with sizes of ~1 µm, which is close to the characteristic PSD of oil droplets in milk as can be seen in Figure 18. The pressure ratio used was stage 2 / stage 1 = 0.2. After homogenization, the equipment was cleaned with 3% NaOH and 0.5% HNO_3 respectively.

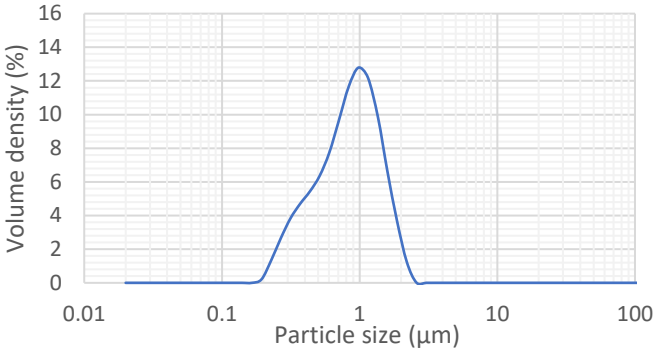

Figure 18: PSD of the average of the model emulsion measured on Mastersizer 2000 at a pressure of 750 bar, homogenized twice.

Fractionation

The model emulsion was fractionated to decrease the PSD, as the oil droplet size was aimed to be as closest as possible to pasteurized milk (~1 µm). For centrifuging, centrifuge tubes of 50 mL filled until 45 mL were used. These samples were centrifuging for 3 minutes at 5000 G using the manual settings of the equipment. The centrifuging time was calculated using Stokes's Law (equation 2), aiming for a particle size of 2 µm in the bottom fraction. The top layer was extracted using a plastic Pasteur pipette before 20 mL of sample was taken from the remaining bottom fraction into a new tube using a micropipette. This sample was then manually homogenized by turning the tube up and down three times. The new sample was then measured on the Mastersizer 2000 and 3000. The stability of both, the unfractionated and fractionated emulsion, were measured on the Mastersizer 2000 by measuring directly after the emulsion was made and after four days, the stability of the emulsion can be seen in Figure 19.

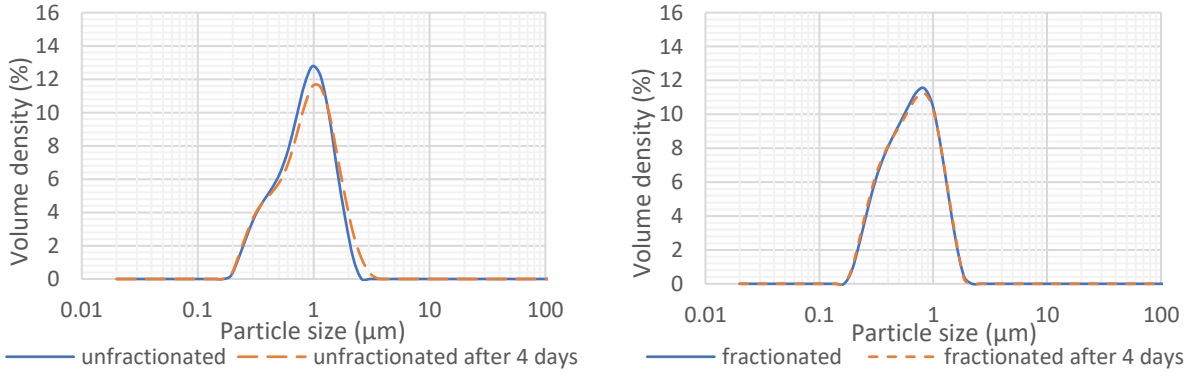

Figure 19: PSD of the averages of the model emulsion measured on Mastersizer 2000, figure on the left shows the unfractionated model emulsion, figure on the right shows the fractionated model emulsion.

4.2.2 Techniques used

Below LD and DLS will be discussed.

4.2.2.1 Laser diffractometry

Sampling

In order to understand when the unexpected peaks would appear, a system was set up on how many samples were taken of each variable. A schematic figure of this system can be seen in Figure 20.

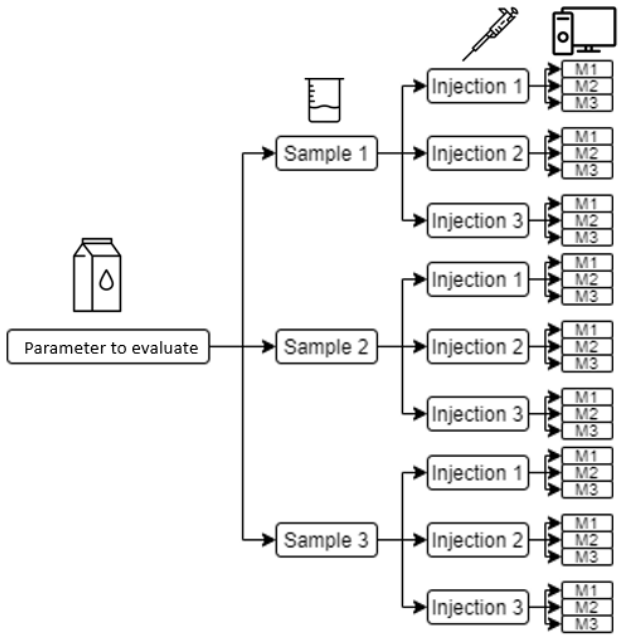

Figure 20: A schematic figure of the sampling method used in order to evaluate each variable and its settings.

To start, three samples of milk were taken from a milk carton, gently shaking the bottle three times in between the samples to ensure a difference of the sampling spot. This is indicated by sample 1, 2 and 3 in the figure. Before analysis, milk samples were diluted according to the Tetra Pak procedure, adding 2 mL of milk, 2 mL of distilled water and 2 mL of solution A (or different amounts when varying the concentration of solution A) to create a sample of 6 mL (or less when using less solution A). This was repeated three times in three glass beakers to create a total of three different samples for each variation. Out of each of these three glass beakers, three samples were taken to inject in the Mastersizer, which can be seen under 'injection' in Figure 20. These injections were measured three times by the Mastersizer software (last column in Figure 20). This brings the total number of measurements to 27 per variable setting (e.g. 0.5% obscuration). For the model emulsion, each sample is injected 3 times and measured three times by the software, creating a total of 9 measurements.

Settings of the Mastersizer

Settings used to measure the samples include a refractive index (RI) of 1.460 and an absorption index of 0.001 for red light and a RI of 1.470 and absorption index of 0.001 for blue light (Tetra Pak, 2019). The refractive index of water for the red laser was set to 1.33. The background measurement was set to 10.00 seconds for both red and blue light, this parameter was set to 30.00 seconds for all model emulsion measurements. The first trial of experiments was executed on the Mastersizer 2000, as this is the equipment available for most of the parties participating in this study, but further experiments were also repeated on the Mastersizer 3000. Similar settings were used on the Mastersizer 3000. The Mastersizer 3000 contains a function were data with bad quality can be identified. Data with bad quality were disregarded from the average for samples of the model emulsion.

4.2.2.2 Dynamic Light Scattering

DLS PSD measurements were conducted with a Malvern Zetasizer Nano ZS, the refractive index for milk fat was set to 1.46. In order to get reproducible results, different concentrations (50%, 10%, 5%, 2%, 1%, 0.5%, 0.2%, 0.1%, 0.01%) of the unfractionated model emulsion were measured on the DLS to find the concentration that provides the most reproducible data. Based on the results, similar concentrations of the fractionated model emulsion (10%, 1%, 0.5%, 0.2%, 0.1%) were studied. These samples were transferred to 1 mm–light path cuvettes using a micropipette, covered with a plastic lid and placed in the equipment for measuring.

5. Results and Discussion

In this chapter the two types of peaks and the reason of their occurrence will be discussed. The right sided unexpected peaks will be discussed in section 5.1, while the left sided unexpected peaks will be discussed in section 5.2. A model emulsion was also made in order to further investigate the left sided unexpected peaks, which will be discussed in section 5.2 as well. DLS was used as a complementary technique to confirm presence of low particle size class, discussed in section 5.2. Best practices will be discussed in Chapter 7.

5.1 Right sided unexpected peaks

The first type of unexpected peak appears on the right side of the main distribution and can mostly be found on the Mastersizer 2000, sometimes occurring on the Mastersizer 3000. These peaks seemed to appear randomly, thus it was of importance to find the conditions in which the occurrence of this type of peak is more probable.

5.1.1 Variables without an effect on right sided unexpected peaks

Below, variable Solution A is studied to see whether it caused a right sided unexpected peak, however it did not. Changing the optical parameter on the Mastersizer 2000 also showed no impact on the right sided unexpected peak, as can be seen in Appendix B. However, as the optical parameters were varied at exceptionally high values, no conclusions can be drawn from these results.

Effect of Solution A

In order to test the hypothesis '*If the concentration of solution A is reduced, then it will affect the PSD by showing an increased number of small particles (i.e. casein micelles)*', the amount of solution A was varied at concentrations of 0, 20, 33 and 50% v/v, keeping the amount of milk and water constant at 2 mL each. Figure 21 below shows four randomly selected curves for each of the concentrations tested.

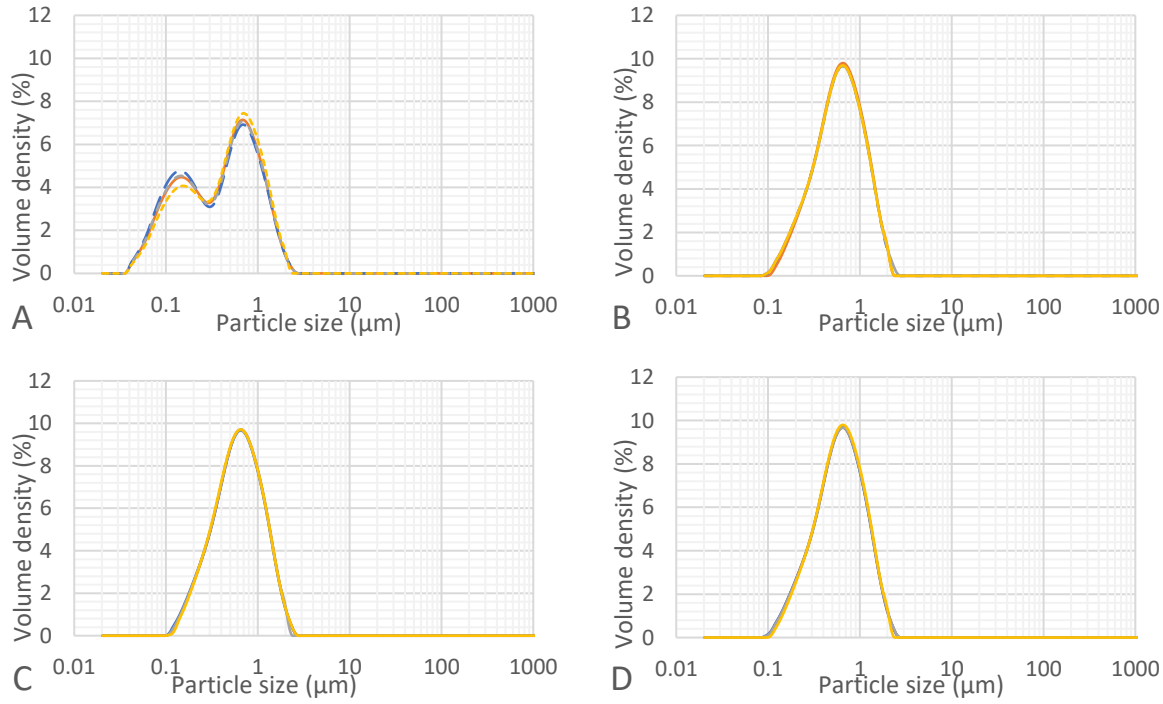

Figure 21: PSD of pasteurized milk measured on the Mastersizer 2000 at different concentrations of solution A of 0% (A), 20% (B), 33% (C) and 50% (D) where four curves were randomly selected for each setting.

As can be observed above, only a concentration of 0% solution A seems to have an impact on the volume distribution. Comparing the curves more closely in Figure 22, there is no impact of the concentration of solution A on the characteristics of the curve when at least 20% of solution A is added. With the absence of solution A, the casein micelles remains stable and can therefore be seen, giving rise to the peak at ~100 nm, as discussed in section '3.1 Milk'. This effect can also be seen in Figure 23, where the Dv90 of each concentration is given. By using solution A, casein micelles are dissociated into such small entities that are no longer possible to observe with LD. This creates a focus on the fat globules when measuring the particle size, which is desired. Therefore, the use of solution A is highly recommended when analyzing the fat globules in milk.

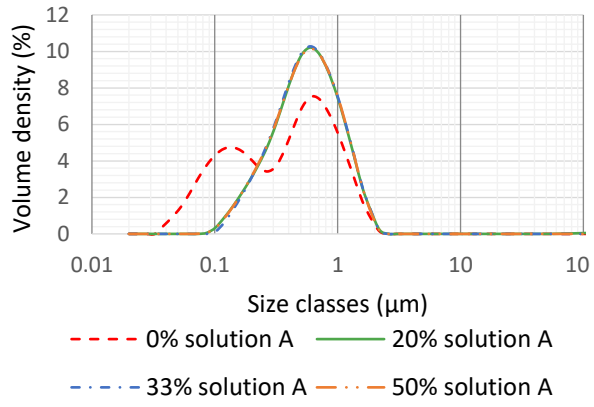

Figure 22: Characteristic PSD curve of different concentrations of solution A in pasteurized milk measured on the Mastersizer 2000 disregarding curves with an unexpected peak.

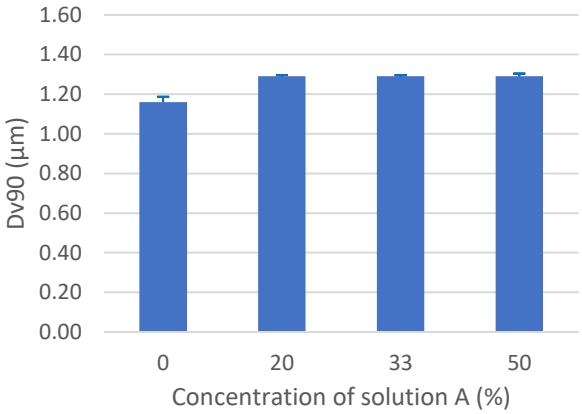

Figure 23: Average particle size Dv90 of different concentrations of solution A in pasteurized milk measured on the Mastersizer 2000 with standard deviations.

When studying the occurrence of right sided unexpected peaks, very few distributions showed an unexpected peak. It can be seen in Figure 24 that there is no significant difference between the amount of right sided unexpected peaks at concentrations of 0, 20, 33 or 50% v/v solution A, as the confidence interval of these concentrations overlaps with the interval of 33% v/v solution A, which is considered the standard. This indicates that the concentration of solution A added to the sample does not have an influence of the occurrence of unexpected peaks. Similar results were obtained for ESL and non-homogenized milk as can be seen in Appendix C.

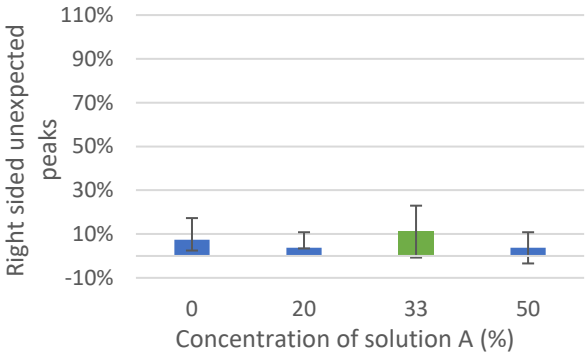

Figure 24: Percentage of right sided unexpected peaks in pasteurized milk measured on the Mastersizer 2000 at different concentrations of solution A using confidence intervals. The standard method of Tetra Pak is marked in green, while other variations are blue.

As discussed above, the amount of solution A does not have a significant impact on the number of unexpected peaks in a measurement but the addition of it is important when focusing on the particle size of fat globules. Thus, the hypothesis is rejected, as no small particles are shown in correlation to the addition of Solution A.

5.1.2. Variables with an effect on right sided unexpected peaks

Below, variables and settings examined to see whether they caused a right sided unexpected peak and will be discussed.

Stirring speed in the dispersion unit

To test the hypothesis '*If the stirring speed is increased, then it will affect the PSD by inducing coalescence or incorporating air*' the stirring speed was varied at 320, 800, 1800 and 2500 rpm on the Mastersizer 2000. Four randomly selected curves of each stirring speed can be seen in Figure 25.

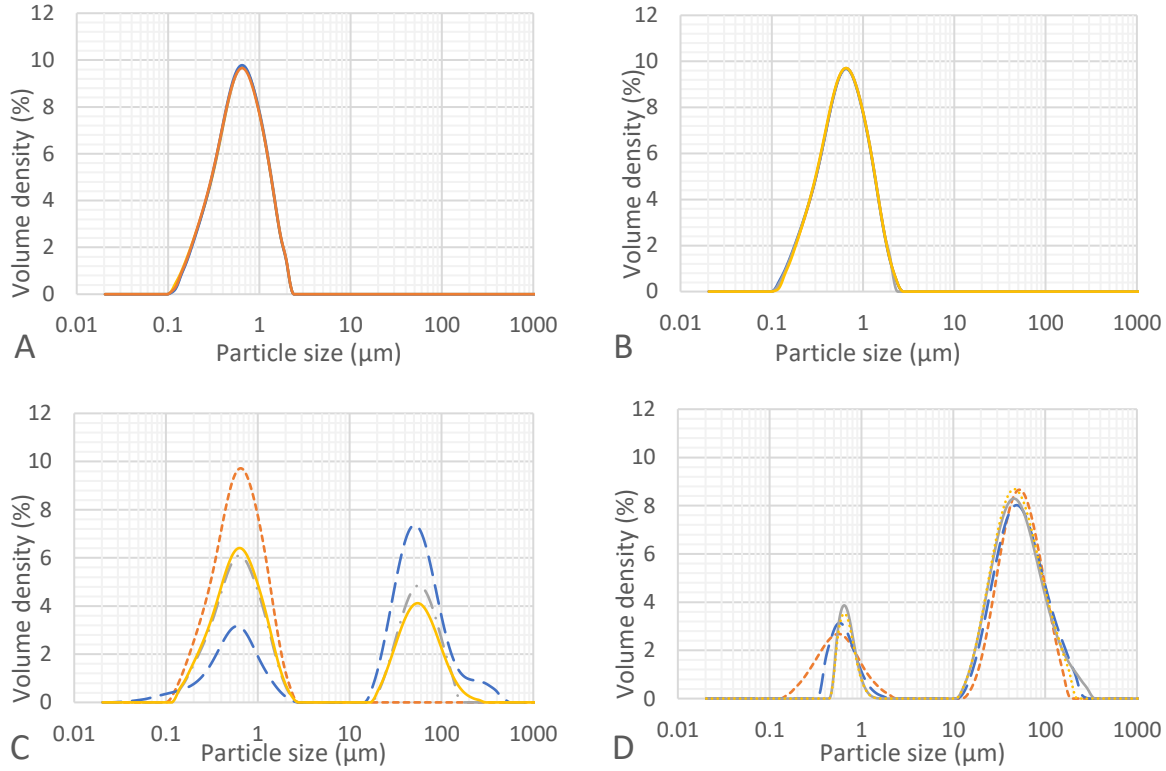

Figure 25: PSD of pasteurized milk measured on the Mastersizer 2000 at different stirring speeds of 320 rpm (A), 800 rpm (B), 1800 rpm (C) and 2500 rpm (D) where 4 out of 27 curves were randomly selected for each setting.

Looking at the results above, the occurrence of right sided unexpected peaks seems to increase at higher stirring speeds of 1800 and 2500 rpm. Since only 4 out of 27 collected curves are shown, the total occurrence of unexpected right sided peaks was further analyzed.

The result of the total number of unexpected peaks occurring when measuring pasteurized milk at different stirring speeds on the Mastersizer 2000 can be seen in Figure 26. Here, an occurrence of 89% unexpected peaks in a stirring rate of 2500 rpm indicates that 24 out of 27 measurements show an unexpected peak on the right side of the main distribution. Interestingly, a correlation can be seen between the increase of the stirring speed and an increase in unexpected peaks. As none of the confidence intervals of the stirring variable seem to overlap with the Tetra Pak method (800 rpm), there is a significant difference at a 5% level between all the different settings tested of this variable. Similar results were obtained using ESL and non-homogenized milk, as can be seen in Appendix C.

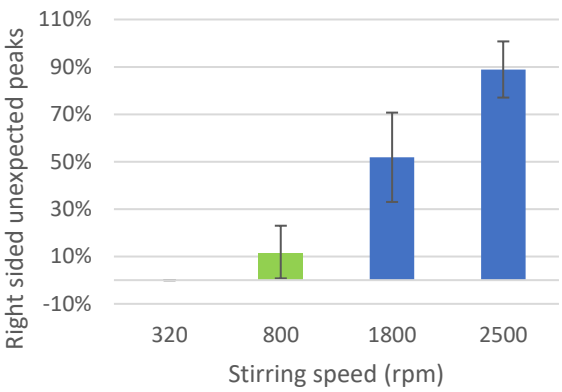

Figure 26: Percentage of unexpected peaks in pasteurized milk measured on the Mastersizer 2000 when changing stirring speed using confidence intervals. The standard method of Tetra Pak is marked in green, while other variations are blue.

This indicates a relation between the stirring speed and number of unexpected peaks on the Mastersizer 2000. When disregarding the curves with an unexpected peak, the stirring speed does not seem to influence the characteristics of the curves as the curve of all stirring speeds seem to overlap (Figure 27). This is confirmed by Figure 28, where the deviation between average particle size (Dv90) of each stirring speed is very little. Indicating that the stirring speed does not influence the particle distribution in curves without these unexpected peaks. Here it should be noted that a stirring speed of 2500 rpm had such a high rate of unexpected peaks curves (which thus had to be disregarded for the average) that the average might not be too reliable.

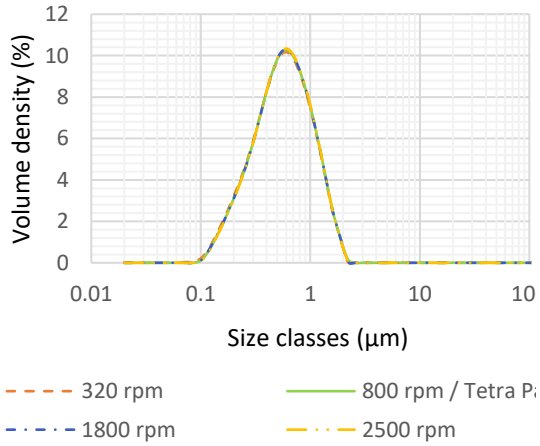

Figure 27: Characteristic PSD curve of changes in the stirring speed in pasteurized milk measured on the Mastersizer 2000 disregarding curves with unexpected peaks.

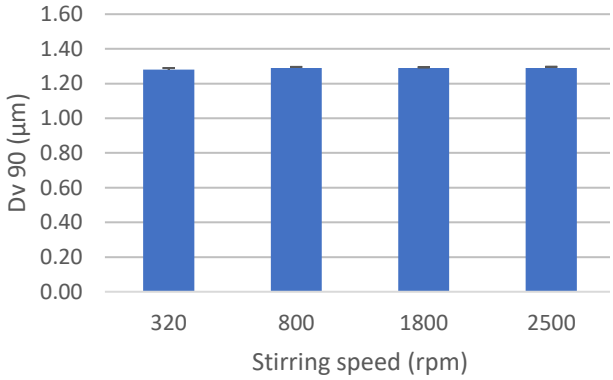

Figure 28: Average particle size Dv90 of different stirring speeds in pasteurized milk measured on the Mastersizer 2000 with standard deviations.

All in all, the stirring speed does not seem to influence the average particle size of pasteurized milk curves disregarding an unexpected right sided peak. However, it does have a significant impact on the appearance of unexpected peaks during different stirring speeds, which indicates that there might be a correlation between the increase in stirring speed and the occurrence of unexpected peaks. An explanation for the increase in unexpected peaks might be because of the increase in air bubbles measured. When the stirring speed is increased, more air might be incorporated in the dispersion unit and thus measured, which could explain the unexpected peaks.

To test this hypothesis, an experiment was conducted by increasing and then decreasing the stirring speed during one measurement (no re-injection of the sample). The results of this can be seen in Figure 29, Figure 29.A shows the measurement when running the dispersion unit at 320 rpm, no unexpected peaks are observed. As can be seen for Figure 29.B, 29.C as stirring speed increases the appearance of unexpected peaks increases until reaching maximum speed (2500 rpm), Figure 29.D. It clearly shows the occurrence of unexpected peaks when the stirring speed is increased. This also creates a high deviation in the volume distribution of the curves. When decreased, some of the unexpected peaks seem to remain in the reservoir, which are then measured at lower stirring speeds (see Figure 29.F and Figure 29.F). However, when lowering the stirring speed back to 320 rpm (Figure 29.G) no unexpected peaks appear anymore and the volume distribution returns to what is believed to be a normal distribution. When repeating the experiments, similar consistent results are obtained. This suggest that the unexpected peaks shown when measuring on the Mastersizer 2000 are most likely air.

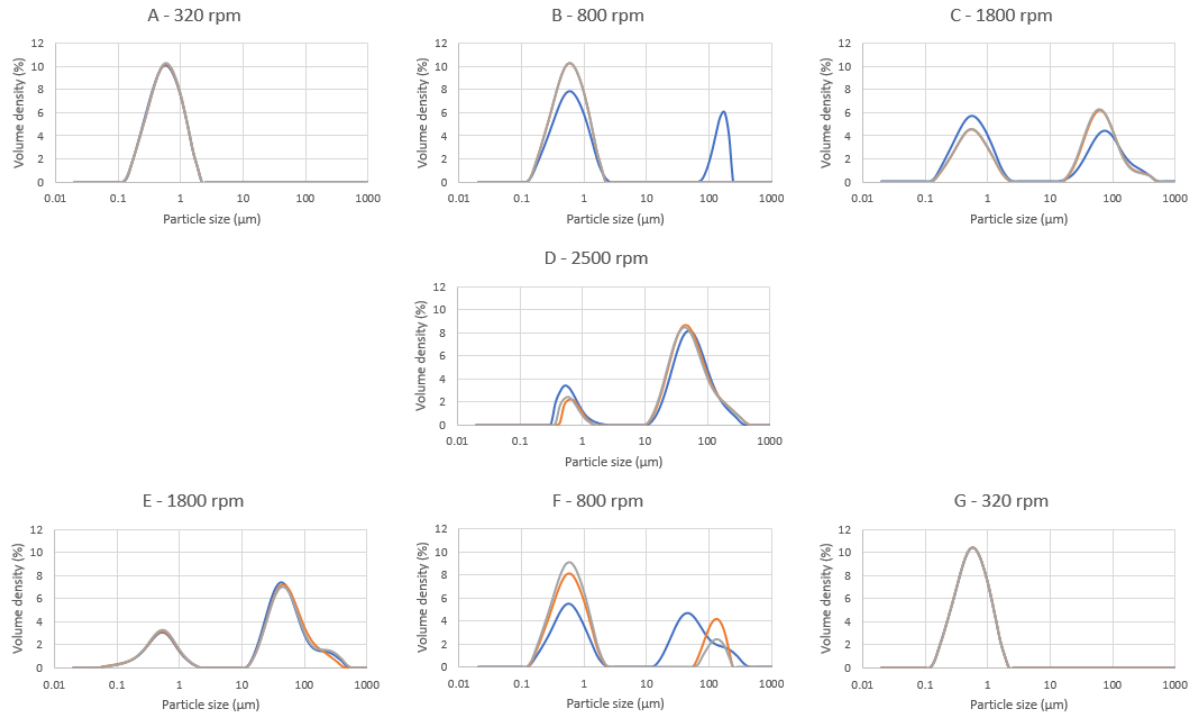

Figure 29: PSD curves of increasing and decreasing the stirring speed of a sample of pasteurized milk measured on the Mastersizer 2000.

This hypothesis is further supported when conducting the same experiment on the Mastersizer 3000. As can be seen in Figure 30, no unexpected peaks appear during the measurements at all except for some small peaks that are believed to be caused by dirt as will be discussed later. Only at a stirring speed of 2500 rpm the distribution becomes narrower. This is believed to be caused by the relation between the stirring speed and the pump speed. As at particularly high stirring rates, the sample will pass through the lasers very quickly, causing abnormalities in the distribution. The experiment was repeated two more times which showed similar results.

This suggests that the appearance of unexpected peaks on the right side of the curve might be correlated to measurements done on the Mastersizer 2000. The reasoning of this is due to the design of the dispersion unit of the Mastersizer 2000, which design allows the equipment tends to incorporate air more easily. Compared to this, the Mastersizer 3000 has a different design of the dispersion unit and a larger volume that is less likely to create a vortex that might incorporate air bubbles into the reservoir. In addition to this, an additional deaeration step is

included in the Mastersizer 3000 equipment, which purpose is to decrease the amount of air bubbles in the dispersant unit before measurements.

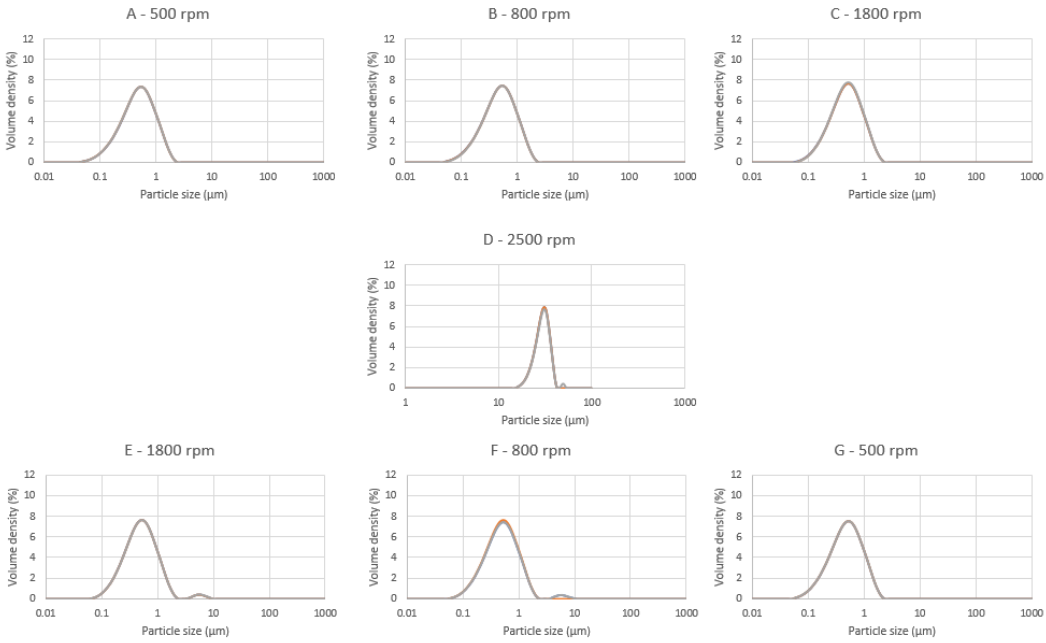

Figure 30: PSD curves of increasing and decreasing the stirring speed of a sample of pasteurized milk measured on the Mastersizer 3000.

Concluding, the hypothesis is partially supported as there was a relation between the number of unexpected peaks and the stirring rate on the Mastersizer 2000 due to the incorporation of air. However, coalescence is not induced by the stirring rate on either equipment, thus this part of the hypothesis can be rejected.

Effect of obscuration rate – Interference of noise

To test the hypothesis '*If the sample concentration is too low, then it will affect the PSD by creating interference between the sample and the background signal'*, the obscuration rate was varied between 0.5, 2, 5, 10 and 20% when measuring pasteurized milk on the Mastersizer 2000. Four randomly selected curves of each of these obscuration rates can be seen in Figure 31.

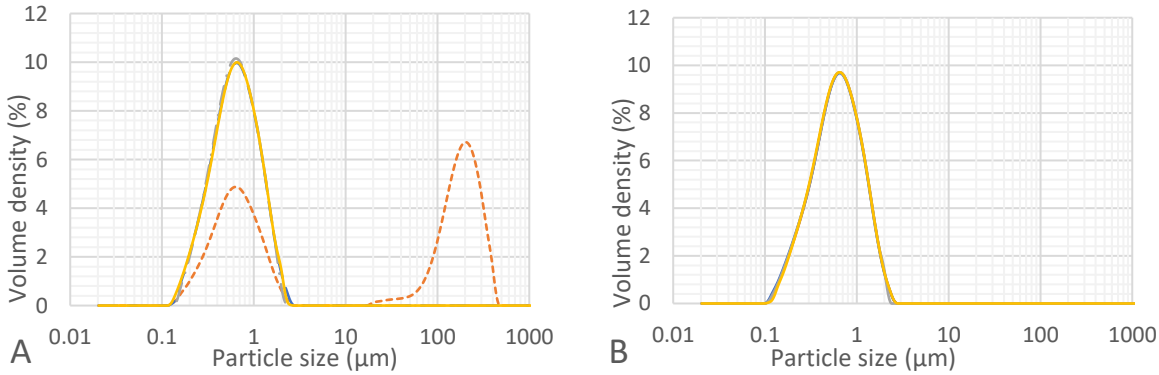

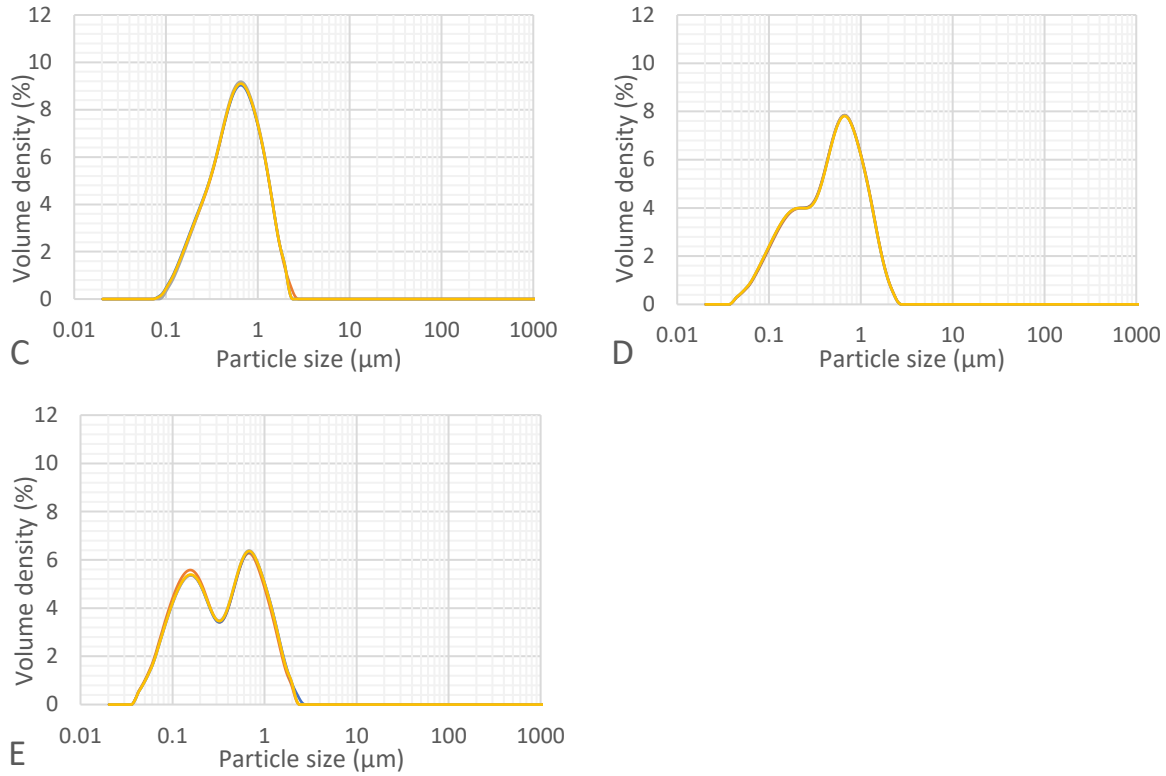

Figure 31: PSD of pasteurized milk measured on the Mastersizer 2000 at different obscuration rates of 0.5% (A), 2% (B), 5% (C), 10% (D) and 20% (E) where four curves were randomly selected for each setting.

What is interesting in this figure is that at an obscuration rate of 0.5% a curve with an unexpected right sided peak can be observed. However, when looking at the occurrence of unexpected peaks in all 27 measurements for each setting in Figure 32, there seems to be no significant difference between number of unexpected peaks and an obscuration rate of 0.5, 2 and 5% as the confidence interval of both 0.5 and 5% overlaps with the interval of 2%. Therefore, the amount of sample added does not appear to influence the number of right sided unexpected peaks. Similar results were obtained testing ESL and non-homogenized milk, as can be seen in Appendix C.

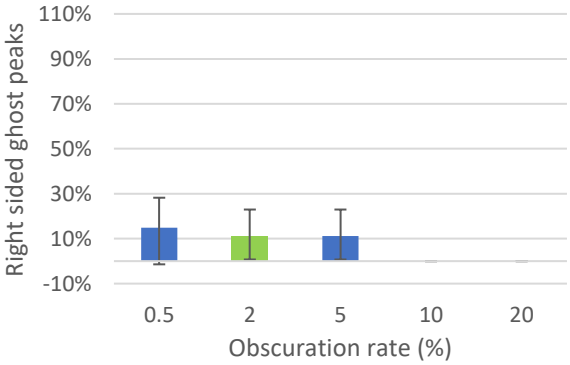

Figure 32: Percentage of unexpected peaks in pasteurized milk measured on the Mastersizer 2000 when changing the obscuration rate using confidence intervals. The standard method of Tetra Pak is marked in green, while other variations are blue.

However, low obscuration rates can cause noise in the background which could be manifested as a high standard deviation and right sided unexpected peaks. To avoid noise in the background, it is suggested by Malvern to avoid too low obscurations as they reduce reproducibility and increase the risk of signal noise in the background during the measurement which could result in unexpected peaks (Malvern Instruments, 2015). Therefore, it is suggested

to keep the obscuration rate above 0.5%. Similar results are obtained on the Mastersizer 3000. Less reproducibility can be seen in Figure 33, where the background seems to interfere with the sample data, showing a higher standard deviation in both the Mastersizer 2000 and Mastersizer 3000 at an obscuration of 0.5%. Another reason for the increase in standard deviation could be explained by the concentration of sample. At low concentrations (i.e. obscuration rates) Malvern suggests increasing the stirring speed to accommodate the low sample concentration and avoid sedimentation in the dispersion unit. As the stirring speed is related to the pump speed, a low obscuration rate in combination with a lower stirring speed can cause a high standard variation as the particle flux passing through the system is not constant. Thus, it can be concluded that using an obscuration rate higher than 0.5% in combination with a stirring rate of 800 rpm should be used to avoid signal noise and multi scattering.

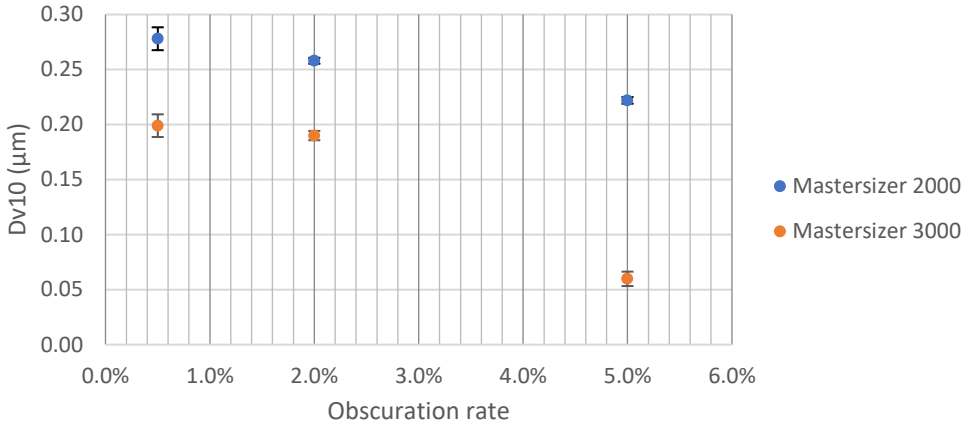

Figure 33: Dv10 for averages of different obscuration rates of pasteurized milk measured on the Mastersizer 2000 and 3000 with standard deviation bars.

All in all, it can be concluded that the hypothesis is true as a low sample concentration (thus obscuration rate) does interfere between the sample and the background and can show unexpected right sided peaks.

Dirt in the Mastersizer

While measuring pasteurized milk and model emulsion on the Mastersizer 2000 and 3000 small unexpected peaks manifested on the right side on the main peak of the PSDs (Figure 34). These unexpected peaks have a particle size around 3.5 and 13 µm. It was believed that there might be a correlation between the obscuration rate and these peaks as they might be caused by noise in the background. However, there seems to be no correlation between obscuration rates and the number of right sided unexpected peaks (R^2 = 0.056). Indicating there should be another explanation. Thus, a hypothesis was formulated stating '*If the background shows disturbances, then it will affect the PSD by showing an unexpected peak*'.

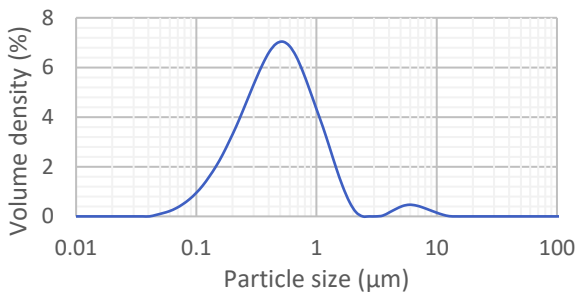

Figure 34: PSD curve of an example of the right sided unexpected peak showing dirt, which can be seen on both the Mastersizer 2000 and 3000.

The inconsistency may be due to dirt in the Mastersizer, as these unexpected peaks had not been seen in previous measurements done at the same settings. Dirt in the Mastersizer can

be seen when looking at the slope of the background. A clean background shows a continuous decreasing, ski slope resembling, curve where detector 1 is under 100 and detector 20 under 20 (Malvern Panalytical, 2017; M. Larsson, personal communication, March 4, 2020). However, when the background gives rise to a peak in the background measurement, unexpected peaks at ~7 µm in the PSD can be interpreted as the dirt. Figure 35 illustrates this, as the background measurement on March 11th (blue long dash line) shows a drastically higher peak around detector number 27 than the measurement on February 27th (orange solid line). Though the detector numbers seem to indicate a clean background, the large peak is alarming. Thus, cleaning of the Mastersizer 3000 was performed and the background returned to a ski slope outline on April 24th (yellow dotted line). Therefore, it is believed the difference is an effect of the cleanliness of the Mastersizer 2000 and 3000.

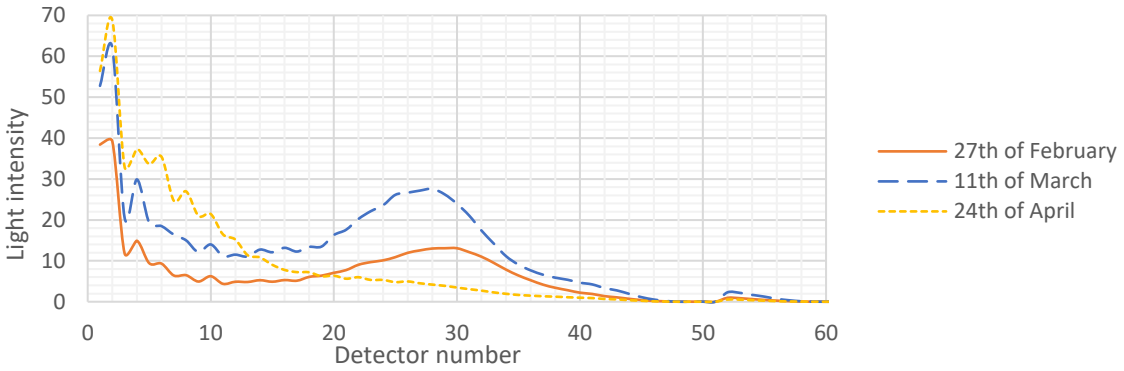

Figure 35: Background measurement of the Mastersizer 3000 on different dates.

Thus, it can be concluded that the cleanliness of the Mastersizer, which shows disturbances in the background when unclean, is of influence on the appearance of right sided unexpected peaks as dirt peaks appear.

5.2 Left sided unexpected peaks

When measuring on the Mastersizer 2000 and 3000, left sided unexpected peaks appeared when varying certain variables. In this section, the reasonings of these peaks will be discussed and the difference between the two models of the Mastersizer will be reviewed.

5.2.1 Effect of obscuration rate

Pasteurized milk on the Mastersizer 2000

To test the hypothesis *'If the sample concentration is too high, then it will affect the PSD by showing multi scattering*', the obscuration rate was varied from 0.5, 2, 5, 10, 20% when measuring pasteurized milk on the Mastersizer 2000. Randomly selected curves can be seen in section 5.1.2, sub-section 'Effect of the obscuration rate – Interference of noise'. Similar to these results, a characteristic curve of each obscuration rate tested on the Mastersizer 2000 (disregarding all right sided unexpected peaks) can be seen in Figure 36. As can be seen in the figure, at higher obscuration rates of 10 and 20%, a left sided shoulder/peak starts to show. Even though there seems to be no significant difference between the obscuration rate and the occurrence of right sided unexpected peaks on the Mastersizer 2000, an effect on the characteristic of the curve is observed. When increasing the obscuration rate from 0.5 to 2%, an increase in the left-sided tail can be seen. When increasing the obscuration from 2 to 5% this tail seems to increase even more. When adding more sample to increase the obscuration rate to 10%, a shoulder can clearly be seen which turns into a second population when increasing the obscuration rate to 20%.

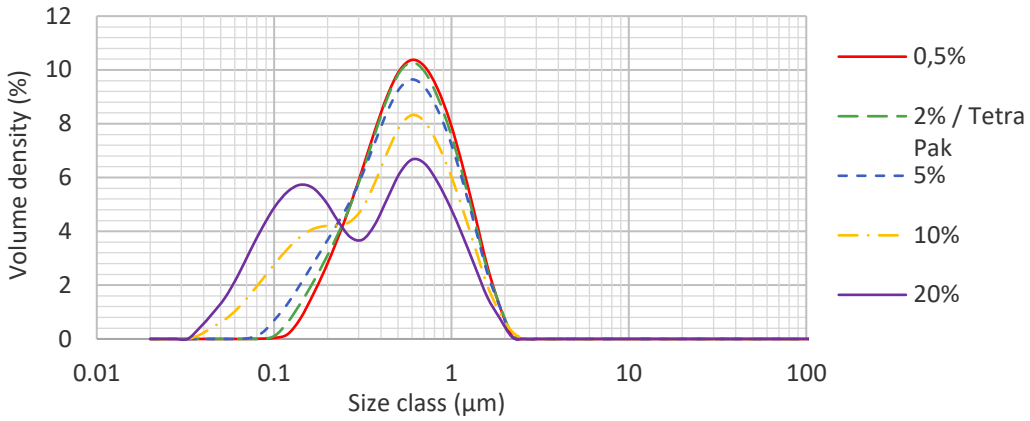

Figure 36: Characteristic PSD curve of changes in the obscuration rate in pasteurized milk measured on the Mastersizer 2000 disregarding curves with unexpected peaks.

There are two hypotheses what would cause this increase of the left-sided unexpected peaks. One hypothesis is that these peaks could occur due to aggregation of oil droplets. However, as mentioned in '2.2.2 Homogenization' it is unlikely that the left sided unexpected peaks are caused by the aggregation of droplets since the left side indicates small droplets (< 0.1µm) while aggregation of droplets is more likely to occur for larger particles due to their higher velocity and thus quicker moving speed.

Another hypothesis is that the effect seen on the left is due to multi scattering. This seems to be more reasonable, as theory suggests that a too high obscuration rate, multi scattering can cause an increased in fine particles population as described in '3.2 Laser Diffractometry'. This theory is supported when looking at Figure 36, where the particle size at higher obscuration rates shifts towards smaller particles. Other arguments supporting this is that it is more likely to occur in samples with particles smaller than 10 µm, since fat droplets in pasteurized milk are around 1 µm this would increase the risk of multi scattering. Furthermore, as mentioned in the background the obscuration should be kept below 5% for particles ranging from 0-1 µm. These recommendations are supported when looking at Figure 36, as a shoulder on the left side of the curve starts to appear when the obscuration rate exceeds 5%.

Pasteurized milk on the Mastersizer 3000

Comparing the Mastersizer 2000 to the Mastersizer 3000, four randomly selected curves for each variation in obscuration rate tested on the Mastersizer 3000 can be seen in Figure 37.

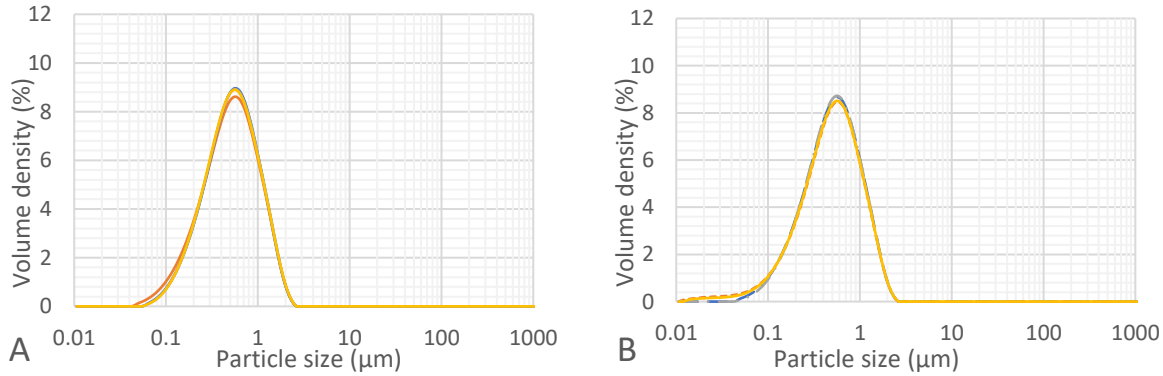

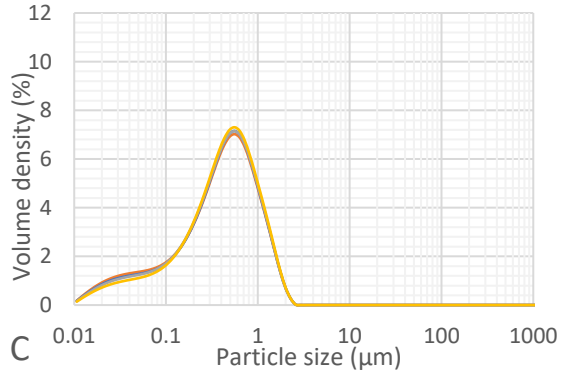

Figure 37: PSD of pasteurized milk measured on the Mastersizer 3000 at different obscuration rates of 0.5% (A), 2% (B), 5% (C) where four curves were randomly selected for each setting.

In Figure 37.C a left sided unexpected peak seems to appear already at an obscuration rate of 5%, which differs from the Mastersizer 2000 where similar behavior was not observed until an obscuration rate of 10%.

Comparing to the Mastersizer 2000 in Figure 38.A, there is a large difference between the two versions of equipment. What stands out in these two figures is the difference in the appearance of an unexpected peak on the left side of the main peak of the PSDs. The PSD of the Mastersizer 3000 shows a great number of small particles, showing a large peak on the left side of the main peak. This difference is even more visible when changing to a surface area curve instead of a volume based curve, as can be seen in Figure 38.B. While a left sided unexpected peak starts to appear on the Mastersizer 2000 as well, the effect is not quite as large. A reason for the peak shown on the Mastersizer 3000 could be because of multi scattering, as too high obscuration can cause multi scattering as mentioned above, which can clearly be seen in Figure 38.

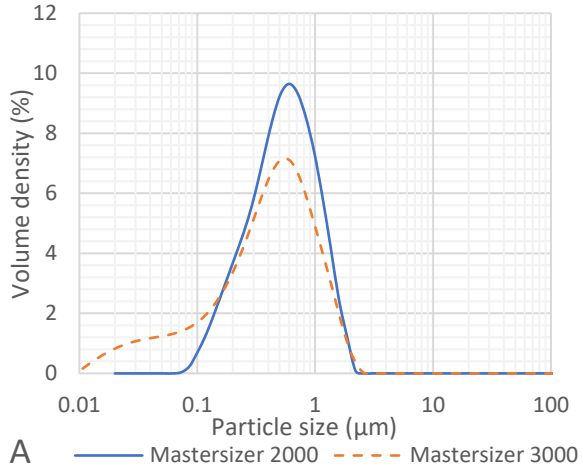

Figure 38.A: PSD curve of the averages of pasteurized milk, disregarding curves containing a unexpected peak, measured on the Mastersizer 2000 and 3000 with a sitrring speed of 800 rpm, an obscuration rate of 5% and 2 mL of Solution A. These graphs show all measurements performed for the selected variable.

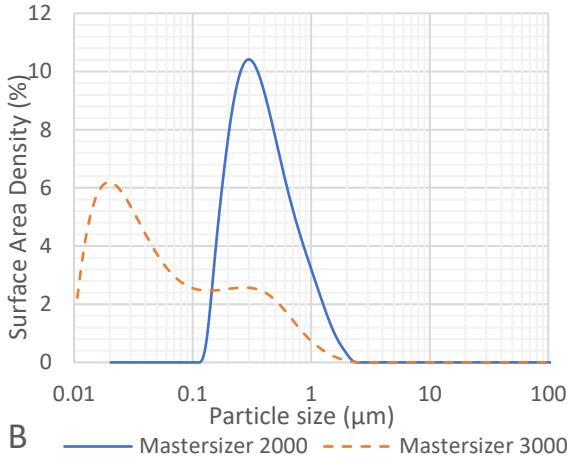

Figure 38.B: Surface Area curve of the averages of pasteurized milk, disregarding curves containing a unexpected peak, measured on the Mastersizer 2000 and 3000 with a sitrring speed of 800 rpm, an obscuration rate of 5% and 2 mL of Solution A. These graphs show all measurements performed for the selected variable.

Though not much of a left sided unexpected peak can be seen on the Mastersizer 2000 at 5% obscuration, at an obscuration of 10% this effect is also clearly visible. While the particle size does decrease for the Mastersizer 2000 as well, the difference between an obscuration of 2 and 5% is much larger in the Mastersizer 3000 than on the Mastersizer 2000 as can be seen

in Figure 39 which shows the Dv10, Dv50 and Dv90 of both equipment. Here, the Dv10 (circled in the figure) of an obscuration rate of 2% shows a difference of 26% between the Mastersizer 2000 and 3000 while an obscuration rate of 5% shows a difference of 73% between the two equipment. The difference of the multi scattering effect between the Mastersizer 2000 and Mastersizer 3000 might be caused by the increase in sensitivity of the Mastersizer 3000, as the lasers alignment changed, the power of the blue light laser was increased and more large-angle back scatter detectors were added as described in section '2.4 Comparing Mastersizer 2000 and 3000'. Due to these changes, Mastersizer 3000 is assumed to be more sensitive to smaller particles, thus being more sensitive to multi scattering as well. This highlights the importance of obscuration rate, as it indicates when the obscuration is too low, unexpected peaks on the right may appear but when the obscuration is too high, unexpected peaks on the left appear.

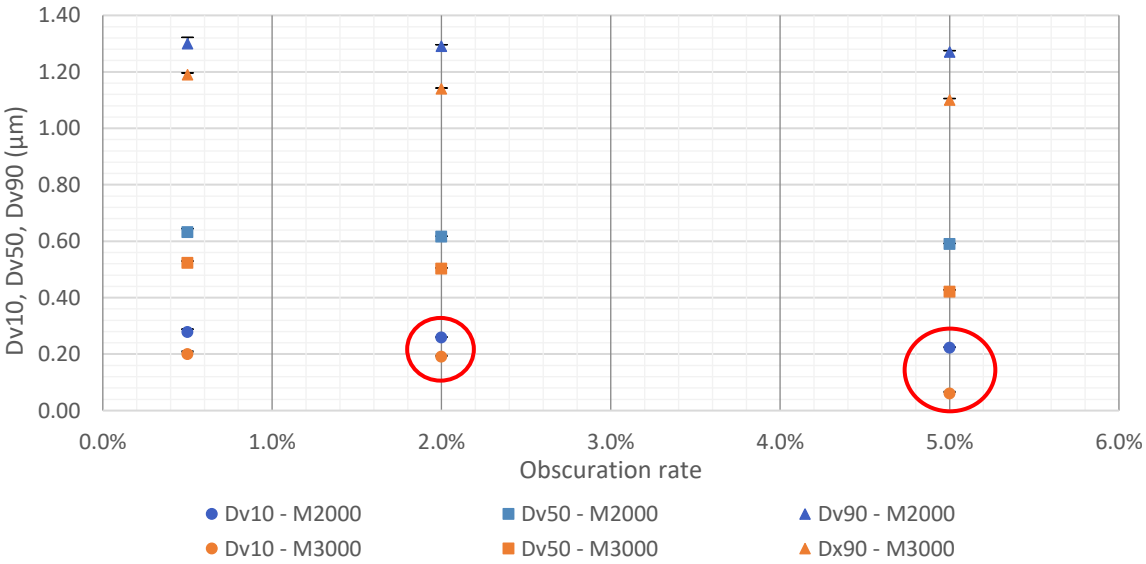

Figure 39: Dv10, Dv50 and Dv90 for averages of different obscuration rates of pasteurized milk measured on the Mastersizer 2000 and 3000 with standard deviation bars.

Unfractionated model emulsion

As described above, the Mastersizer 3000 seems to be more sensitive to show a left sided unexpected peak when measuring pasteurized milk. This is expected to be caused by multi scattering. In order to verify whether this left sided peak on the Mastersizer 3000 is an artifact (e.g. multi scattering), protein particles or small oil droplets, the investigation of a more simplified system was conducted. This was done by using a model emulsion, in which the presence of milk proteins is not a factor of concern.

The unfractionated model emulsion was tested at different obscuration rates, using an obscuration of 2% on the Mastersizer 2000 and 0.5, 0.8, 1, 2 and 5% on the Mastersizer 3000. Of these obscuration rates, four randomly selected PSDs of each can be seen in Figure 40.

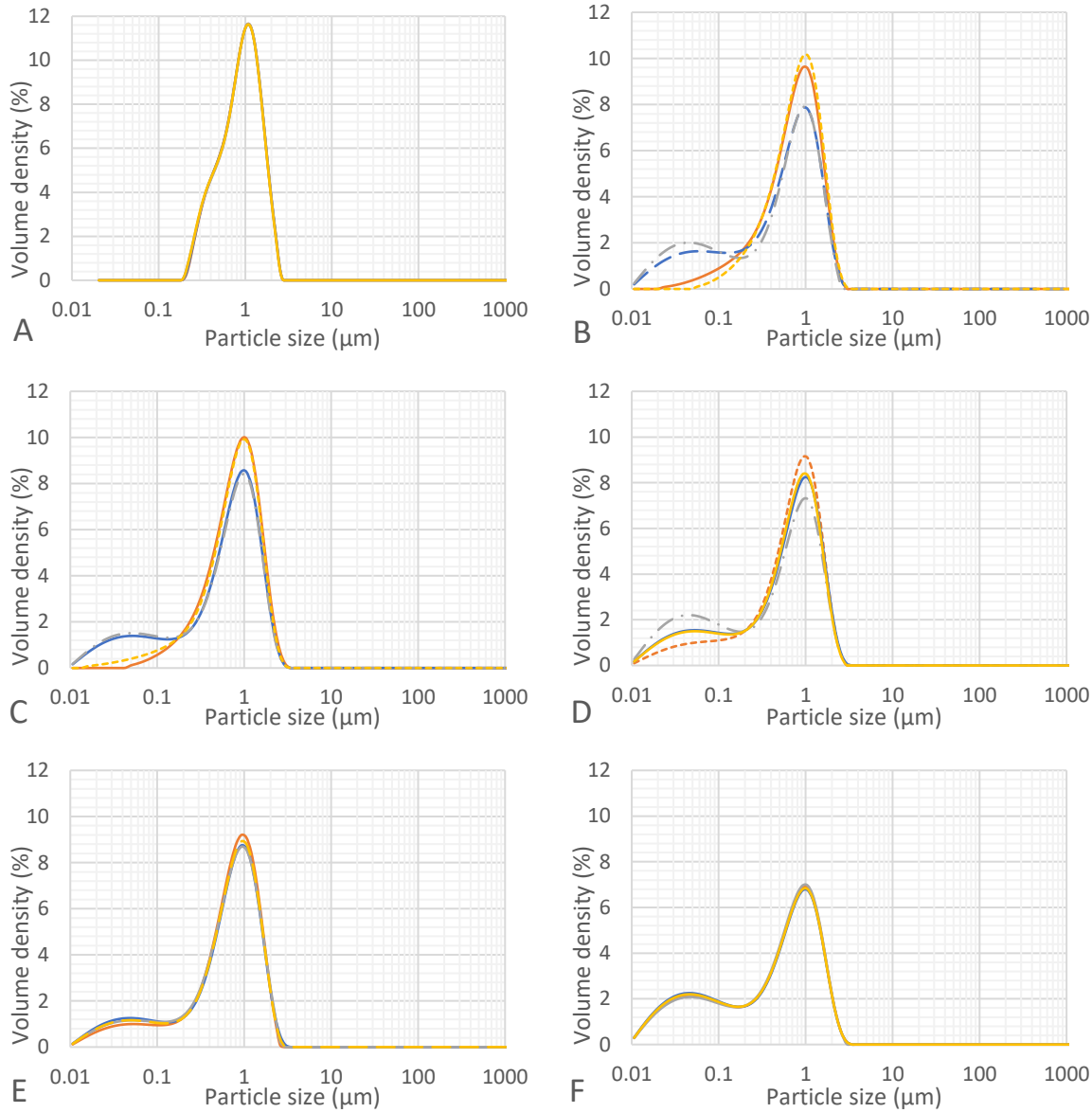

Figure 40: PSD of the unfractionated model emulsion at different obscuration rates measured on the Mastersizer 2000 at an obscuration rate of 2% (A) and on the Mastersizer 3000 at obscuration rates of 0.5% (B), 0.8% (C), 1% (D), 2% (E) and 5% (F) where four PSDs were randomly selected for each setting.

What can be seen in the figure is the occurrence of a left sided unexpected peak when the obscuration rate is increased. However, while the unexpected peak does seem to reduce at lower obscuration rates, it does not completely disappear at any occasion and even shows a high deviation between the different PSDs. When comparing to the Mastersizer 2000 (Figure 40.A), the distributions of the Mastersizer 3000 appear to show a smaller particle size peak in each of the obscuration rates as the Mastersizer 2000 indicates the absence of particles below 0.2 µm.

Comparing all average distributions of the unfractionated model emulsion in Figure 41, an effect of what is believed to be multi scattering on the left side of the distribution can be seen for the unfractionated model emulsion. Here, the left sided unexpected peak lowers when the obscuration is decreased, apart from an obscuration of 1% which seems to have a higher left sided unexpected peak than an obscuration at 2%. This might be explained by the variation in the number of PSDs per obscuration rate. As the number of measurements for each obscuration rate were unequal, the number of peaks with and without a left sided unexpected

peak differed, which could have impacted the average PSDs of the unfractionated emulsion. Nevertheless, the effect that is believed to be multi scattering can be seen in the figure.

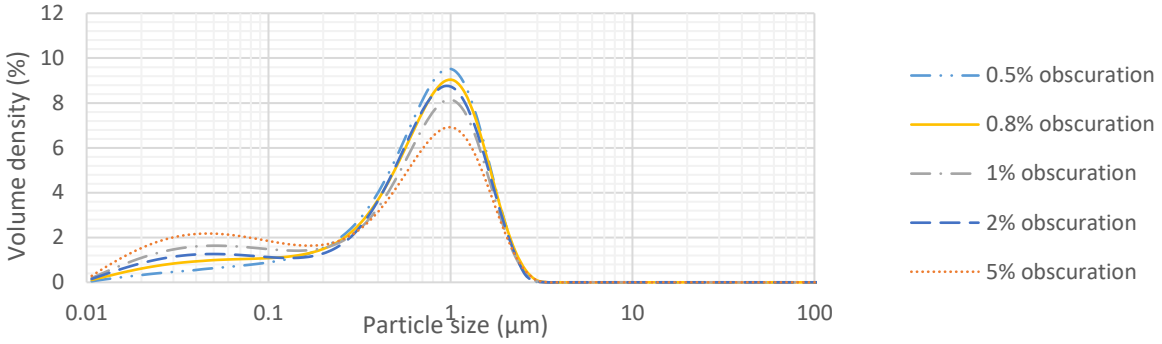

Figure 41: PSD of the averages of the unfractionated model emulsion measured on the Mastersizer 3000 with an obscuration rate of 0.5%, 0.8%, 1%, 2% and 5%.

These results further strengthen the theory of multi scattering, as the Mastersizer 3000 shows a relation between the obscuration rate and the size of the left sided unexpected peak. The Mastersizer 3000 is also considered to be more sensitive than the Mastersizer 2000, which could be due to a different alignment of the lasers which may cause the equipment to be more sensitive to multi scattering, as described in section '2.4 Comparing Mastersizer 2000 and 3000'.

The results of the unfractionated model emulsion show a difference compared to pasteurized milk. This effect is believed to be caused by multi scattering, which occurs at lower obscuration rates in the unfractionated model emulsion. This suggests that it might be needed to perform an experiment varying the obscuration rate for every product and product variation.

Low obscuration rates - High standard deviation

However, a too low obscuration rate also seems cause left sided unexpected peaks. As suggested in the hypothesis '*If the variables of the LD equipment are not optimized, then it might increase the standard deviation of the PSD'*, the occurrence of a high standard deviation might be due to amongst others a too low obscuration rate. As can be seen in Figure 42, a lower obscuration rate in the unfractionated emulsion causes a higher standard deviation between the measurements. This effect is believed to be caused due to a variation in the particles passing through the system at low obscuration rates, which can result in a high standard deviation between measurements. Thus, it is also not recommended to use too low obscuration rate. Another issue with low obscuration rates is that they seem to have a lower percentage of curves showing good data quality. Based on this, the hypothesis seems to be correct as the standard deviation increases significantly at very low obscuration rates. Thus, it is suggested to use an obscuration rate of at least 0.8% for the unfractionated model emulsion.

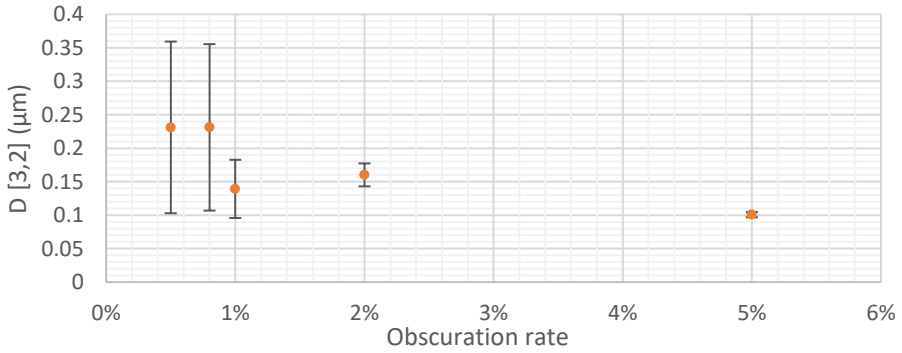

Figure 42: D [3,2] of averages of the unfractionated model emulsion measured on the Mastersizer 3000 at different obscuration rates with standard deviation.

Comparing Mastersizer 2000 and 3000

An obscuration of 0.8% is chosen for the unfractionated model emulsion, as these measurements show a low number of unexpected peaks. When comparing the average distribution of the Mastersizer 2000 to an obscuration of 0.8% on the Mastersizer 3000, considerably different distributions can be seen (Figure 43). While it was expected for both equipment to have similar comparable PSDs, the PSDs obtained measuring the unfractionated emulsion on the Mastersizer 3000 showed a left sided unexpected peak and no shoulder on the left of the main peak, which can be seen when measuring on the Mastersizer 2000. Yet, the main peak of both PSDs is around 1 µm and both PSDs show no larger particles than 2.5 µm. This would indicate that the left sided unexpected peaks could be an artifact or very small oil droplets, but it is very unlikely that these peaks are protein as this is not present in the model emulsion.

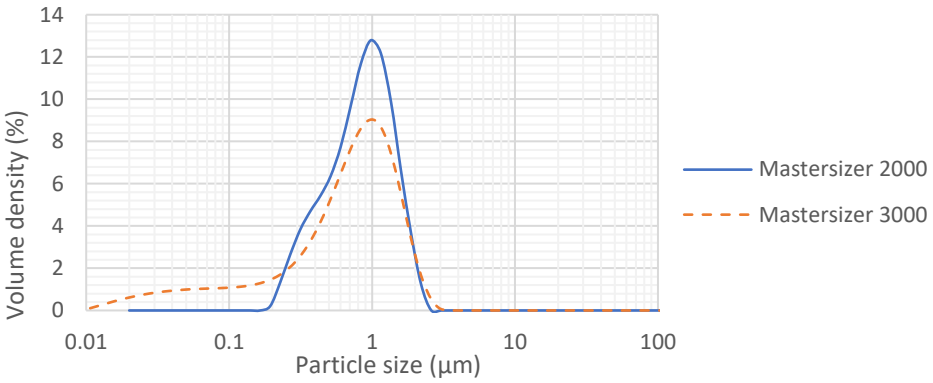

Figure 43: PSD of the average distributions of the unfractionated model emulsion measured on the Mastersizer 2000 (2% obscuration) and 3000 (0.8% obscuration).

A similar difference between equipment can be seen when comparing the Dv10, Dv50 and Dv90 values of the unfractionated model emulsion (Figure 44), as a difference can be seen between the Mastersizer 2000 and 3000 for all Dv-values. However, the difference between the equipment at different obscuration rates cannot be evaluated since the obscuration rate on the Mastersizer 2000 was only measured at 2%.

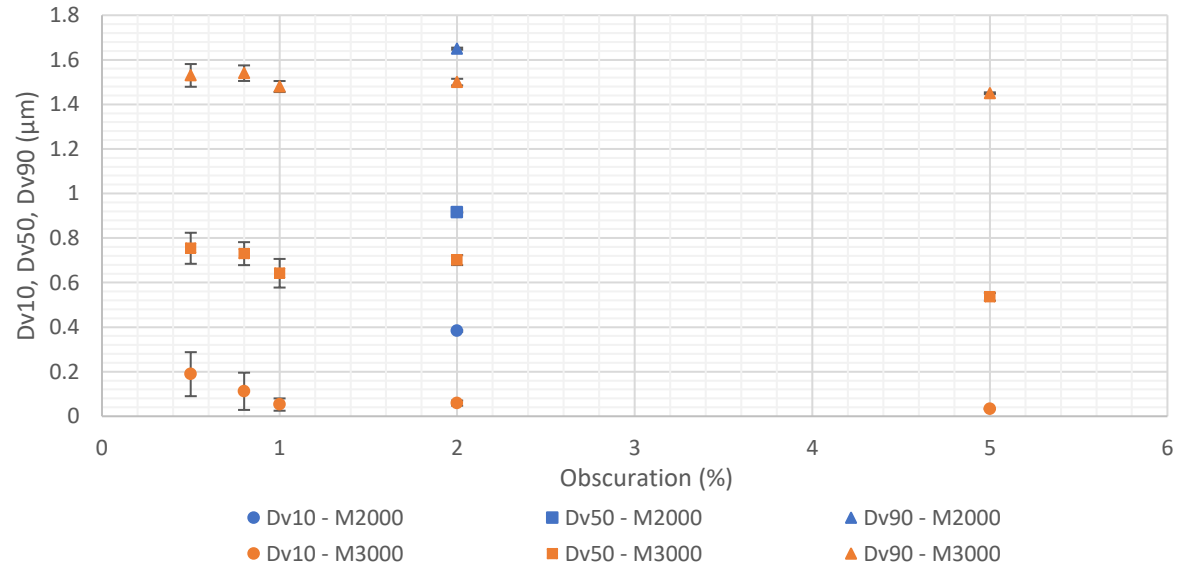

Figure 44: Dv10, Dv50 and Dv90 for averages of different obscuration rates of the unfractionated model emulsion measured on the Mastersizer 2000 and 3000 with standard deviation bars.

Comparing to DLS

The hypothesis that the left sided unexpected peaks could be caused by casein micelles can be disregarded, since a left sided peak can still be seen in the unfractionated model emulsion, even though such system does not contain any protein. However, difference between the distribution of the unfractionated model emulsion on the Mastersizer 2000 and 3000 cannot yet be explained. Therefore, the results were compared with DLS, in order to confirm whether what is seen with the Mastersizer 3000 can be ascribed to artifacts or to the presence of very small oil droplets. Sizes detectable with the DLS vary in the range of 10 nm to 10 µm, considerably smaller than those for the Mastersizer. DLS should therefore be more accurate when measuring sizes below 1 µm. Concentrations series in the range of 0.01 to 50% were measured and a concentration of 0.5% was most reproducible for the unfractionated emulsion. Raw data of all concentrations analyzed can be found in Appendix D. Three PSDs can be seen in Figure 45.

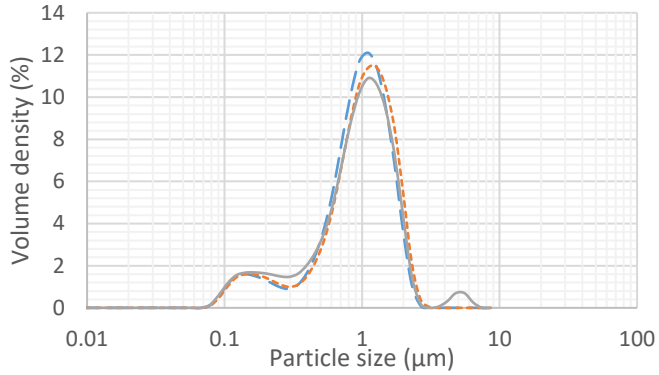

Figure 45: PSD of the unfractionated model emulsion at a concentration of 0.5% measured on the DLS, showing three PSDs for each concentration.

As can be seen in the figure, all distributions show a left sided unexpected peak besides the main distribution, some of the measurements also show a right sided unexpected peak besides the main distribution.

Comparing all three equipment in Figure 46 below, it should be noted that different concentrations were used for each equipment, optimizing the concentration per equipment based on reproducibility and reduced number of left sided unexpected peaks. On the Mastersizer 2000, an obscuration rate of 2% was used, on the Mastersizer 3000 an obscuration of 0.8% and on the DLS a concentration of 0.5%. Comparing the average distributions of the unfractionated emulsion of the Mastersizer 2000 and 3000 in Figure 46, the distributions have some characteristics in common, as they exhibit the presence of a large population of particles with sizes of approximately 1 µm. Furthermore, the presence of particles with smaller sizes are detectable using three instruments, resulting in either a separate population (i.e. a second peak) or a larger distribution (i.e. a shoulder to the left of the main peak). While the Mastersizer 2000 shows more of a shoulder, the Mastersizer 3000 shows a tail and the DLS shows a bimodal distribution of oil droplet sizes. As mentioned above, the PSDs of the Mastersizer 2000 and 3000 show the presence of a largest drop size at ~2.5 µm, but the DLS measurement shows the presence of a small peak at ~6 µm. This larger particle size was not present in all measurements of the DLS as can be seen above. The largest difference can be seen on the left side. As the Mastersizer 3000 indicates the presence of particles as small as 0.01 µm, the Mastersizer 2000 only indicates the presence of particles above 0.18 µm while the measurement on the DLS indicates the presence of droplets as small as 0.07 µm. This makes it difficult to draw any conclusion on which distribution shows the true PSD, but what can be said is that both the DLS and Mastersizer 2000 can confirm that there are no particles smaller than 0.07 µm. Another issue that can be seen in the figure is that the volume distribution seems quite different for each measurement. Therefore, a cumulative curve was created to ensure that all curves add up to 100%, indicating an even volume

distribution. These can be seen in Appendix E, where it can be concluded that the volume distributions of both Mastersizers and the DLS are all equal.

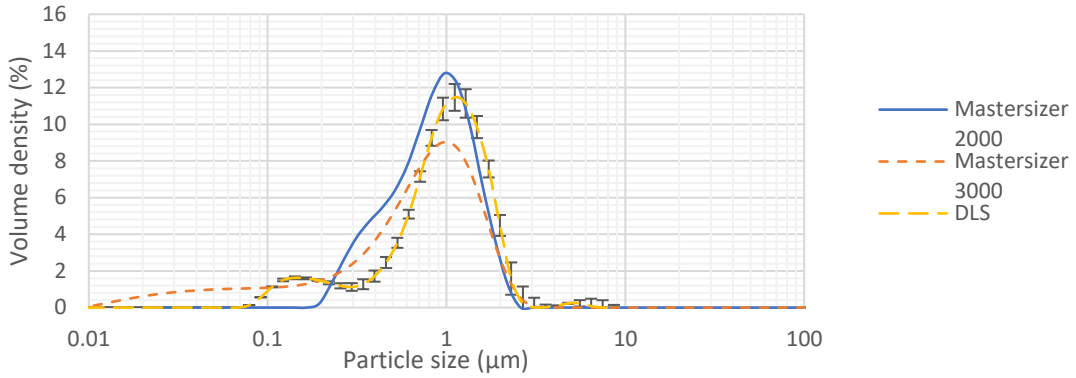

Figure 46: PSD of the average distributions of the unfractionated model emulsion measured on the Mastersizer 2000 (2% obscuration), Mastersizer 3000 (0.8% obscuration) and DLS (0.5% concentration, with standard deviation).

Fractionated model emulsion

To decrease the particle size for more precize measurements on the DLS, the model emulsion was fractionated. Four randomly selected PSDs for each of the different obscuration rates of the fractionated model emulsion measured on the Mastersizer 2000 at an obscuration rate of 2% and on the Mastersizer 3000 at an obscuration rate of 1 and 2% can be seen in Figure 47.

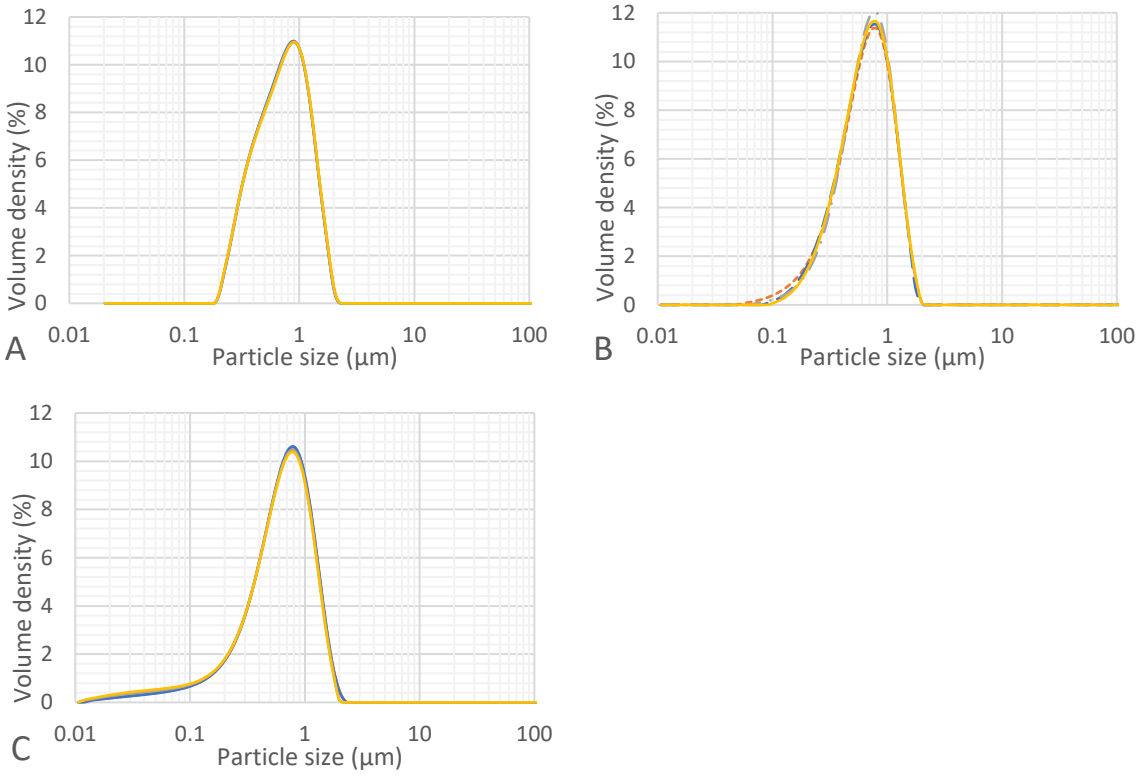

Figure 47: PSD of the fractionated model emulsion at different obscuration rates measured on the Mastersizer 2000 at an obscuration rates of 2% (A) and on the Mastersizer 3000 at obscuration rates of 1% (B) and 2% (C) where four PSDs were randomly selected for each setting.

What can be seen in the fractionated emulsion is the difference between obscuration rates measured on the Mastersizer 3000, as the left sided unexpected peak lowers when the obscuration rate is decreased. The Mastersizer 2000 does not seem to show any sort of unexpected peak on the left.

Comparing the average PSDs of different obscurations of the fractionated model emulsion in Figure 48, it shows an effect which is believed to be multi scattering. As can be seen in the figure, when the fractionated model emulsion is studied at an obscuration rate of 2% the results indicate a presence of smaller particles which can be seen as a left sided tail. This effect is smaller, if even present, at 1%. This suggests that the underlying cause could be the effect of multi scattering, as this is observed in the small particle sizes.

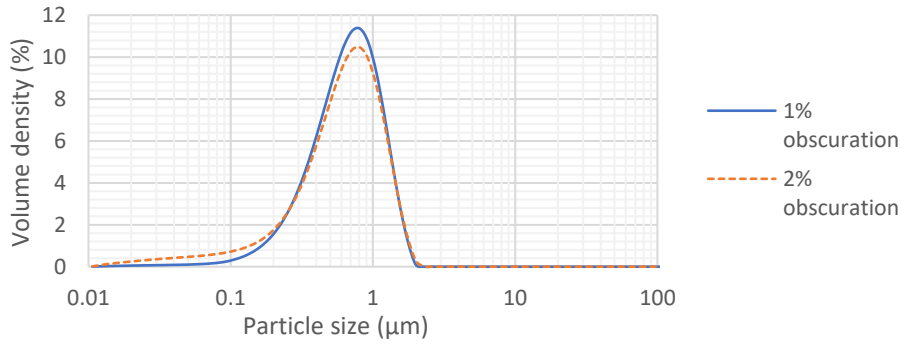

Figure 48: PSD of the averages of the fractionated model emulsion measured on the Mastersizer 3000 with an obscuration rate of 1% and 2%.

To investigate whether the left sided unexpected peak is indeed caused by multi scattering, a modeling program was used to determine the effect that fractionation should have on the model emulsion. This was compared with the PSD measured before and after fractionation of the model emulsion for both the Mastersizer 2000 and 3000.

The results of this comparison can be seen in Figure 49.A, where the unfractionated model emulsion was measured on the Mastersizer 2000 and compared with the simulated effect of the fractionation. Figure 49.B shows the effect of the fractionation measured compared to the simulated effect of the fractionation on the Mastersizer 2000. What is interesting in these figures, is that the starting point of all distributions is almost identical. Figure 49.B shows a comparable volume distribution, but the effect of fractionation is not as much as it should have been, as the particle size is reduced to 2 µm instead of the simulated 1.3 µm. Even though the PSDs do not match completely, this variation is considered acceptable since the focus of this experiment is on the left side of the main distribution.

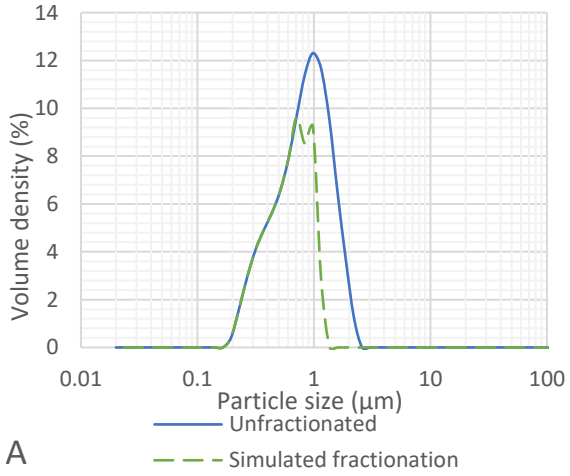

Figure 49.A: PSD of the average of the unfractionated model emulsion measured on the Mastersizer 2000 at an obscuration of 2% and the PSD of its simulated fractionation.

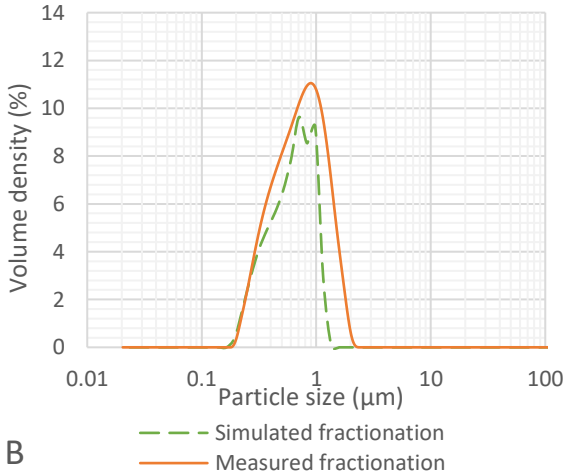

Figure 49.B: PSD of the simulated fractionated of the model emulsion (measured on the Mastersizer 2000 at an obscuration of 2%) and the PSD of the measured fractionated model emulsion on the Mastersizer 2000 at an obscuration of 2%.

The simulation of the fractionation measured on the Mastersizer 3000 showed different results. Here, Figure 50.A shows the difference between the measured unfractionated model emulsion at an obscuration of 0.8% on the Mastersizer 3000, compared to the simulated fractionation of this PSD. Similar differences can be seen as when measuring on the Mastersizer 2000, as only a reduction of the larger particles can be seen. A bigger difference can be seen when comparing the simulated and measured fractionated emulsion on the Mastersizer 3000. The smallest particle size (left side of the distribution) does not overlap for the PSD of measured obscuration rates of 1 or 2% and the simulated fractionation. The simulation shows no change in the smaller particle size of the distribution (Figure 50.A) as the fractionation should only affect the largest particle size (right side of the distribution). However, when measuring the fractionated emulsion on the Mastersizer 3000 (Figure 50.B) the small particle size of the distribution is affected. The reason of this difference remains unknown to the authors. The results of fractionation should therefore be interpreted with some caution.

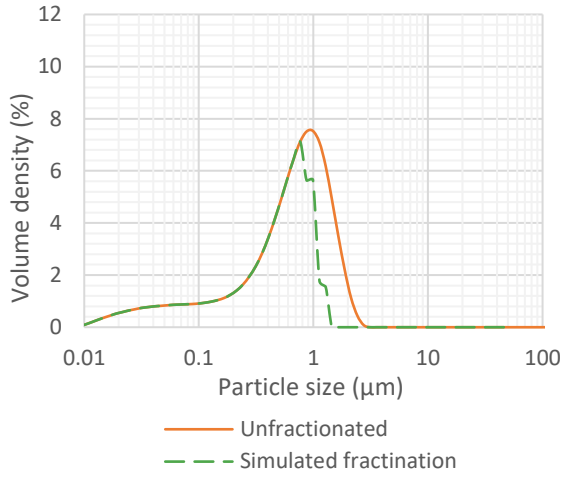

Figure 50.A: PSD of the average of the unfractionated model emulsion measured on the Mastersizer 3000 at an obscuration of 0.8% and the PSD of its simulated fractionation.

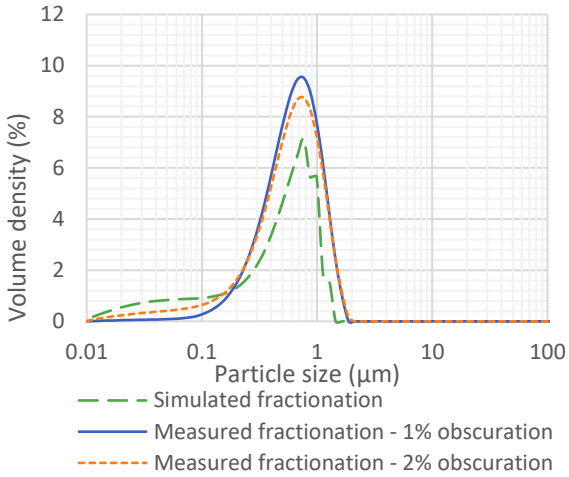

Figure 50.B: PSD of the simulated fractionated of the model emulsion (measured on the Mastersizer 3000 at an obscuration of 0.8%) and the PSDs of the measured fractionated model emulsion on the Mastersizer 3000 at an obscuration of 1 and 2%.

Nevertheless, comparing the results of the Mastersizer 2000 and 3000, the results seem to match more than the unfractionated model emulsion. An obscuration of 1% was chosen to be most accurate for the fractionated model emulsion on the Mastersizer 3000 due to repeatability and appearance of multi scattering. As can be seen in Figure 51, both distributions show the presence of a largest drop size at ~2 µm and exhibit the presence of a large population of particles with sizes of ~1 µm. Here the main difference can be seen in the start of the distribution. While the distribution on the Mastersizer 2000 starts at around 0.18 µm, the distribution on the Mastersizer 3000 starts around 0.04 µm. It was thought that the unexpected left sided peak of the unfractionated emulsion could be explained by multi scattering, but this is not likely to be the case for the fractionated emulsion as the obscuration rate is kept low to prevent multi scattering. Yet, a difference between equipment can still be seen.

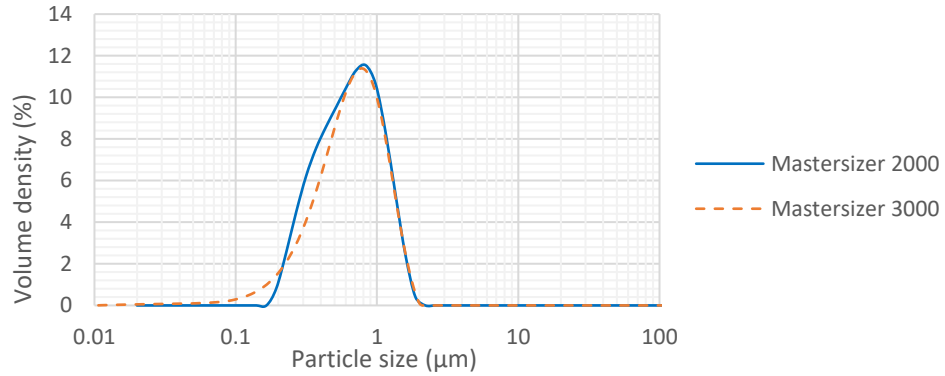

Figure 51: PSD of the average distributions of the fractionated model emulsion measured on the Mastersizer 2000 (2% obscuration) and 3000 (1% obscuration).

Comparing to DLS

Even when the obscuration is lowered to prevent multi scattering in the fractionated emulsion, a difference in particle size can still be seen between the Mastersizer 2000 and 3000. Thus, the results were compared to the data from the DLS. The fractionated model emulsion was tested in a range of concentrations between 0.1 to 10%, the raw data of these distributions can be found in Appendix D. A concentration of 0.2% was used for measurements on the DLS as this had the lowest deviation for the fractionated emulsion. Three distributions for a concentration of 0.2% can be seen in Figure 52.

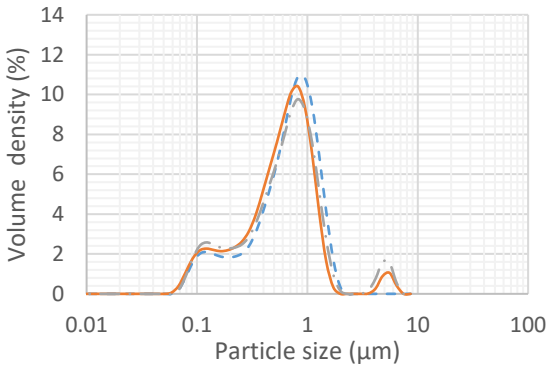

Figure 52: PSD of the fractionated at a concentration of 0.2% measured on the DLS, showing three PSDs for each concentration.

The distribution shows a left sided unexpected peak of the main distribution, some of the measurements also show a right sided unexpected peak of the main distribution.

Comparing the fractionated model emulsion measured on the Mastersizer 2000 and 3000 to the DLS in Figure 53, the PSD obtained by DLS, shows similar characteristics as the one for the unfractionated emulsion. Again, not all measurements exhibit the presence of the population with larger particle size as can be seen by the error bars. Besides the DLS, both the Mastersizer 2000 and 3000 show the presence of a largest drop size around 2 µm. All three distributions exhibit the presence of a large population of particles with sizes of approximately 0.8 µm. The left side of the distribution looks very similar to the unfractionated emulsion for both the Mastersizer 2000 and the DLS, only the Mastersizer 3000 shows a difference on the left side as the distribution shows the presence of smaller sizes around 0.06 µm. This matches the DLS measurement quite closely. This would suggest that what shows on the unfractionated model emulsion measured on the Mastersizer 3000 as sizes smaller than 0.1 µm could be an artifact and therefore would not represent actual particles of that size. However, more experimental research is needed in order to draw this conclusion.

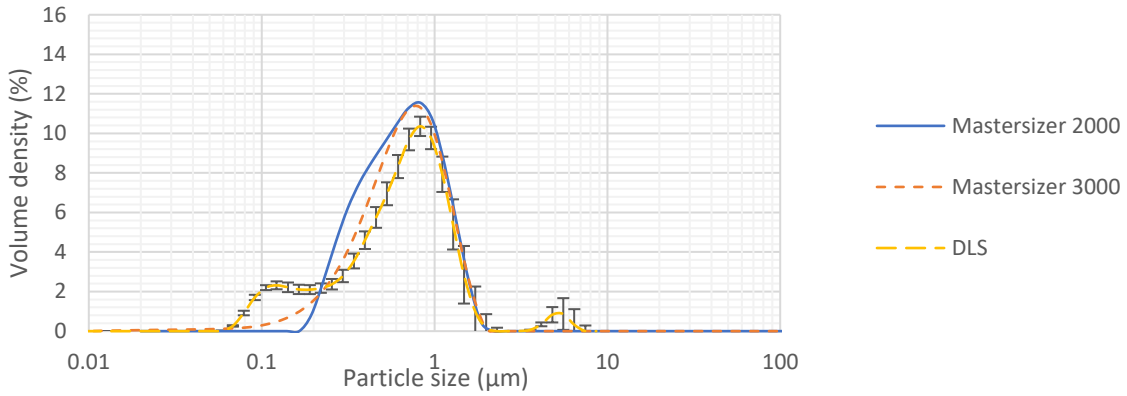

Figure 53: PSD of the average distributions of the fractionated model emulsion measured on the Mastersizer 2000 (2% obscuration), Mastersizer 3000 (1% obscuration) and DLS (0.2% concentration, with standard deviation).

Concluding, the hypothesis of multi scattering for pasteurized milk samples can be confirmed, as left sided unexpected peak showed on the Mastersizer 2000 and 3000 can be prevented by lowering the obscuration rate. However, this is not the case for the unfractionated model emulsion, as a left sided unexpected peak appears no matter the obscuration rate.

5.2.2 Effect of stirring rate

To test the hypothesis '*If the variables of the LD equipment are not optimized, then it might increase the standard deviation of the PSD'*, several parameters were tested at different settings. Some of these settings, such as low obscuration rate as mentioned above, showed a high standard deviation compared to the standard deviation of other parameters. Another of the reasons causing a high standard deviation, which creates somewhat of a left sided unexpected peak can be the stirring speed. This can be seen in Figure 54, which shows four randomly selected curves for each stirring speed tested on the Mastersizer 3000: 800 and 1800 rpm.

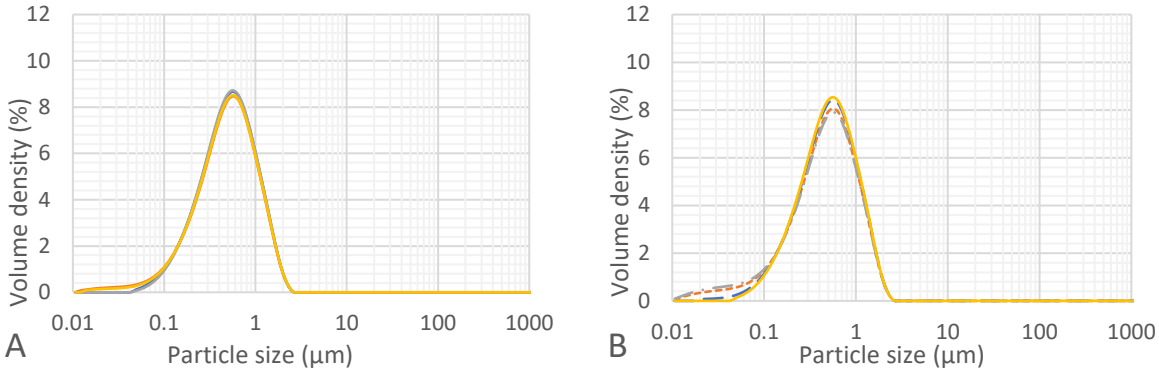

Figure 54: PSD of pasteurized milk measured on the Mastersizer 3000 at different stirring speeds of 800 rpm (A) and 1800 rpm (B) where four curves were randomly selected for each setting.

The randomly selected curves show a larger variation when stirring at 1800 rpm on the Mastersizer 3000. While a variation between measurements can be seen in all measurements performed on the Mastersizer 3000, the difference in standard deviation of stirring at 1800 rpm has doubled when comparing to other variables. This can be seen in Figure 55, showing the Dv10 of a stirring rate of 800 and 1800 rpm. Here a stirring rate of 1800 rpm has a standard deviation five times as high as the standard deviation of 800 rpm. A reasoning for this could be the relation between the stirring rate and the pump speed, as the pump speed increases when the stirring rate increases. This may cause a higher flux of the sample through the laser at higher stirring rates, which causes a higher variation between measurements.

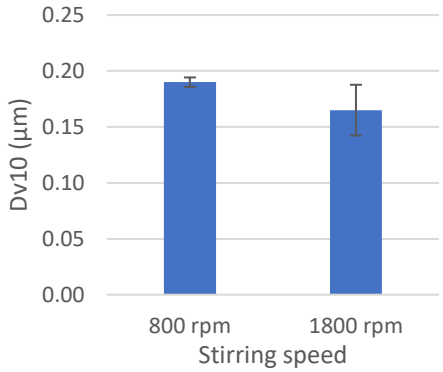

Figure 55: Dv10 of pasteurized milk measured on the Mastersizer 3000 at 800 and 1800 rpm with error bars.

This further confirms the hypothesis that the variables of the Mastersizer need to be optimized in order to avoid a high standard deviation that could appear as a left sided unexpected peak. To avoid the formation of the left sided unexpected peak, it is suggested to keep the stirring speed below 1800 rpm. This is confirmed when comparing to the Mastersizer 2000, as it strongly indicates that stirring speed of 1800 rpm is too high as right sided unexpected peaks occur as well.

5.2.3 Difference in sensitivity

As described in '2.4 Comparing Mastersizer 2000 and 3000', there is a difference between the two versions of equipment. Therefore, the hypothesis '*If the sensitivity of the LD equipment is increased, then it will affect the PSD'* was tested. Figure 56 shows the difference in volume (Figure 56.A) and surface area (Figure 56.B) density between the Mastersizer 2000 and 3000 at a stirring speed of 800 rpm and an obscuration rate of 2%. These settings are used by Tetra Pak to measure all milk samples and were expected to provide good results (Tetra Pak, 2019).

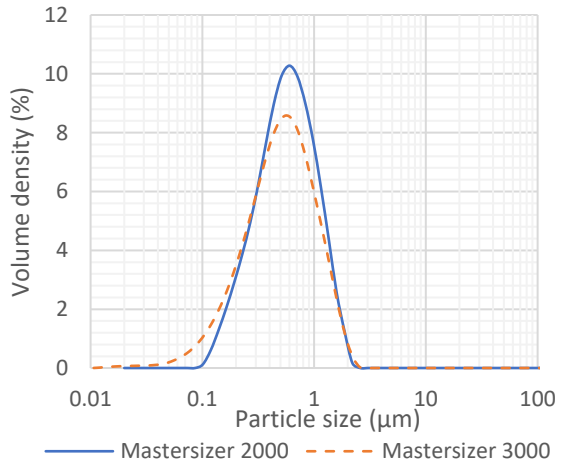

Figure 56.A: PSD curve of the average curves of pasteurized milk, disregarding curves containing a unexpected peak, measured on the Mastersizer 2000 and 3000 with a stirring speed of 800 rpm, an obscuration rate of 2% and 2 mL of solution A.

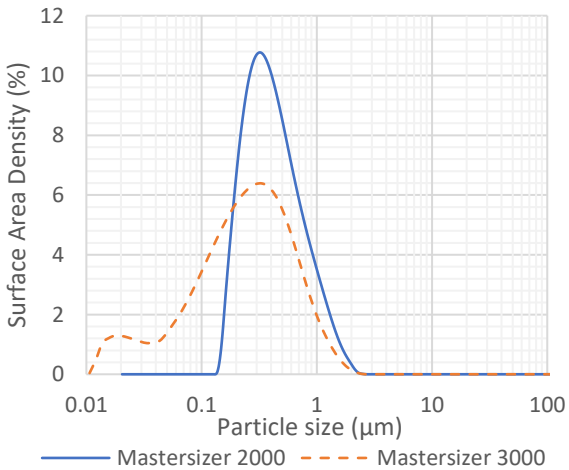

Figure 56.B: Surface area curve of the average curves of pasteurized milk, disregarding curves containing a unexpected peak, measured on the Mastersizer 2000 and 3000 with a stirring speed of 800 rpm, an obscuration rate of 2% and 2 mL of solution A.

As can be seen, the particle size seems to be lower for the Mastersizer 3000 as the curve shows a particle size smaller than 0.1 µm. This effect is even stronger when looking at the surface area of the Mastersizer 2000 and 3000 as can be seen in Figure 56.B.

When comparing the D [3,2] of the Mastersizer 2000 and 3000 in Figure 57, a smaller value for the Mastersizer 3000 can be seen at all obscuration rates comparing to the Mastersizer 2000, indicating a smaller average droplet size based on surface area moment mean. While multi scattering is believed to be a possible explanation for the left sided unexpected peak or

bump on the Mastersizer 3000, the D [3,2] value of measurements on the Mastersizer 3000 is always smaller than on the Mastersizer 2000. Indicating that obtaining similar results could be unachievable even when different obscuration rates are used. What is also of interest is that there seems to be a strong correlation between the obscuration rate and particle size.

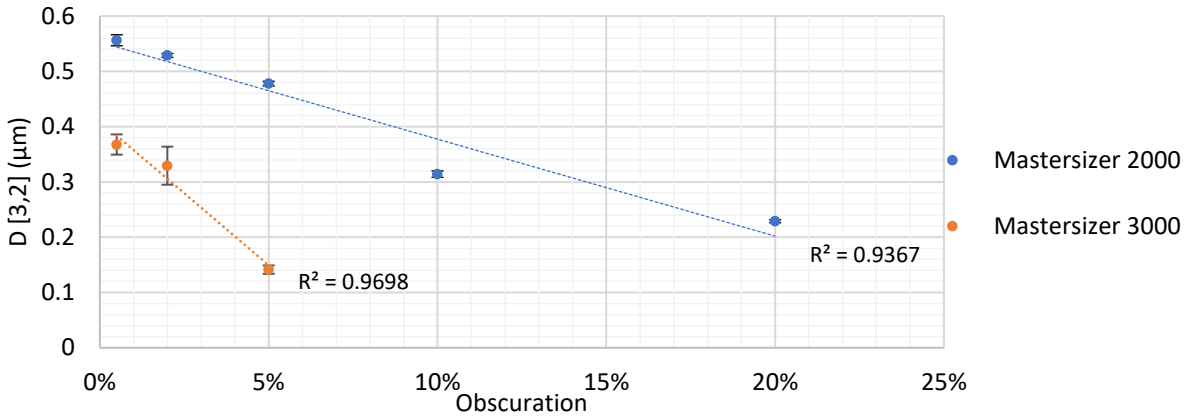

Figure 57: D [3,2] of averages of pasteurized milk measured at different obscuration rates on the Mastersizer 2000 and 3000 with standard deviation.

The correlation between the obscuration rate and particle size (D [3,2]) is not as strong for the unfractionated model emulsion compared to pasteurized milk. Figure 58 shows the difference in D [3,2] for the Mastersizer 2000, Mastersizer 3000 and DLS. Similar to milk, there is quite a high variability between the three equipment. The D [3,2] at 2% obscuration of the Mastersizer 2000 is 4x higher than the same value on the Mastersizer 3000. What is also of interest is the correlation between different obscuration rates on the Mastersizer 3000, as the D [3,2] value decrease when the obscuration increases. However, the correlation is not very strong, and more measurement points are needed to ensure whether this is a strong correlation or not. The D [3,2] of the DLS does not seem to match either the Mastersizer 2000 or 3000, but its value is closer to the Mastersizer 2000. Here it should be noted that the DLS does not use obscuration rate, and 0.5% should thus be seen as a dilution factor and not as an obscuration rate.

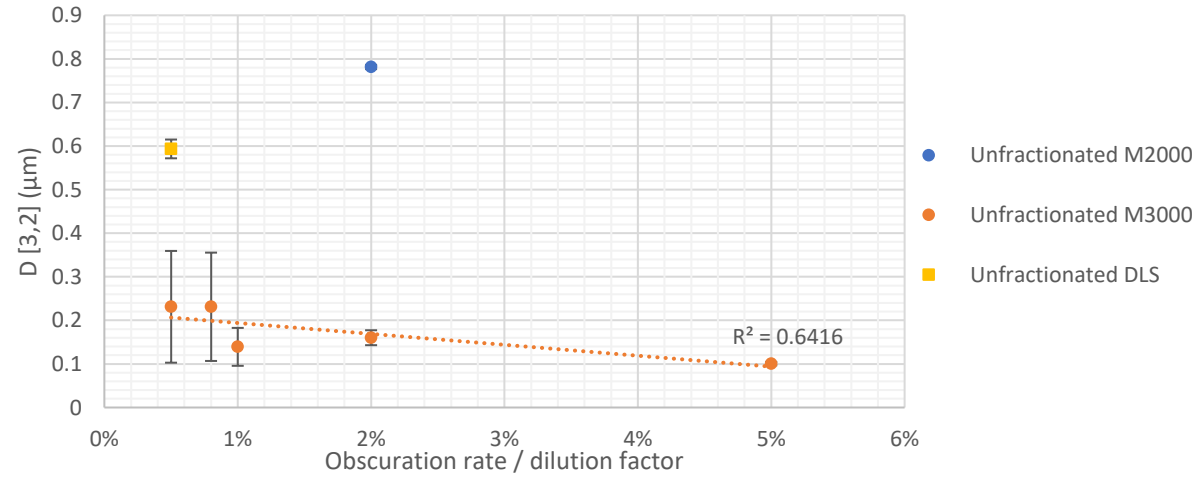

Figure 58: D [3,2] of the unfractionated model emulsion, averages taken from measurements on the Mastersizer 2000, Mastersizer 3000 and DLS.

Moving on to the D [4,3], also known as the volume moment mean, there seems to be a strong correlation as well between particle size and obscuration rate when measuring pasteurized milk for both the Mastersizer 2000 and 3000 (Figure 59). Nonetheless, the Mastersizer 3000 constantly shows a smaller value than the Mastersizer 2000. Indicating similar matters as mentioned above.

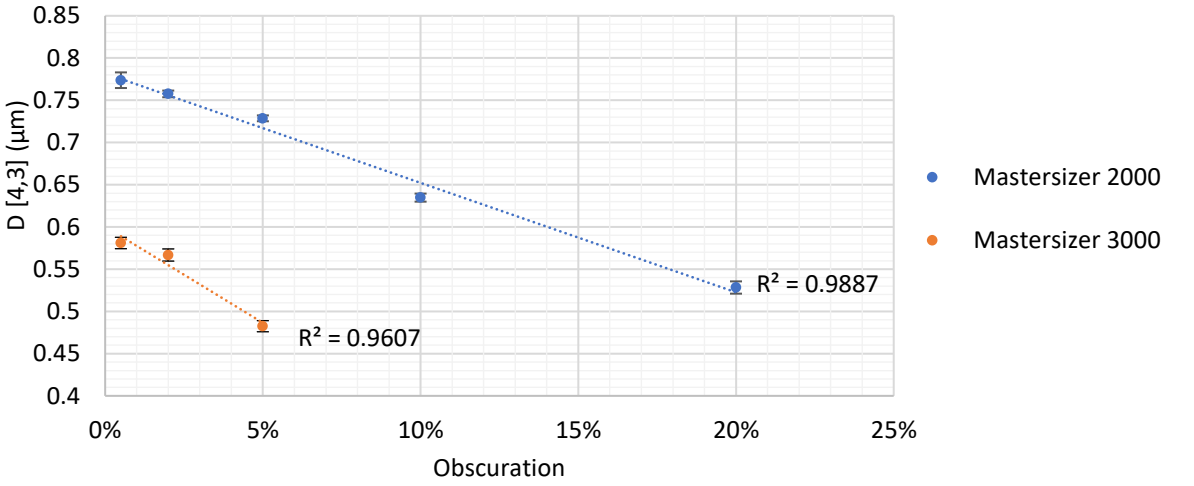

Figure 59: D [4,3] of averages of pasteurized milk measured at different obscuration rates on the Mastersizer 2000 and 3000 with standard deviation.

Comparing the D [4,3] of pasteurized milk with the D [4,3] of the unfractionated model emulsion, a similar trend can be seen once again. Figure 60 shows the D [4,3] value of the unfractionated model emulsion of the Mastersizer 2000, Mastersizer 3000 and DLS. What is interesting in this figure is the D [4,3] value of the Mastersizer 2000, which is 40% higher than the Mastersizer 3000 and shows thus less variation between equipment than when using the D [3,2]. The D [4,3] of the DLS measurement seems to match the Mastersizer 2000 quite closely, as they are both around 1.04 µm. Again, a trend can be seen in the correlation of different obscuration rates on the Mastersizer 3000. This once more shows a decreasing particle size as the obscuration rate decreases.

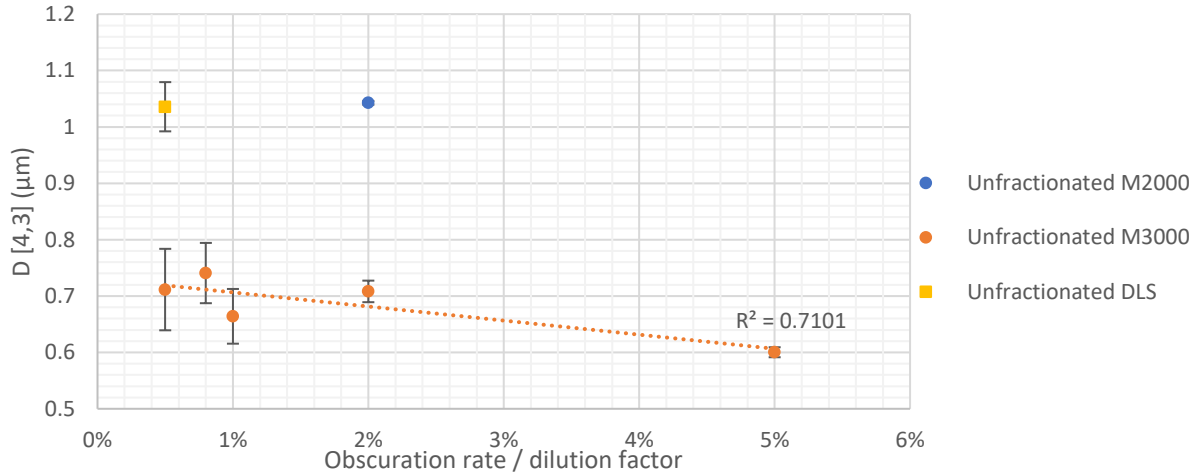

Figure 60: D [4,3] of the unfractionated model emulsion, averages taken from measurements on the Mastersizer 2000, Mastersizer 3000 and DLS.

As all measurements for both pasteurized milk and the unfractionated model emulsion on the Mastersizer 3000 have a lower D [3,2] and D [4,3] values compared to the Mastersizer 2000 and DLS. A way to explain this variation could be the difference in laser sensitivity between the two Mastersizers. As mentioned in section '2.4 Comparing Mastersizer 2000 and 3000', the Mastersizer 3000 can measure particles as small as 0.01 µm while the Mastersizer 2000 can only measure particles larger than 0.02 µm. This difference is caused by the upgrade of the equipment. The Mastersizer 3000 has more large angle detectors, more backscatter detectors and a larger measuring angle. The newer equipment also has a different laser path alignment of the blue light, as the blue and red laser path are the same in the newer model.

Another difference is the milliwatt of the blue light, which is increased to 10 milliwatt instead of 0.3 milliwatt on the Mastersizer 2000. Furthermore, the algorithm has been changed in the Mastersizer 3000, which may be due to the changes in the newer model. Because of the increased sensitivity of smaller particles, the equipment is most likely more sensitive to variations and disturbances as well.

Use of a different Absorption Index

Due to the difference in sensitivity as mentioned above, results between the Mastersizer 2000 and 3000 differ considerably from each other. This difference may be lowered by changing the optical parameters of the Mastersizer 3000, as the increase in sensitivity has a big impact on the use of the correct optical parameters. Since the Mastersizer 2000 is not as sensitive to small particles and thus not as sensitive to changes to the RI and ABS, the results of the Mastersizer 2000 do not require a change in its absorption index.

To test this hypothesis, the effect on the PSD of the unfractionated model emulsion was examined by increasing and decreasing the ABS BL for measurements done on the Mastersizer 3000, varying at 0.0005, 0.001 (standard), 0.005 and 0.01. The result can be seen in Figure 61.

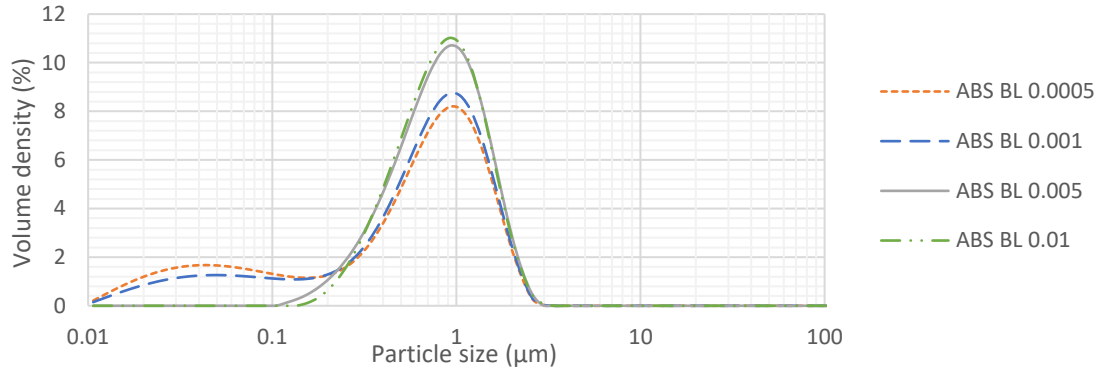

Figure 61: PSD of the average curve of the unfractionated model emulsion at an obscuration rate of 0.8% and stirring speed of 800 rpm, using different absorption indexes for the blue light (ABS BL).

As can be seen in the figure, changing the ABS BL has a significant impact on the characteristics of the PSD. Here, an ABS BL 0.001 is the standard used in all experiments. What is interesting in this figure is that a change of a factor of 5 and 10 prevents a left sided unexpected peak to occur. The hypothesis was also tested on pasteurized milk using an ABS BL of 0.0005, 0.001, 0.005 and 0.01 to investigate the changes of the PSD when changing the ABS BL on this sample. A similar effect could be seen, as the distribution of the unexpected left sided peak lowers when the ABS BL is increased.

When comparing these different values of the ABS BL to the PSD from the unfractionated model emulsion measured on the Mastersizer 2000, an ABS BL of 0.01 on the Mastersizer 3000 seems to match the PSD of the Mastersizer 2000 quite closely (Figure 62).

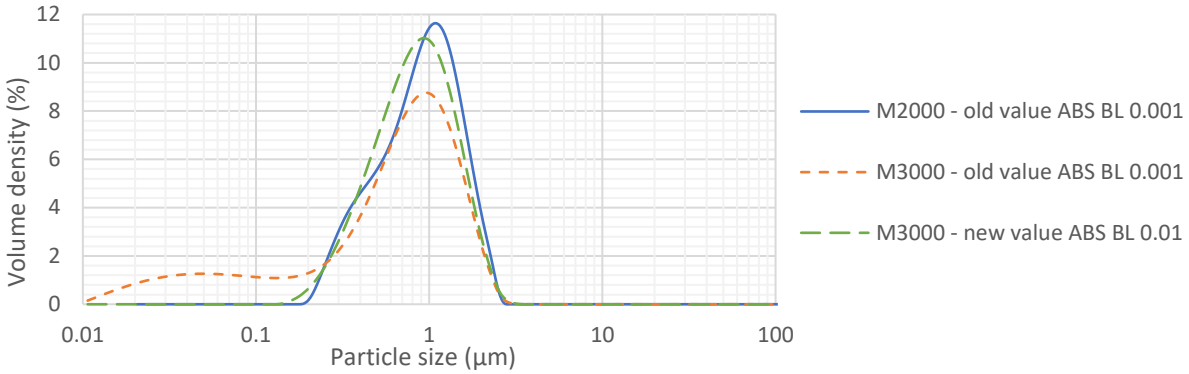

Figure 62: PSDs of the unfractionated model emulsion measured on the Mastersizer 2000 and 3000 with a stirring speed of 800 rpm and an obscuration rate of 0.8%, comparing the 'old values' of ABS BL 0.001 (measured on the Mastersizer 2000 and 3000) compared to the 'new value' of ABS BL 0.01 (measured on the Mastersizer 3000).

Therefore, an ABS BL of 0.01 was used on all obscuration rates of the unfractionated model emulsion measured on the Mastersizer 3000 to investigate the impact of the new ABS BL on the PSD at different obscuration rates. This can be seen in Figure 63.

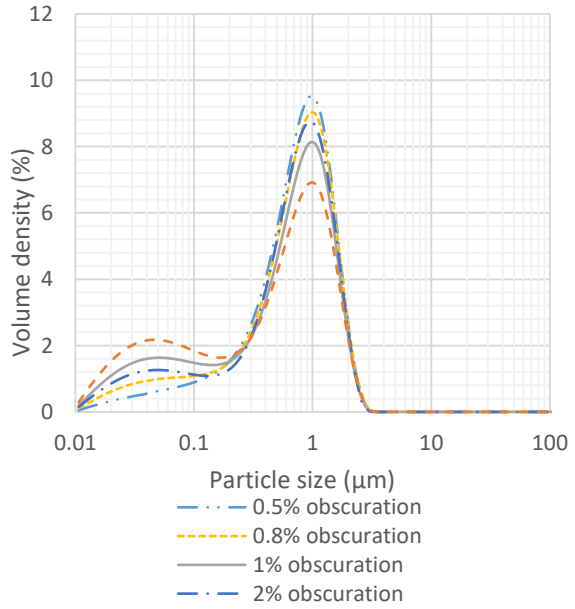

Figure 63.A: PSD of the averages of the unfractionated model emulsion measured on the Mastersizer 3000 with an obscuration rate of 0.5%, 0.8%, 1%, 2% and 5% using an ABS BL of **0.001**.

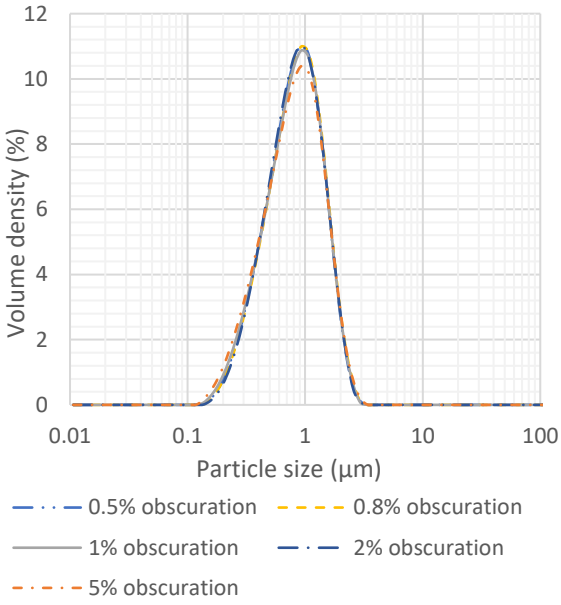

Figure 63.B: PSD of the averages of the unfractionated model emulsion measured on the Mastersizer 3000 with an obscuration rate of 0.5%, 0.8%, 1%, 2% and 5% using an ABS BL of **0.01**.

In the figure a remarkable difference can be seen. At an ABS BL of 0.001 a left sided unexpected peak can be seen at all obscuration rates (Figure 63.A), which is considered to be caused by multi scattering. However, all left sided unexpected peaks are eliminated when changing with a factor of 10 to an ABS BL of 0.01 (Figure 63.B). Similar results are obtained when changing the absorption of the fractionated model emulsion.

Moving to pasteurized milk, an ABS BL of 0.005 on the Mastersizer 3000 seemed to match the Mastersizer 2000 more closely than an ABS BL of 0.01 that is used for the unfractionated model emulsion. The comparison of the 'old' and 'new' ABS BL for pasteurized milk can be seen in Figure 64.

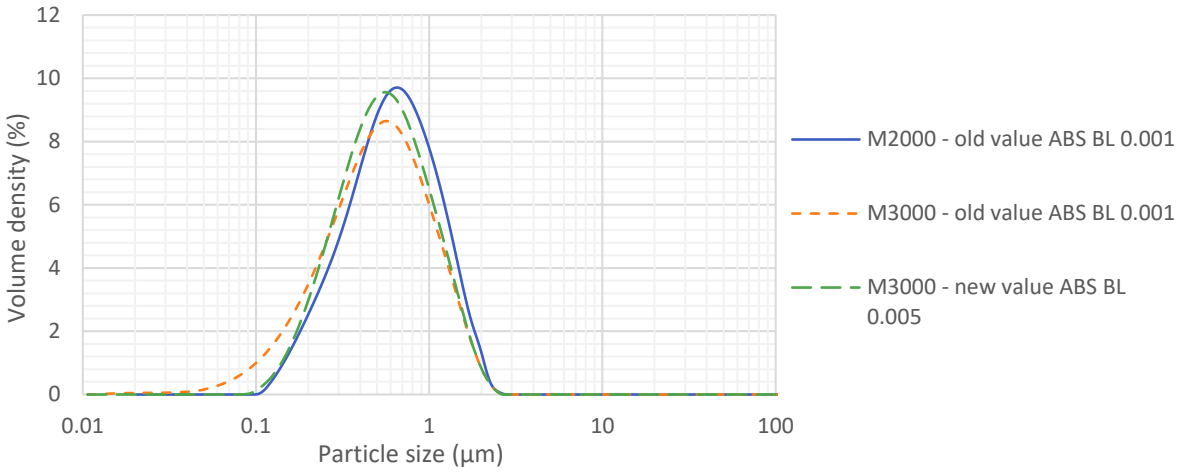

Figure 64: PSDs of the average curves of pasteurized milk, disregarding curves containing a unexpected peak, measured on the Mastersizer 2000 and 3000 with a stirring speed of 800 rpm, an obscuration rate of 2% and 2 mL of solution A, comparing the 'old values' of ABS BL 0.001 (measured on the Mastersizer 2000 and 3000) compared to the 'new value' of ABS BL 0.005 (measured on the Mastersizer 3000).

As can be seen in the figure, using a different ABS BL on pasteurized milk also shows results matching the Mastersizer 2000 more closely.

Using an ABS BL of 0.005 on pasteurized milk also impacts the D [3,2] greatly, as the difference between the D [3,2] measured on the Mastersizer 2000 and 3000 at an obscuration of 2% is reduced to 21% instead of 38% when using an ABS BL of 0.001 (Figure 65).

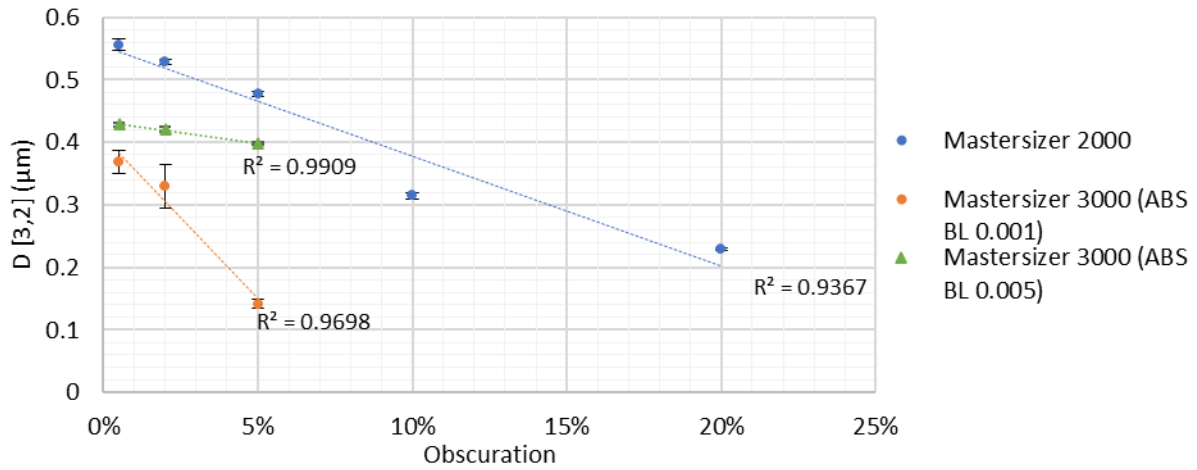

Figure 65: D [3,2] of averages of pasteurized milk measured at different obscuration rates on the Mastersizer 2000 and 3000 with standard deviation comparing an ABS BL of 0.001 with 0.005.

Comparing the D [3,2] of the unfractionated model emulsion using an ABS BL of 0.001 and 0.01 in Figure 66, a large difference can be seen between the two ABS BL as well. Using the ABS BL of 0.01, a 12% difference between the Mastersizer 2000 and 3000 at an obscuration rate of 2%. Which is significantly smaller than the difference of 80% between the Mastersizer 2000 and 3000 when using an ABS BL of 0.001 on the Mastersizer 3000.

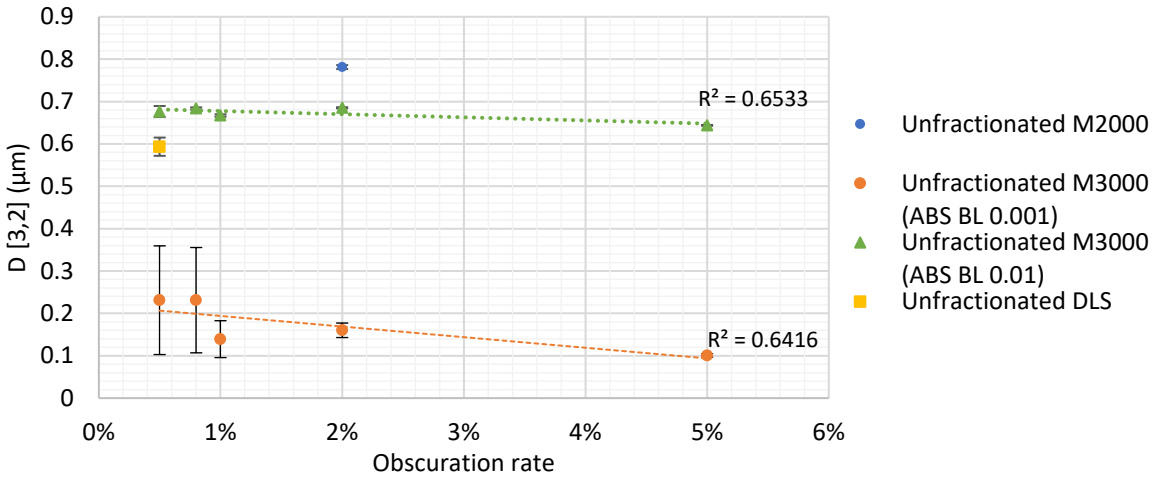

Figure 66: D [3,2] of averages of the unfractionated model emulsion measured at different obscuration rates on the Mastersizer 2000 and 3000 with standard deviation comparing an ABS BL of 0.001 with 0.01.

Similar results are obtained when comparing the D [4,3] of pasteurized milk at 2% obscuration with an ABS BL of 0.001 and 0.005. The difference between the Mastersizer 2000 and 3000 is reduced to 20% when using an ABS BL of 0.005 instead of 25% when using an ABS BL of 0.001. For the model emulsion, using an ABS BL of 0.01 reduces the difference between the Mastersizer 2000 and 3000 to 12% instead of 32% when using an ABS BL of 0.001. In general, therefore, it seems that when comparing the D-values of the Mastersizer 2000 and 3000 at an obscuration of 2% a margin of error of 20% should be considered. This is the largest difference that can be seen when comparing the D-values of the Mastersizer 2000 and 3000.

As can be seen above, the results of the PSD and D-values of the 'new' ABS BL on the Mastersizer 3000 seems to match the Mastersizer 2000 more closely than when using the 'old' ABS BL for the Mastersizer 3000. As mentioned in section '3.2 Laser Diffractometry', absorption can be defined as how much laser light is absorbed by the particle during the experiment. Because of the different laser path of the blue light, stronger laser power and increased number of detectors the Mastersizer 3000 has an increased sensitivity for smaller particles. By increasing the ABS BL, the software interprets that less light is going through the sample, resulting in the diffraction of less light. This will lead to less sensitivity to smaller particles, which reduces or even prevents the left sided unexpected peak.

It should be noted that the ABS BL might need to be optimized depending on the sample tested, since different ABS BL were used depending on the sample measured. A note of caution is due here since no literature or similar experiments were found to confirm this change in ABS BL due to increased sensitivity. Furthermore, this change in ABS BL was not investigated in depth due to lack of time, thus it is recommended further study this variable.

Concluding, the sensitivity of the equipment is of great influence of the PSD as can be seen when comparing the PSD of the Mastersizer 2000 and 3000. This confirms the hypothesis of the influence of sensitivity on the PSD. It is believed this difference may be created due to the increased sensitivity of the Mastersizer 3000 compared to the Mastersizer 2000, this difference could be minimized by increasing the ABS BL. It is uncertain to which extend the ABS BL needs to be increased in order to obtain comparable PSDs of the Mastersizer 2000 and 3000 for samples other than mentioned above. The chosen ABS BL for pasteurized milk and the model emulsion were determined by comparing to the Mastersizer 2000. Therefore, these results need to be interpreted with caution since the ABS BL needs to be determined empirically or by experience.

6. Conclusion

This research has identified that there are several possible reasons for why unexpected peaks appear when measuring oil droplets in homogenized milk and likewise products. First, a large difference is identified between the two versions of the laser diffraction (LD) equipment (two different models still in use, made by the same manufacturer).

On the older model (Mastersizer 2000), unexpected peaks have mainly been observed on the right side of the main distribution. These unexpected peaks are most likely caused by air since the dispersing unit has a small volume, is manually controlled and lacks a deaeration function. Other reasons for right sided unexpected peaks are dirt in the equipment and too low sample concentration (i.e. obscuration rate), causing fluctuation between the measured sample and the background which can result in an unexpected peak. All in all, it can be concluded that the right sided unexpected peaks are artifacts and thus not real.

The second finding is focused on unexpected peaks on the left side of the main distribution. This problem has mainly occurred on the newer model of LD equipment (Mastersizer 3000). There are several reasons for why these peaks occur. The first type of left sided unexpected peak is believed to be caused by a too high sample concentration, which results in the effect of multi scattering. This occurs in both models of the equipment, however the level of sample concentration needed to get a multi scattering effect is different in each model as the newer model has an increased sensitivity to smaller particles which increases the risk of multi scattering. Another type of left sided unexpected peaks is an increased standard deviation caused by using unoptimized variables of the LD equipment (e.g. too high stirring speed or too low sample concentration). This occurs mainly in the newer model of the equipment. A high stirring speed causes a higher deviation due to a higher flux of the sample through the laser at higher stirring speeds. While low sample concentration can cause a high standard deviation as the particles passing through the system are not constant. Both types of the left sided unexpected peaks are believed to be artifacts.

Besides multi scattering and a high standard deviation, another type of left sided unexpected peak can be seen on the newer model of the equipment. This type of unexpected peak shows a variation in particle size distribution (PSD) between the older and newer version of equipment. This is believed to be caused by an increase in sensitivity towards fine particles on the newer model due to changes in the detection system, different alignment and increase in power of the blue light laser. By increasing the absorption index blue light, left sided unexpected peaks can be modified. This may provide more comparable results of the older and newer model. However, more research should be done to support this theory. Concluding that measurements made on LD equipment should be evaluated carefully, as the refractive index and absorption index have a significant impact on the PSDs provided by the newer model. When similar PSDs are obtained, it is suggested to consider a margin of error when comparing between the older and newer model of equipment.

7. Best practices

While searching for reasons for why the right and left sided peaks occur, some best practices were developed as an effect of how to get the best results. These findings will be listed below. The findings are only valid for the Mastersizer 2000 and 3000.

General recommendations

First, the importance of a correct refractive index and absorption index should be mentioned. It is extremely crucial that these values are correct for the sample used or else the data will be not reliable. To check the fit of the refractive index and absorption index, the weighted residual can be used. This is a value provided on the Mastersizer software which indicates how well the calculated data was fitted with the measured data (Malvern Instruments, 2013). The value should be under 1% in order to provide reliable data. If the value is over 1%, the refractive index and absorption value might need adjustments.

Another important issue is the quality of the data. This can be checked on the Mastersizer 3000 software. While the Mastersizer 2000 does not have such a function, the data can be imported in the Mastersizer 3000 software to use the data quality. The data quality function checks how well the obscuration rate works for the sample and if the residual is a good fit. Even a different cycle of the same measurement, the data quality can differ. It is therefore important to check the data quality and disregard the samples with a warning for the overall data quality.

Also, the use of an average measurement is recommended in order to ensure reliable data. The data of this project is mainly gathered by injecting three different samples, which are each measured three times. This provides nine measurements for each sample/setting. Tetra Pak follows a procedure where a sample is injected once and measured six times, which would also provide multiple PSDs. Before creating an average, curves of which the data quality is insufficient or curves that show an air bubble and/or dirt on the right side of the curve should be deleted. Thus, it is recommended to measure enough PSDs in order to create an average when some data must be disregarded. This typically seems to be 6 or more PSDs.

Furthermore, when a high standard deviation can be seen between measurements of the same sample, it is suggested to check several possible causes. The obscuration rate might be too low, causing a slight variation in particles passing through the laser with time which could result in a high standard deviation. Other reasons for a too high deviation are a too high stirring rate or an unstable background.

Background check

As described in section ‘5.1.2, sub-section Dirt in the Mastersizer’ can cause the occurrence of right sided unexpected peaks. To avoid this, the background should be checked and show a curve that resembles a ski slope where detector 1 is under 100 and detector 20 under 20 (Malvern Panalytical, 2017; Larsson, 2020). An example of a clean background can be seen in Figure 67 below. When the background indicates an unclean Mastersizer by e.g. showing a bump in the curve, the Mastersizer should be cleaned. For cleaning guidelines, see Appendix F.

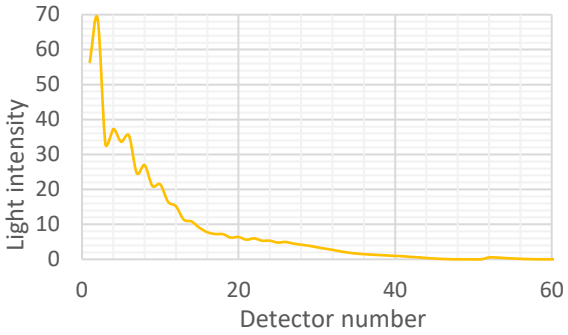

Figure 67: Background curve indicating a clean Mastersizer on the Mastersizer 3000

Besides a check of the cleanliness of the background, the stability of the background should also be checked. This can be done after adding the sample. The Mastersizer shows a 'light scattering graph', a stable background shows variation and jumps from positive to negative peaks in this graph. If there is a lot of negative peaks, one should wait with the measurement and make sure the background is stable.

Varying obscuration rate

When investigating the unexpected peak now found on the left side on the Mastersizer 3000, additional experiments were done to determine the optimal obscuration rate on the Mastersizer 3000. It was discovered that an obscuration rate optimal on the Mastersizer 2000 is not necessarily the obscuration rate that should be used on the Mastersizer 3000. While on the Mastersizer 2000 no left sided unexpected peak seems to appear at an obscuration rate of 5%, this does happen on the Mastersizer 3000. As mentioned before, this peak is most likely caused by multi scattering. It might be said that an obscuration of 2% could be considered too high for the Mastersizer 3000, as the curve shows a lower particle size than the Mastersizer 3000. To find the optimal obscuration rate, an obscuration-titration test can be performed. This is done by testing obscuration rates at an increasing interval and determining when the multi scattering effect occurs by studying the Dv10, Dv50 and Dv90. This was done for unfraction model emulsion at obscuration rates between 1.0 and 2.0%, with an interval of 0.2%. Besides that, 0.5% and 5% was also tested. When multi scattering occurs, the Dv10 and Dv90 will decrease, indicating more smaller particles and less larger particles as the curve shifts towards the left.

As can be seen in Figure 68, the average of both the Dv10 and Dv90 stay quite stable between obscurations of 1 and 2%. However, at 5% there is a decrease of the Dv10, Dv50 and Dv90, indicating a shift towards a smaller particle size and thus multi scattering. Dv90 seems higher at an obscuration of 0.5%, which can be explained by the error of the noise when the obscuration is too low. From these results it can be concluded that there is no difference in the effect of multi scattering between 1 and 2%. Therefore, it is suggested to keep the obscuration rate at 2% to avoid background noise in the measurement for the unfractionated model emulsion.

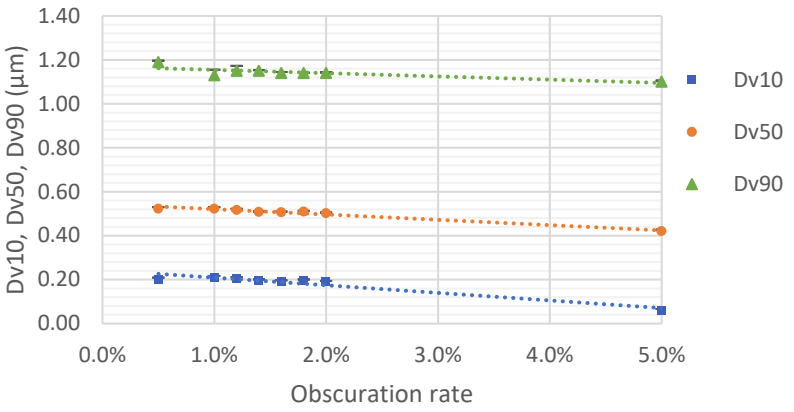

Figure 68: Average particle size and standard deviation for the unfractionated model emulsion with obscuration rates between 0.5 and 5.0% measured on the Mastersizer 3000, disregarding curves with unexpected peaks.

When measuring other variations of milk or completely different products, it is recommended to repeat the obscuration-titration experiment as the effect of multi scattering might occur at different obscuration rates depending on the particle size of the product. It is thought that in general, the bigger the particles, the higher the obscuration rate can be before multi scattering occurs.

Stirring speed

As mentioned above, variations in stirring speed can cause right and left sided unexpected peaks. Stirring at a high speed can result in right sided unexpected peaks on the Mastersizer 2000 and a high standard deviation, which might show as a left sided unexpected peak, on the Mastersizer 3000. To avoid this, it is recommended to keep the stirring rate below 1800 rpm. A stirring rate of 800 rpm provides a low standard deviation and no air bubbles on the Mastersizer 3000 and is thus considered an optimal stirring rate. On the Mastersizer 2000 there are some air bubbles when measuring at 800 rpm, however it is unclear if this is caused by the stirring rate or the fact that the Mastersizer 2000 has a manual stirring unit without a degas function. Insufficient research has been done on stirring rates below 800 and between 800 and 1800 rpm to compare and examine any possible differences in the occurrence of unexpected peaks on the Mastersizer 2000. However, a speed of 320 rpm seems to cause no right sided unexpected peak on the Mastersizer 2000 as described in ‘5.1.2, sub-section Stirring sped in the dispersion unit’, but this is considered extremely low and may cause a high standard deviation. As recommended by Malvern a stirring rate of 1200 rpm would be preferable, but testing needs to be done to confirm the use of this stirring speed. In order to give adequate recommendations for the Mastersizer 2000 more research would be needed on stirring between 320 and 800 rpm and between 800 and 1800 rpm.

8. Next steps

The recommendations for further research and improvements are stated below.

- Further research is needed to fully map the validity and reliability of laser diffraction methods when applied to determining the details of the drop size distributions in emulsions. At the moment, there seems to be a difference between all three methods. Therefore, it is recommended to investigate this further. This would preferably be done with a direct method to remove the uncertainties that indirect methods bring.
- It is believed that there is a correlation between obscuration rate and the apparent particle size as estimated by the laser diffraction equipment. The suggested correlation is the bigger the particles in a sample, the lower the obscuration rate needed but this would need to be further investigated with a range of different products (e.g. different types of milk) to be confirmed.
- The model emulsion was homogenized at a very high pressure but gave a higher particle size than expected at this pressure. It is recommended to investigate the efficiency of the homogenizer by comparing it to a different brand of homogenizer and testing at different pressures. What could also be of interest is trying different settings such as a different ratio between the first and second stage.
- To further investigate the influence of a broad particle size range on the newer model of LD equipment, a range of model emulsion with different ranges of particle sizes could be measured. This would show whether the accuracy of the older model is depended on the particle size range or not.
- The manufacturer of the equipment tested in this project has suggested to adjust the stirring speed to 1200 rpm to avoid sedimentation in the dispersing unit. While this may not work for the older model, since it is expected that this would increase the amount of air bubbles. This may improve the standard deviation on the newer model since a slower stirring speed needs a longer time for the background to stabilize. Therefore, it is suggested to test different stirring speeds and examine the influence on the standard deviation.
- Further research is needed in order to confirm that left sided unexpected peaks on the newer model can be prevented by increasing the absorption index blue light. If that is the case, research needs to be done to experimentally obtain the most adequate value of the absorption index of the blue light on the newer model.
- If absorption index blue light does need to be adjusted and the value is known, further investigation is needed to indicate an expected margin of error from the two models.

References

Anton Paar. (n.d.). *The principles of dynamic light scattering.* Retrieved 2 June 2020, from https://wiki.anton-paar.com/en/the-principles-of-dynamic-light-scattering/

Born, M., & Wolf, E. (1999). *Principals of optics: Electromagnetic theory of propagation, Interference and diffraction of light*. Cambridge University Press.

Bylund, G. (2015). *Dairy processing handbook* (3rd ed.). Tetra Pak.

Driscoll, D., Etzler, F., Barber, T., Nehne, J., Niemann, W., & Bistrian, B. (2001). Physicochemical assessments of parenteral lipid emulsions: light obscuration versus laser diffraction. *International Journal Of Pharmaceutics,* 219(1-2), 21-37. https://doi.org/10.1016/s0378-5173(01)00626-3

Haugaard, G., & Pettinati, J. (1959). Photometric Milk Fat Determination. *Journal Of Dairy Science,* 42(8), 1255-1275. https://doi.org/10.3168/jds.s0022-0302(59)90730-1

Heuer, M., & Leschonski, K. (1985). Results Obtained with a New Instrument for the Measurement of particle size distributions from diffraction patterns. *Particle & Particle Systems Characterization*, 2(1-4), 7-13. https://doi.org/10.1002/ppsc.19850020102

Hirleman, E.D. (1988). Modeling of Multiple Scattering Effects in Fraunhofer Diffraction Particle Size Analysis. *Particle & Particle Systems Characterization*, 5(2), 57-65. https://doi.org/10.1002/ppsc.19880050202

Horiba. (n.d.). *Choosing Laser Diffraction or Dynamic Light Scattering (DLS) - Horiba.* Retrieved 28 April 2020, from https://www.horiba.com/uk/scientific/products/particle-characterization/education/general-information/practical-tips/choosing-laser-diffraction-or-dynamic-light-scattering-dls/

Horiba-Instruments. (2004). *Theory and techniques of light scattering* (pp. 446–7422).

Hulst, H. (1981). *Light scattering by small particles.* Dover.

ISO. (2020). *Particle size analysis - Laser diffraction methods*. Standard number: ISO 13320:2020. Retrieved from https://www.iso.org/standard/69111.html

Keck, C.M., & Müller, R.H. (2008). Size analysis of submicron particles by laser diffractometry—90% of the published measurements are false. *International Journal Of Pharmaceutics*, *355(1-2)*, 150–163. https://doi.org/10.1016/j.ijpharm.2007.12.004

Malvern Instruments. (2013). *Mastersizer 3000 User Manual* [Ebook] (2nd ed.). Malvern Instruments. Retrieved from https://www.malvernpanalytical.com/en/learn/knowledge-center/user-manuals/MAN0474EN

Malvern Instruments. (2015). *A basic guide to particle characterization* [Ebook] (pp. 6-7). Retrieved 26 April 2020, from https://www.cif.iastate.edu/sites/default/files/uploads/Other_Inst/Particle%20Size/Particle%20Characterization%20Guide.pdf

Malvern Instruments. (2015). *Mastersizer S, Mastersizer 2000 and Mastersizer 3000: Method transfer –how to get the same results on all three systems*. Presentation.

Malvern Instruments. (2020). *Zetasizer Nano Series* [Ebook]. Worcestershire, UK: Malvern Instruments. Retrieved from https://www.malvernpanalytical.com/en/products/product-range/zetasizer-range/zetasizer-nano-range/zetasizer-nano-s

Malvern Panalytical. (2017). *Mastersizer 3000 Customer Training Course Part 1: Basic Principles and Data Quality*. Presentation.

Malvern Panalytical. (2017). *Mastersizer 3000 Customer Training Course Part 1: Basic Principles and Data Quality* [Ebook].

Malvern Panalytical. (2019). *Mastersizer 3000 Smarter particle sizing* [Ebook] (p. 8). Retrieved 26 May 2020, from https://www.malvernpanalytical.com/en/products/product-range/mastersizer-range/mastersizer-3000?creative=311633610439&keyword=%2Bmastersizer&matchtype=b&network=g&device=c&gclid=CjwKCAjw2a32BRBXEiwAUcugiCj4kAE0XQIf-l7JDB1wOrSoJtGcgIcUz1e6Z7lqZiyvG-0XLFTZxBoCzjYQAvD_BwE.

Malvern Panalytical. (2020). *Dynamic light scattering: an introduction in 30 minutes.* Retrieved from https://www.malvernpanalytical.com/en/learn/knowledge-center/technical-notes/TN101104DynamicLightScatteringIntroduction

Michalski, M., Briard, V., & Michel, F. (2001). Optical parameters of milk fat globules for laser light scattering measurements. *Le Lait,* 81(6), 787-796. https://doi.org/10.1051/lait:2001105

Mie, G. (1908). Beiträge zur Optik trüber Medien, speziell kolloidaler Metallösungen. *Annalen Der Physik*, 330(3), 377-445. https://doi.org/10.1002/andp.19083300302

Müller, R., & Schumann, R. (1996). *Teilchengrössenmessung in der laborpraxis*. Stuttgart.

Nielsen, C., Kjems, J., Mygind, T., Snabe, T., & Meyer, R. (2016). Effects of Tween 80 on Growth and Biofilm Formation in Laboratory Media. *Frontiers In Microbiology*, *7*. https://doi.org/10.3389/fmicb.2016.01878

Obiols-Rabasa, M., Grusch, M., Persson, L., & Lundberg, D. (2019). *Effect of refractive index and absorbance in the output data in laser diffraction experiments* [Ebook]. Lund: CR Competence AB.

Qi, P. (2007). Studies of casein micelle structure: the past and the present. *Le Lait,* 87(4-5), 363-383. https://doi.org/10.1051/lait:2007026

Ransmark, E., Svensson, B., Svedberg, I., Göransson, A., & Skoglund, T. (2019). Measurement of homogenisation efficiency of milk by laser diffraction and centrifugation. *International Dairy Journal*, *96*, 93-97. https://doi.org/10.1016/j.idairyj.2019.04.011

Rawle, A. (2006). *Optical Properties: the Gladstone Dale Approach*. Malvern Instruments.

Römpp, H. (1995). *Chemie-Lexikon*. Thieme.

Stratton, J. (1941). *Electromagnetic theory*. McGraw-Hill Companies.

Tetra Pak. (2019). *Tetra Pak Milk SOP*. Tetra Pak.

Walstra, P., Wouters, J., & Geurts, T. (2005). *Dairy Science and Technology*. Boca Raton: CRC Press. https://doi.org/10.1201/9781420028010

Appendix

Appendix A: Concentration of Emulsifier

The amount of emulsifier needed depends on:

CMC = critical micelle concentration [mmol/l]

Diameter of the oil droplet $d_{oil\ droplet}$ = 1 x10^{-6} [m]

Part of oil in the emulsion mixture α = 3 [% wt]

The radius, *r*, the volume, *V*, and area, *A*, of one oil droplet can be calculated by:

$$r_{oil\ droplet} = \frac{d_{oil\ droplet}}{2} \quad [m]$$

$$V_{oil\ droplet} = \frac{4\pi r^3{}_{oil\ droplet}}{3} \quad [m^3]$$

$$A_{oil\ droplet} = 4\pi r^2{}_{oil\ droplet} \quad [m^2]$$

The critical micelle concentration, *CMC*, and molar weight, *M,* of the emulsifier is

$CMC_{emulsifier}$ = 0.012 [mmol/l]

$M_{emulsifier}$ = 1.22754 [g/mmol]

The amount of emulsifier needed to cover a particular surface is given by the:

Γ = 3x10^{-3} [g/m^2]

The density of the emulsion, $\rho_{emulsion}$, depends on the density of oil, ρ_{oil}, the density of the water, ρ_{water}, and α:

$$\rho_{water} = 1 \quad [kg/l]$$

$$\rho_{oil} = 0.910 \quad [kg/l]$$

$$\rho_{emulsion} = \rho_{water} \cdot (1-\alpha) + \rho_{oil} \cdot \alpha \quad [kg/l]$$

Note that the density of the emulsifier is to be negligible

$$V_{emulsion} = 1 \quad [l]$$

$$V_{oil} = V_{emulsion} \cdot \alpha \quad [l]$$

$$V_{water} = V_{emulsion} \cdot (1-\alpha) \quad [l]$$

Note that the volume of the emulsifier is considered to be negligible

Amount of oil droplets, *n*, is:

$$n = \frac{V_{oil}}{V_{oil\ droplet}} \quad [\text{number of droplets in the emulsion}]$$

The amount of Tween 80 needed in the emulsion is

$$V_{emulsifier} = \frac{M_{emulsifier} \cdot CMC_{emulsifier} \cdot V_{emulsion} + n \cdot \Gamma \cdot A_{oil\ droplet}}{\rho_{emulsion}} \quad [l]$$

$$V_{emulsifier} = \frac{1.22754\ \frac{g}{mmol} \cdot 0.012 \frac{mmol}{l} \cdot 1\ l + 5.73x10^{16} \cdot 3\text{x}10^{-3} \frac{g}{m^2} \cdot 3.14\text{x}10^{-12}\ m^2}{997.3\ \frac{g}{l}} \quad [l]$$

$V_{emulsifier}$ = 0.008 l

Appendix B: Changes to the optical parameter

In order to understand to what extend the results are influenced by a change of the optical parameters, variations of the particle size distribution due to changes of the refractive index (RI) and the absorption index (Abs) in pasteurized milk PSD were investigated on the Mastersizer 2000. The Malvern Mastersizer software allows changes of the optical parameters also after the measurement itself. The simulations of possible results were performed by adjusting the standard RI and absorption index used (RI red light 1.46, RI blue light 1.47, Abs red light 0.001). Different combinations were made changing RI red light ±10%, RI blue light ±10% and a combination of the two both adjusted ±10%. The Abs red light was adjusted to 0.01 and 0.0001.

The simulations of the measurements can be seen in below. Most show dramatic and unexpected high influence of the optical parameters on the analysis results. Changes in the optical parameters not only influence the mean particle size but also the particle size distribution. However, they do not have an influence on the appearance of right sided unexpected peaks. For example, the change of the RI red light causes multi-modal or a high peak in the volume distribution which is not what one would expect when measuring the particle size of pasteurized milk. The impact of changing the refractive index in the PSD is higher compared with changes in the Absorption Index, similar results were obtained by M. Keck & H. Müller (2008). Thus, it can be concluded that the right sided unexpected peaks are not created due to a wrongly chosen optical parameters on the Mastersizer 2000 software.

These optical parameters were used for the simulations, the raw data was re-calculated combining each parameter in pasteurized milk curve. All changes were done on one curve using a stirring speed of 800 rpm, obscuration rate of 2% and 2 mL of solution A.

Refractive Indices Red light – RI red (632.8 nm)	Refractive Indices Blue Light - RI blue (470 nm)	Absorption Indices red light
1.46	**1.47**	**0.001**
Increase 10% SOP RI		
1.606	**1.47**	**0.001**
1.46	1.617	**0.001**
1.606	1.617	**0.001**
Decrease 10% SOP RI		
1.314	**1.47**	**0.001**
1.46	1.323	**0.001**
1.413	1.323	**0.001**
Absorption Indices		
1.46	**1.47**	0.01
1.46	**1.47**	0.0001

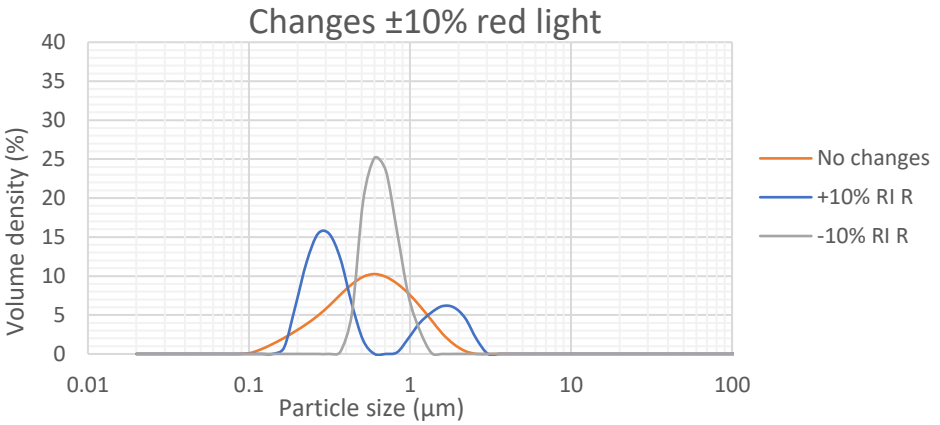
Changes ±10% red light
Volume density (%)
Particle size (µm)
No changes
+10% RI R
-10% RI R

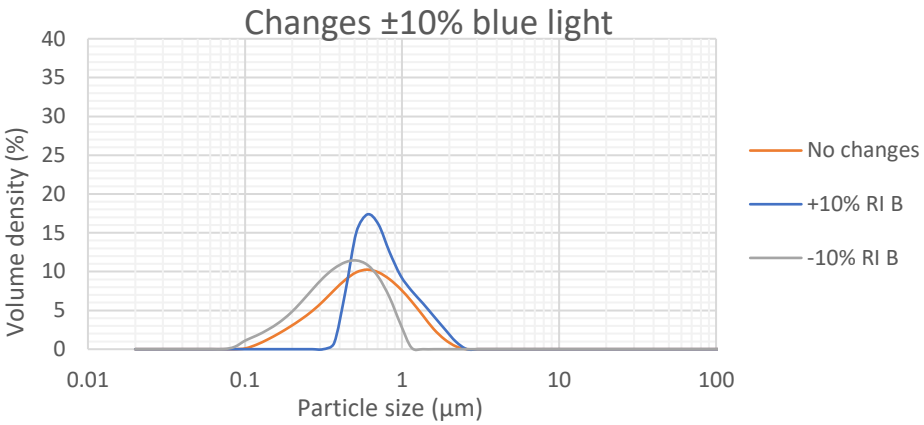
Changes ±10% blue light
Volume density (%)
Particle size (µm)
No changes
+10% RI B
-10% RI B

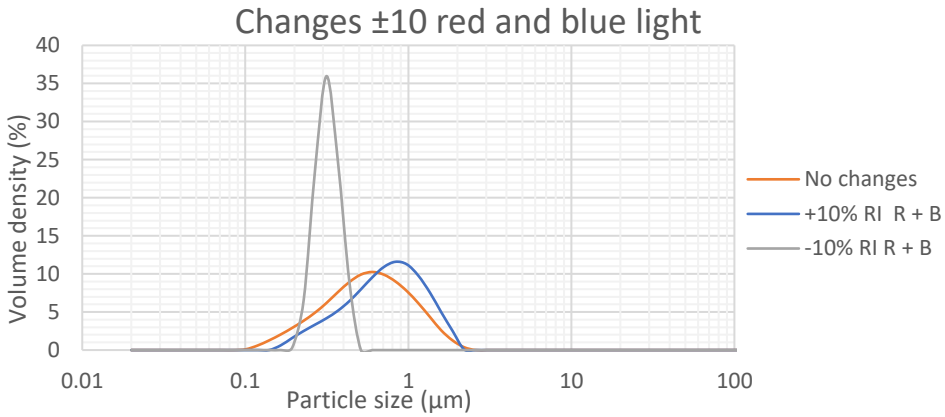
Changes ±10 red and blue light
Volume density (%)
Particle size (µm)
No changes
+10% RI R + B
-10% RI R + B

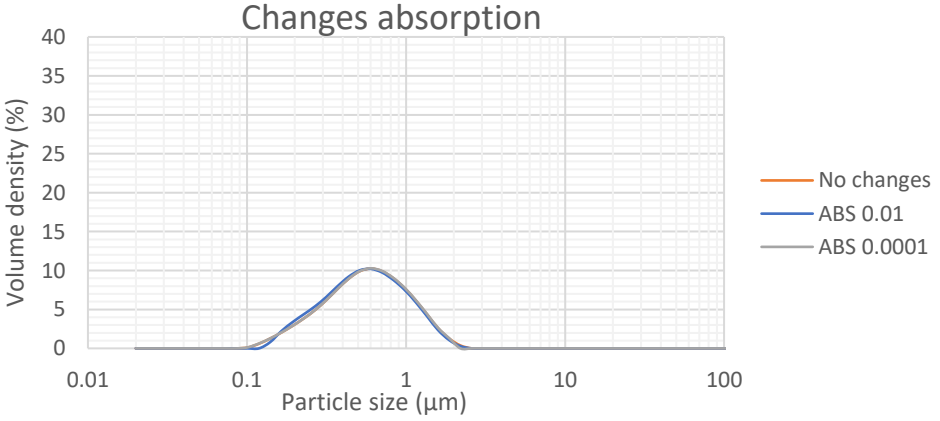
Changes absorption
Volume density (%)
Particle size (µm)
No changes
ABS 0.01
ABS 0.0001

Appendix C: Comparison of pasteurized, ESL and non-homogenized milk

Average curves of variation of Solution A (disregarding curves with right sided unexpected peaks):

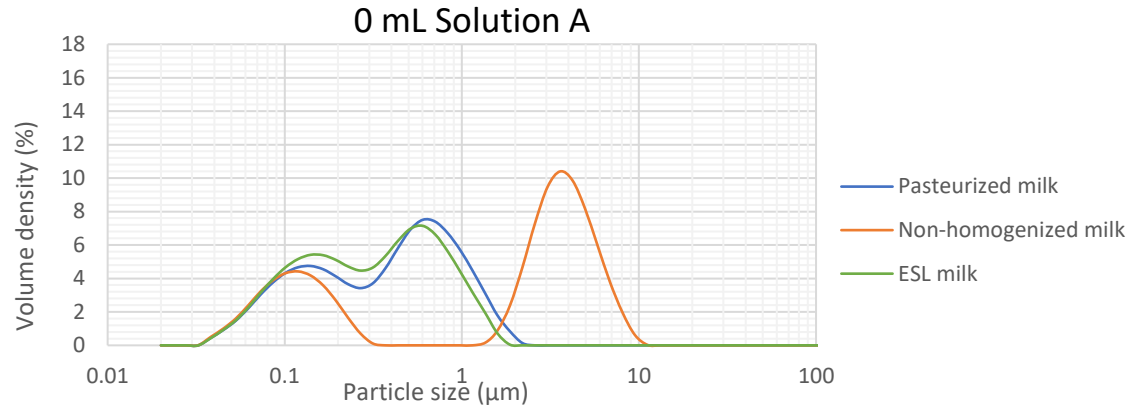

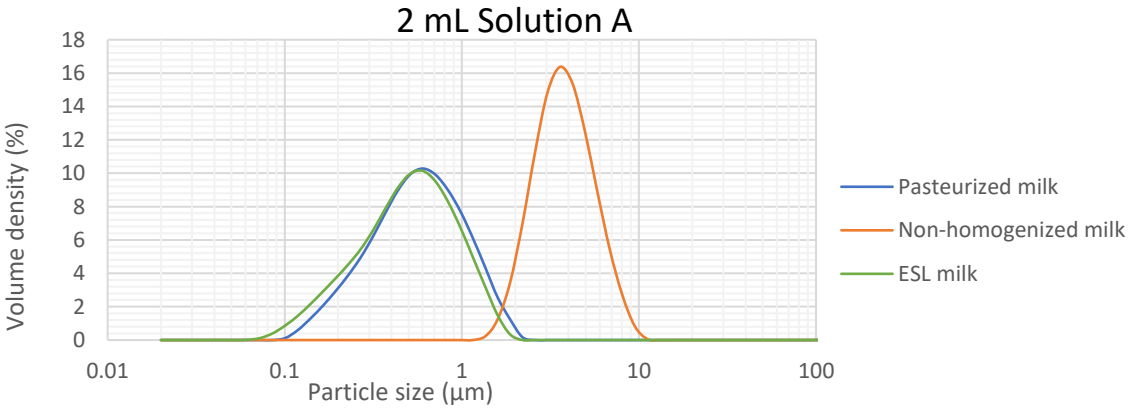

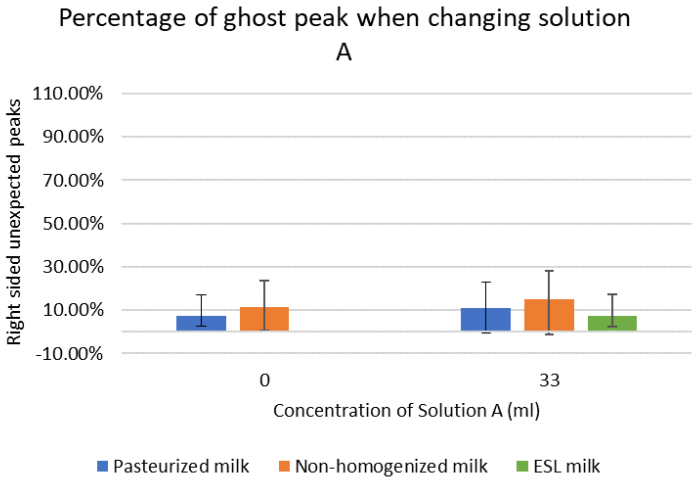

Average curves of variation of stirring rate (disregarding curves with right sided unexpected peaks):

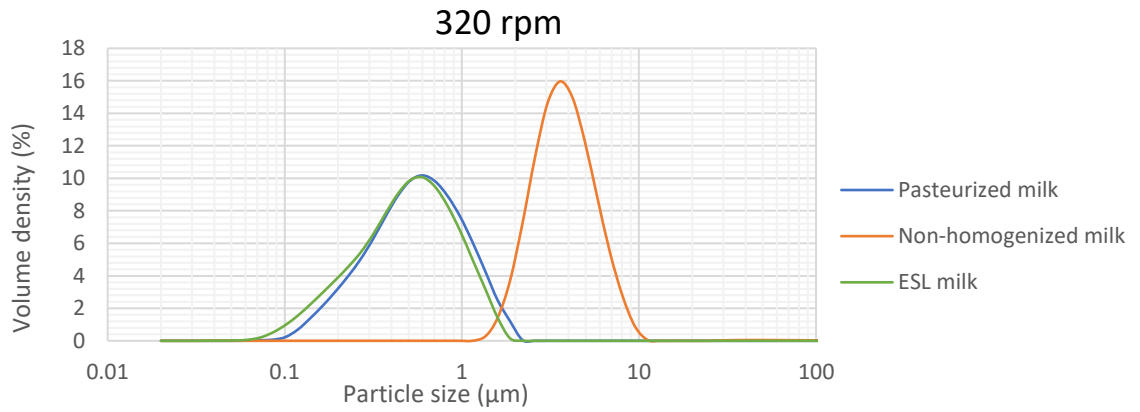

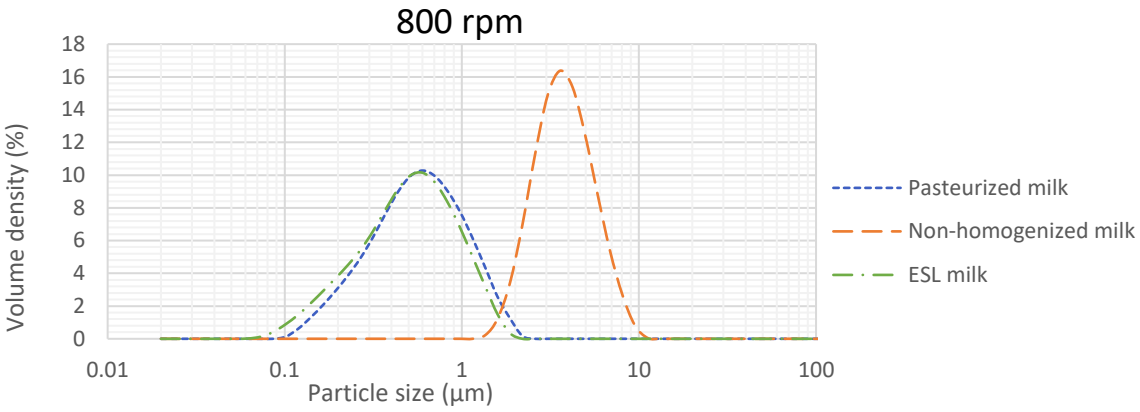

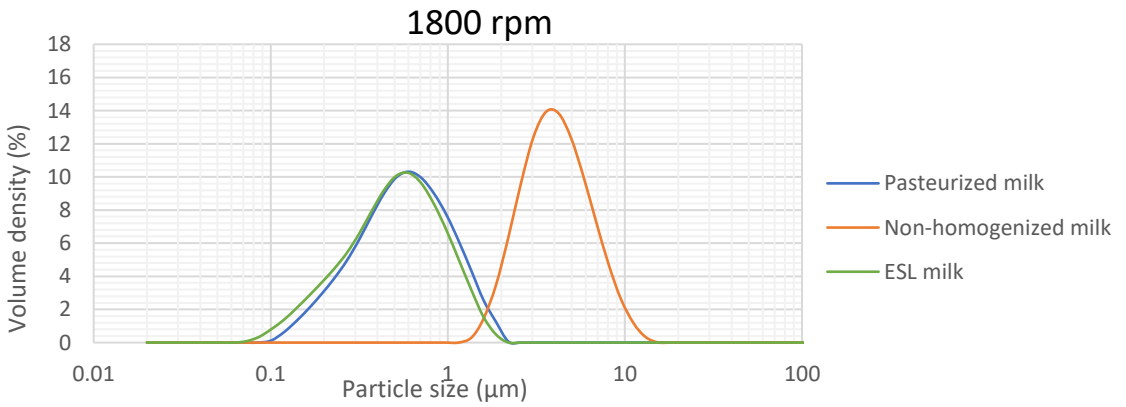

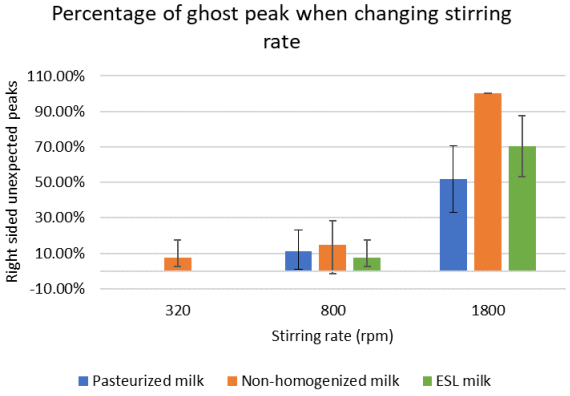

Average curves of variation in obscuration rate (disregarding curves with right sided unexpected peaks):

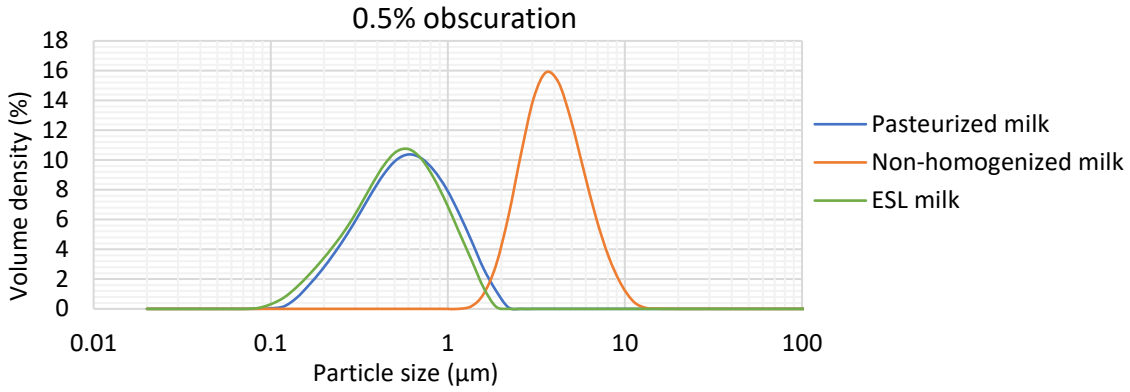

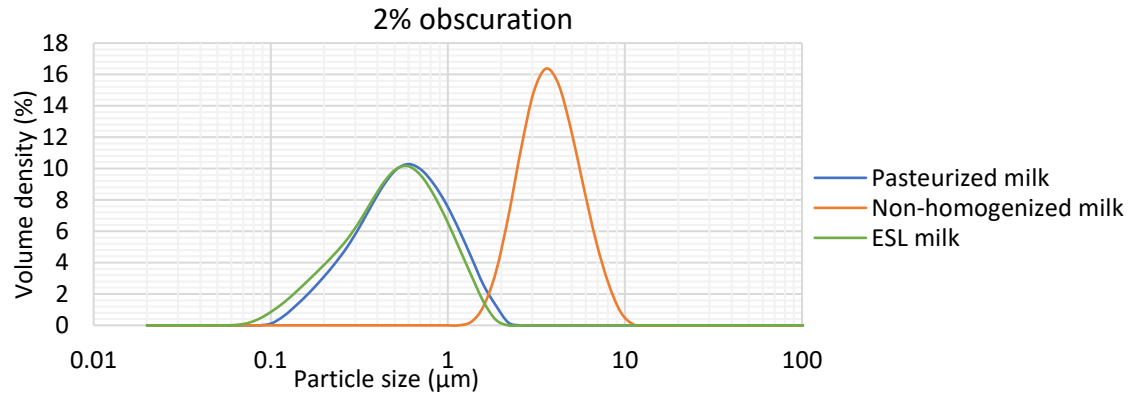

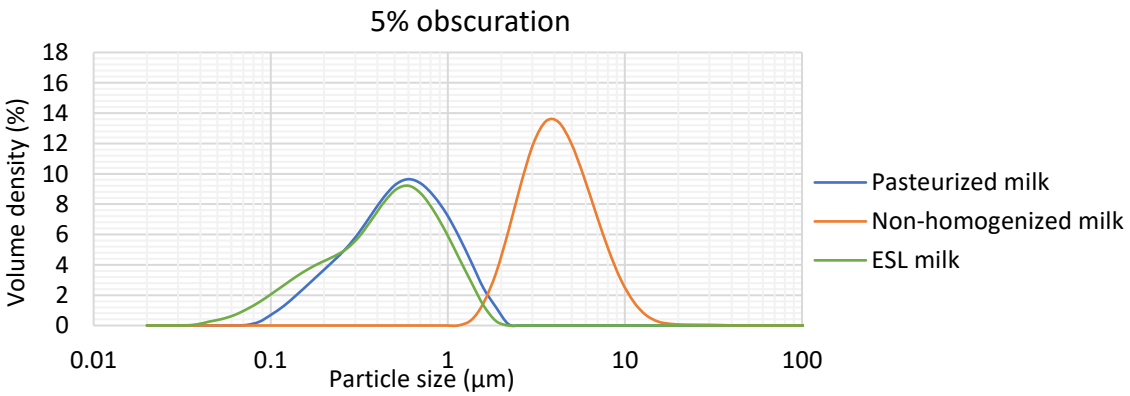

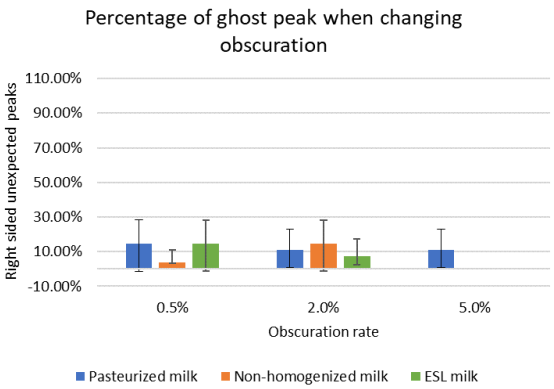

Appendix D: Raw data of the unfractionated and fractionated emulsion measured on the DLS

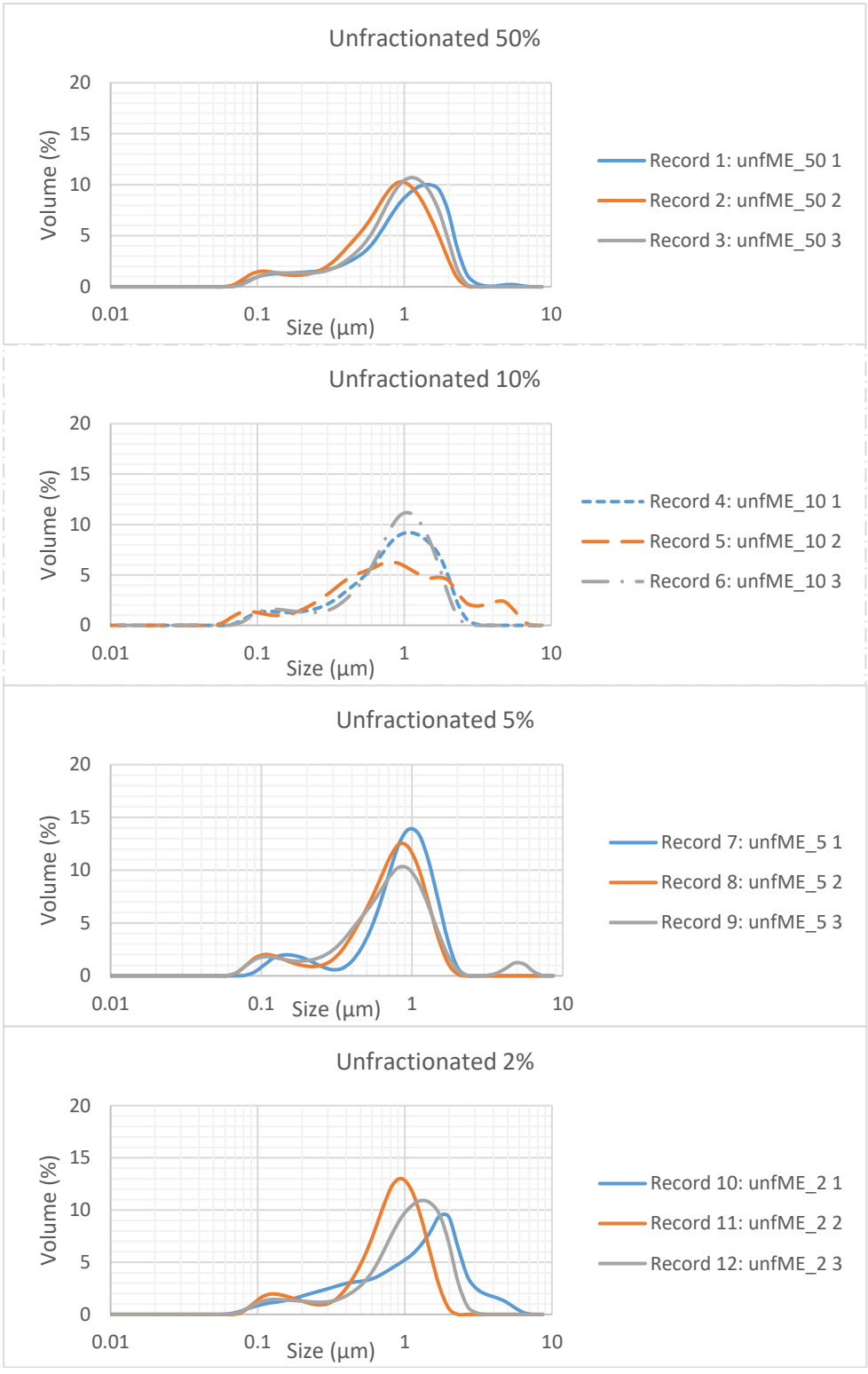

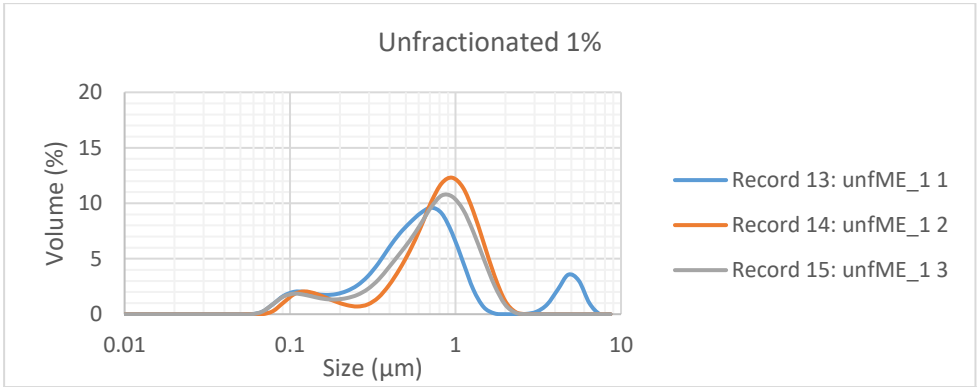
Unfractionated 1%
Volume (%)
20
15
10
5
0
0.01
0.1
1
10
Size (µm)
Record 13: unfME_1 1
Record 14: unfME_1 2
Record 15: unfME_1 3

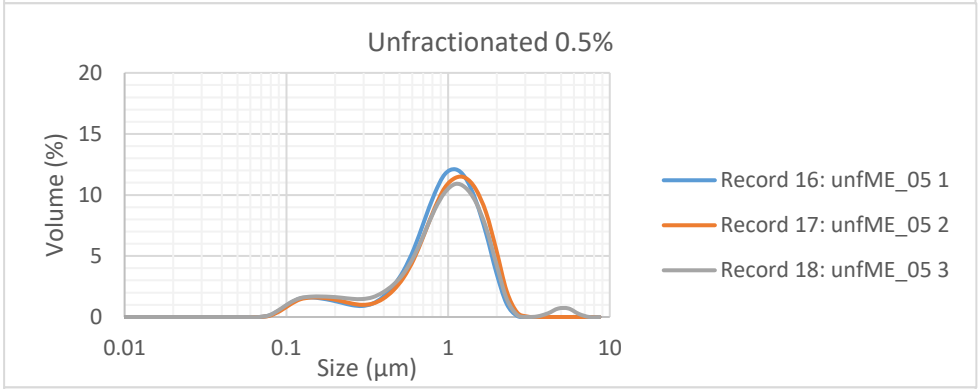
Unfractionated 0.5%
Volume (%)
20
15
10
5
0
0.01
0.1
1
10
Size (µm)
Record 16: unfME_05 1
Record 17: unfME_05 2
Record 18: unfME_05 3

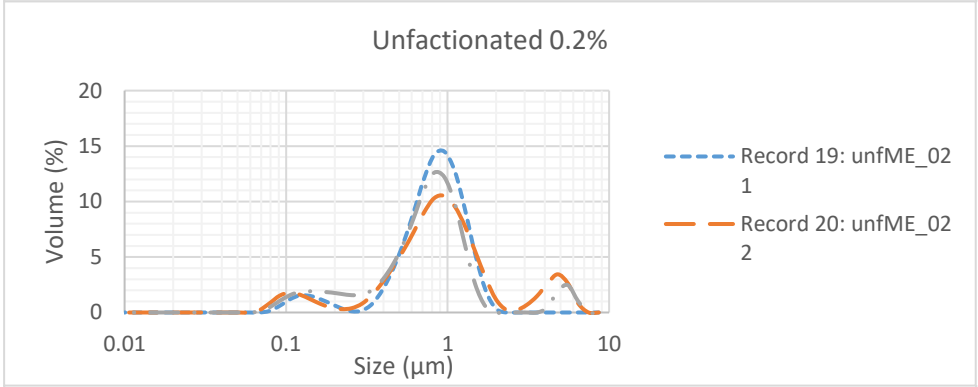
Unfactionated 0.2%
Volume (%)
20
15
10
5
0
0.01
0.1
1
10
Size (µm)
Record 19: unfME_02 1
Record 20: unfME_02 2

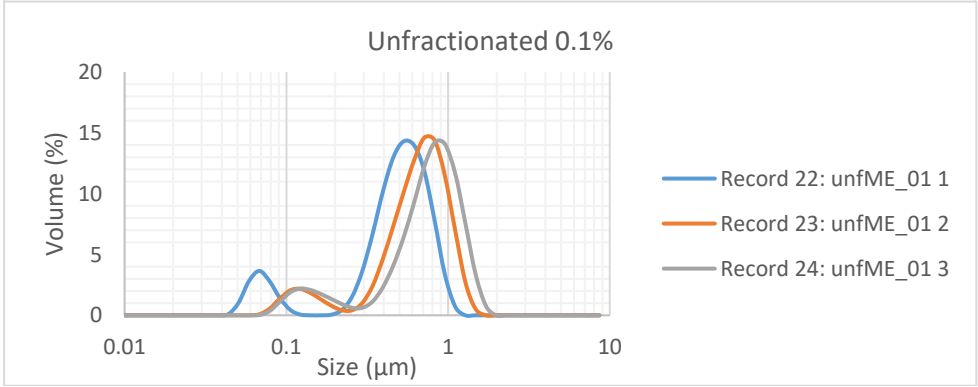
Unfractionated 0.1%
Volume (%)
20
15
10
5
0
0.01
0.1
1
10
Size (µm)
Record 22: unfME_01 1
Record 23: unfME_01 2
Record 24: unfME_01 3

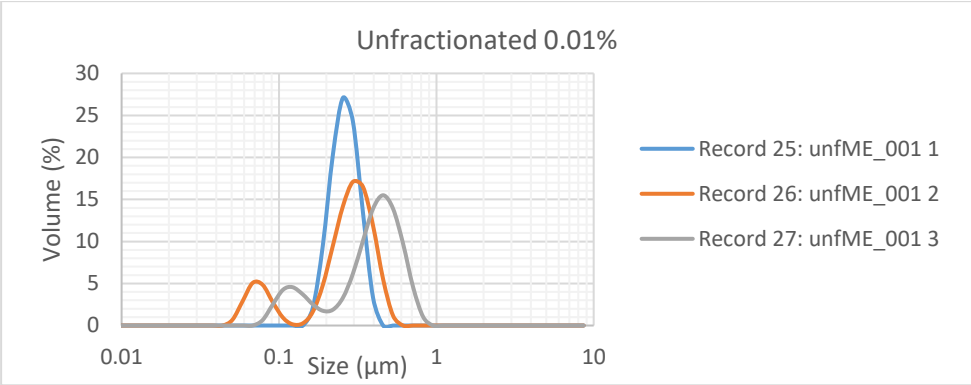

Fractionated:

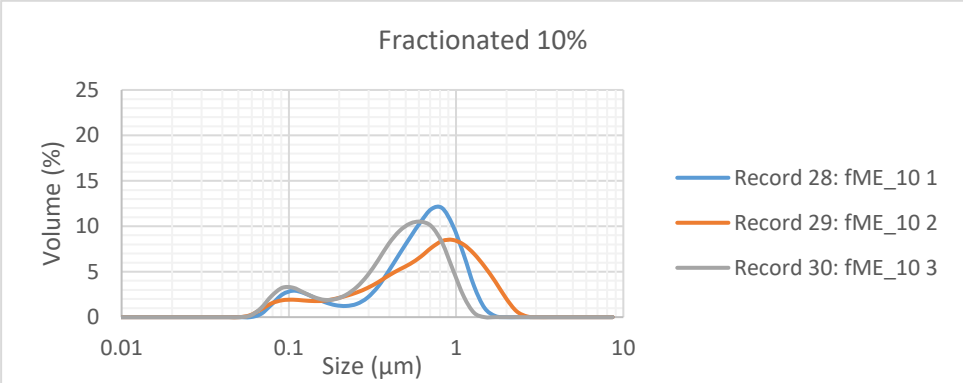

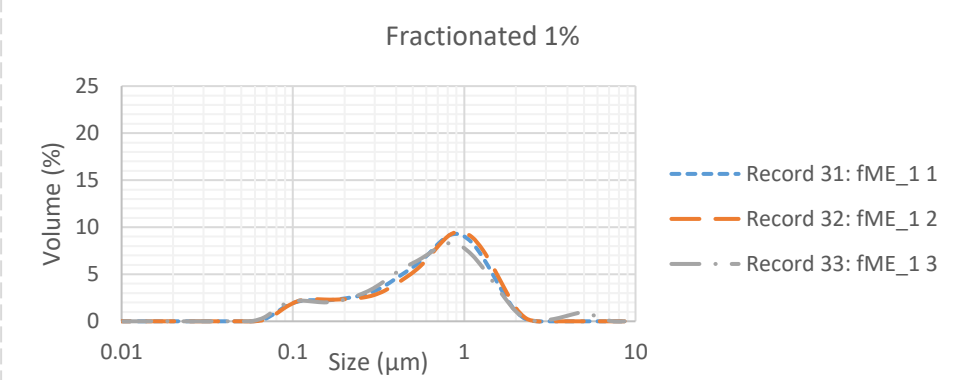

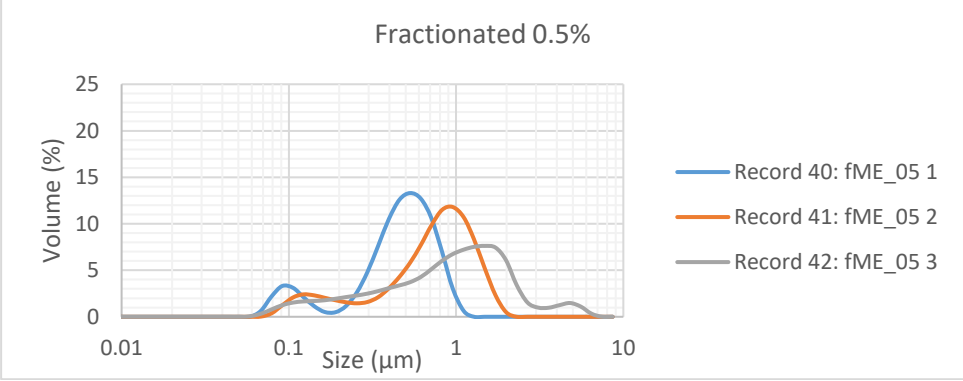

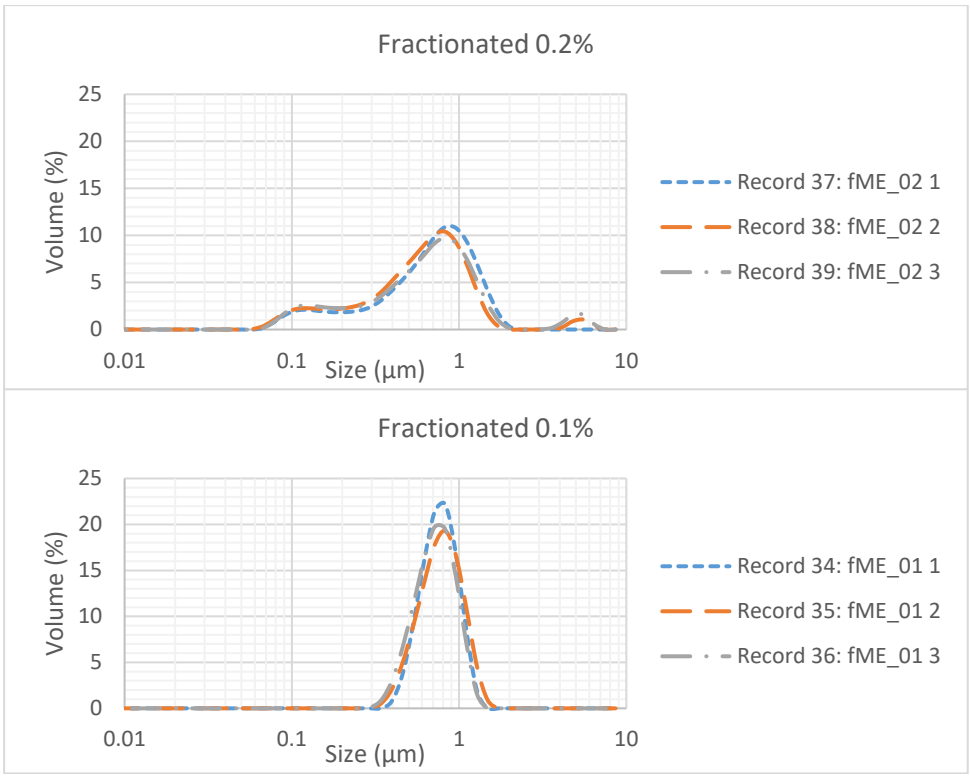
Fractionated 0.2%
Volume (%)
25
20
15
10
5
0
0.01
0.1
1
10
Size (µm)
Record 37: fME_02 1
Record 38: fME_02 2
Record 39: fME_02 3
Fractionated 0.1%
Volume (%)
25
20
15
10
5
0
0.01
0.1
1
10
Size (µm)
Record 34: fME_01 1
Record 35: fME_01 2
Record 36: fME_01 3

Appendix E: Cumulative curves of the Mastersizer 2000, 3000 and DLS

Cumulative curves of the average curves of the unfractionated model emulsion measured on the Mastersizer 2000, Mastersizer 3000 and DLS:

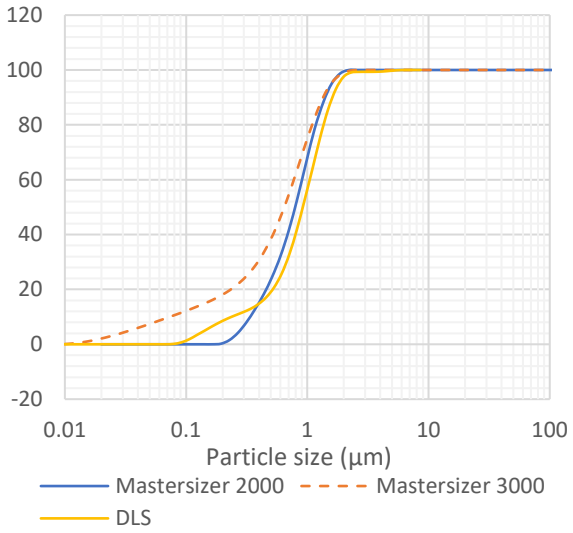

Cumulative curves of the average curves of the fractionated model emulsion measured on the Mastersizer 2000, Mastersizer 3000 and DLS:

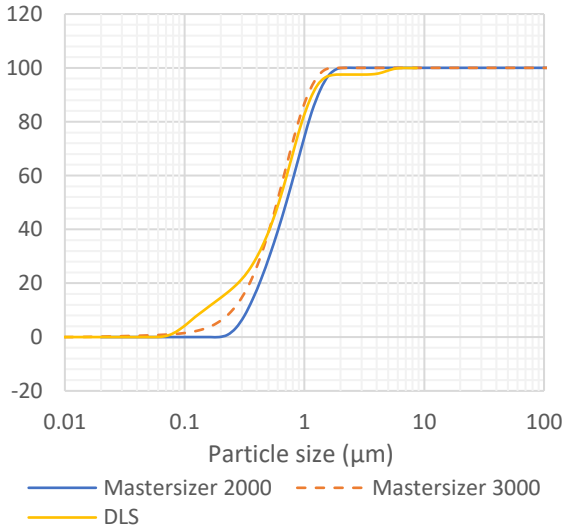

Appendix F: Cleaning plan Mastersizer 3000

As suggested by Malvern, it has been decided to split up the cleaning procedure in two steps. Step one consists of the following:

1. Use the cleaning sequence available on the Mastersizer 3000 software to clean the dispersion unit
2. Rinse the dispersing unit with water and detergent (contains both anionic and non-ionic surfactants)
3. Clean with ethanol
4. Clean with water
5. Check background to see if there is still a bump in the background curve (see image below)

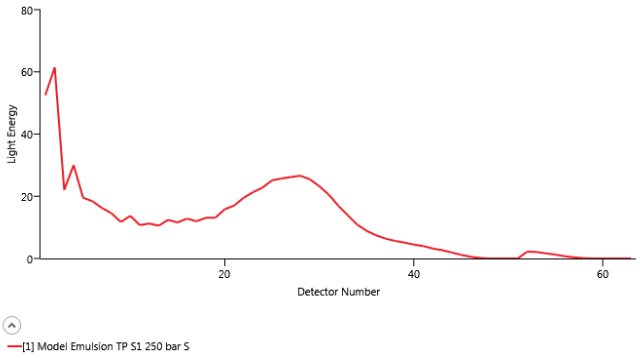

If bump is still visible, the cell windows need to be cleaned. Cleaning first with ethanol, then with water and detergent, next with ethanol again followed by just water. The following steps should be followed:

1. Rinsing the stationary and removeable cell windows with ethanol, isopropanol or water. Use a spray bottle and rinse over sink. Check for that no debris or smears appear on windows before continuing to the next step
2. Cleaning cell windows with a damp lint free tissue/ cloth. Apply cleaning fluid not to the whole tissue but only to the top part that is going to be swept across the surface of the cell window. Use water or alcohol as cleaning fluid. Repeat until windows are clean and change cleaning area of tissue/ cloth so not to smear windows with removed dirt. If possible, change tissue/cloth between cleanings.
3. Now the windows should be clean and to avoid that the evaporation drying that can form deposits on cell windows than can be difficult to remove, the cell windows should be wiped dry. Take a dry lint free tissue/ cloth and wipe the windows dirt. Do not use excessive force during wiping since it can remove the optical coating of the cell windows. The cell window drying can need multiple dryings with clean lint free tissue/ cloth until windows are dry. Make sure that cell windows are completely dry and free from smears, if not repeat cleaning procedure again
4. Repeat for the cell with fixed cell windows. Please note how the cell is positioned on picture. Cell has a drain valve to the front of cell so that all the wash fluid will be drained from cell area.
5. Repeat the cleaning with a tissue/ cloth gently soaked at one edge with dispersant. Use either water or alcohol. Repeat until cell window is clean from dirt and smears.
6. When cell windows are clean from dirt and smears dry the fixed windows the same way as removable window to avoid the drying due to evaporation. Check for cleanliness of cell windows. If satisfied, the next step is to remount the cell windows in cell.
7. When both cell windows are clean remount the removable cell window into the cell. Please check that seal is in correct position. If not press the cell down with finger without smearing cell windows. Fit the grooves of removable cell window over the pin in the fixed cell window half.

8. Lock the cell window in position by reversing the action using the Cell Holder lever. Turn Cell Holder Lever 90 degrees anti-clockwise. Press lever down to tighten the two windows and the seal to avoid leakage. If hoses have been removed, attach them again and add water as dispersant in your Hydro unit. Check by manual cleaning that the system has no leakages outside of instrument. If cell is leaking, remove windows and check the seals.
9. Check to see if the bump in the background curve is gone. To check if the Mastersizer is clean, measure using only water, to see if there are unexpected peaks with no sample. Repeat this several times if needed.

If there are oat fibers sitting on cell windows they are probably adhering to some other contamination or dirt. In the worst-case new cell windows needs to be purchased since in oat fibers are sticking to cell widows it can be hard to remove without destroying the optical treatment of the glasses. New cell windows can be ordered on Malvern Store or contacting Tomas Sandberg who is account manager for Pharma and Food in Sweden/Denmark. Article number for only cell window is MAZ2011, but there is a Standard Hydro LV consumables kit MAZ4130 including QAS standards, Tygon tubings, Lens tissues and wet measurement cell windows and seals.